OFDM Techniques for Multimedia Data Transmission

A thesis submitted in fulfilment of the requirements for the degree of Doctor of Philosophy

Katrina L. Neville
B.Eng(Communication)
M.Eng

School of Electrical and Computer Engineering
College of Science, Engineering and Health
RMIT University

February 2, 2011

Declaration

I certify that except where due acknowledgement has been made, the work is that of the author alone; the work has not been submitted previously, in whole or in part, to qualify for any other academic award; the content of the thesis is the result of work which has been carried out since the official commencement date of the approved research program; and, any editorial work, paid or unpaid, carried out by a third party is acknowledged.

Signed: ..... Date: .....

Acknowledgments

I would like to acknowledge the help and support of my supervisor Assoc. Prof. Zahir Hussain who has helped me along the way to produce this dissertation and has given up time to answer my technical questions about this work.

I would also like to thank Assoc. Prof. James Scott and Prof. Ian Burnett who have also given me much support and help in the final stages of my thesis write-up, without their help this thesis would not be at the point it is now.

I'd also like to acknowledge the help of my colleagues in the digital signal processing research group at RMIT who have all been so much fun to work with: Dr. Noura Al-Hinai, Dr. Khaizuran Abdullah, Dr. Fawaz Al-Qahtani, Mr. Khalifa Al-Mawali and Mr. Arun Gurung.

Finally I'd like to thank Dr. Glenn Matthews and my family who have all been so supportive of me and the work I've been doing.

Publications

Below are the publications in conjunction with the author during her PhD candidacy.

Journal Publications

1. K. L. Neville and Z. M. Hussain, "A Compressive OFDM Transceiver System," submitted for publication.

Conference Publications

1. K. L. Neville and Z. M. Hussain, "Effects of Wavelet Compression of Speech on its Mel-Cepstral Coefficients," Proceedings of *International Conference on Communication, Computer and Power (ICCCP'09)*, Muscat, February 15-18, 2009.

2. K. L. Neville and Z. M. Hussain, "FFT-OFDM for Compressed Image Transmission: Performance Using Structural Similarity," Proceedings of

IEEE Advanced Technologies in Communications Conference (ATC'08), Hanoi, October 6-9, 2008.

3. K. L. Neville, F. Al-Qahtani, Z. M. Hussain, and M. Lech, "Recognition of Modulated Speech over OFDMA," Proceedings of *TENCON'06*, Hong Kong, November 14-17, 2006.

4. K. L. Neville, J. Jusak, Z. M. Hussain, and M. Lech, "Performance of a Text-Independent Remote Speaker Recognition Algorithm over Communication Channels with Blind Equalisation," Proceedings of *TENCON'05*, Melbourne, November 22-24, 2005.

Joint Publications

The author has also contributed to the following joint publications:

1. S. M. Lajevardi, K. L. Neville and Z. M. Hussain, "Facial Expression Recognition Over FFT-OFDM," Proceedings of *IEEE Advanced Technologies in Communications (ATC'09)*, Haiphong, Vietnam, October 12-14, 2009.

2. K. Abdullah, K. L. Neville, and Z. M. Hussain, "An Interference Cancellation Algorithm for Fourier-Based and Wavelet-Based OFDM Systems," Proceedings of *IEEE Advanced Technologies in Communications Conference (ATC'08)*, Hanoi, October 6-9, 2008.

3. N. Al-Hinai, K. L. Neville, A. Z. Sadik, and Z. M. Hussain, "Compressed Image Transmission over FFT-OFDM: A Comparative Study," Proceed-

ings of *Australasian Telecommunication Networks and Applications Conference (ATNAC'07)*, Christchurch, December 2-5, 2007.

Other Publications Not Related to This Thesis

1. K. L. Neville, P. Burton and I. Burnett, "A Second Life Virtual Studio as an Online Teaching Environment," Proceedings of *ASEE Annual Conference and Exposition*, Louisville, Kentucky, USA, June 20-23, 2010.

2. K. L. Neville, and Z. M. Hussain, *Digital Signal Processing 3 Learning Package*, RMIT Press, 2008.

3. K. L. Neville, and Z. M. Hussain, *Communication Engineering Learning Package*, RMIT Press, 2007.

4. K. L. Neville, "Channel Compensation for Speaker Recognition Systems," Dissertation for Masters of Engineering, RMIT University, November 2006.

Keywords

Orthogonal frequency division multiplexing, wireless transmission, signal processing, data compression, multimedia data transmission, video processing, image processing, discrete wavelet transform.

Contents

List of Figures

Abstract

Orthogonal Frequency Division Multiplexing (OFDM) is an efficient parallel data transmission scheme that has relatively recently become popular in both wired and wireless communication systems for the transmission of multimedia data. OFDM can be found at the core of well known systems such as digital television/radio broadcasting, ADSL internet and wireless LANs.

Research into the OFDM field continually looks at different techniques to attempt to make this type of transmission more efficient. More recent works in this area have considered the benefits of using wavelet transforms in place of the Fourier transforms traditionally used in OFDM systems and other works have looked at data compression as a method of increasing throughput in these types of transmission systems.

The work presented in this thesis considers the transmission of image and video data in traditional OFDM transmission and discusses the strengths and weaknesses of this method. This thesis also proposes a new type of OFDM system that combines transmission and data compression into one block. By merging these two processes into one the complexity of the system is reduced, therefore promising to increase system efficiency.

The results presented in this thesis show the novel compressive OFDM

method performs well in channels with a low signal-to-noise ratio. Comparisons with traditional OFDM with lossy compression show a large improvement in the quality of the data received with the new system when used in these noisy channel environments. The results also show superior results are obtained when transmitting image and video data using the new method, the high correlative properties of images are ideal for effective transmission using the new technique.

The new transmission technique proposed in this thesis also gives good results when considering computation time. When compared to MATLAB simulations of a traditional DFT-based OFDM system with a separate compression block, the proposed transmission method was able to reduce the computation time by between a half to three-quarters. This decrease in computational complexity also contributes to transmission efficiency when considering the new method.

Acronyms

ACE	Active Constellation Mapping
AM	Amplitude Modulation
ASK	Amplitude Shift Keying
AWGN	Additive White Gaussian Noise
CWT	Continuous Wavelet Transform
DCT	Discrete Cosine Transform
DSBSC	Double Sideband Suppressed Carrier AM
DFT	Discrete Fourier Transform
DWPT	Discrete Wavelet Packet Transform
DWT	Discrete Wavelet Transform
FFT	Fast Fourier Transform
FM	Frequency Modulation
FSK	Frequency Shift Keying
IDFT	Inverse Discrete Fourier Transform
IDWPT	Inverse Discrete Wavelet Packet Transform
IDWT	Inverse Discrete Wavelet Transform

ICI	Inter-Channel Interference
ISI	Inter-Symbol Interference
ML	Maximum Likelihood
OFDM	Orthogonal Frequency Division Multiplexing
OQPSK	Offset Quadrature Phase Shift Keying
PAPR	Peak-to-average power ratio
PDF	Probability Density Function
PEP	Peak Envelope Power
PLC	Power line communication
PM	Phase Modulation
PSK	Phase Shift Keying
QAM	Quadrature Amplitude Modulation
QPSK	Quadrature Phase Shift Keying
RLE	Run-length encoding
SSIM	Structural Similarity

Chapter 1

Introduction

Since the discovery of wireless transmission using radio waves in the late 1800s wireless information transmission has become increasingly important in society. In today's world it is taken for granted that breaking news can be received almost as soon as it happens, that people can speak to each other in real-time even if they are located on the other side of the world and that e-mails can be read, files transferred and the Internet can be accessed even when taking a lunch break in the park. Almost all of these activities are made possible due to advances in wireless communication technology with mobile/satellite telephones and wireless computer networks aiding in the communication network that covers the globe today.

Some of the important historical advances that launched the wireless communication revolution and ultimately allowed for these diverse ranges of communication tools include: the early wireless telegraphy system where data was transmitted in the form of the Morse code 'dots' and 'dashes' (short and long electrical impulses) [1]-[3], the analogue modulation techniques used in audio

and speech transmission in AM and FM radios and the development of wireless video transmission as used in television broadcasting [4].

During the early development years of these technologies, the data and modulation techniques used were all based on analogue technology with analogue signal processing methods being employed in the systems. With the onslaught of digital technology and techniques in the 1960s and 1970s these wireless transmission systems gained new life and began to evolve further. The digital era allowed the digitisation of analogue signals to occur which opened the door to the development of signal processing using digital hardware and software devices (DSP) and digital modulation techniques to efficiently transmit these digital data streams. The versatility and reliability of digital signals and systems has led to many governments making the transition from analogue television and radio broadcasting to new digital broadcasting methods [4] - [6]. Telecommunication companies are also making this change from analogue to digital technology for mobile and landline telephone systems [6].

As well as the evolution of the old, well known technologies, such as radio and television, new technologies have also developed out of the popularity of computers, wireless LANs are one type of system which aims to make Internet and file-sharing available to everyone, no matter where they are located.

With the increasing complexity of these communication systems comes increasing complexity in the type of content being transmitted and received. The early content of plain speech/audio and basic black and white images used in early radio and television has developed into high definition audio and video streams; and with the introduction of computers into the mix even more complex content needs to be considered from images, video and audio to medical

and financial data. Techniques are continuously being developed to maximise data throughput and efficiency in these wireless communication systems while endeavouring to keep data loss and error to a minimum.

For data transmission systems and networks increasing the performance and efficiency of a system can be tackled by considering both the physical-layer issues where modulation, multiplexing, channel equalisation and error correction occurs and also from a compression perspective where application specific compression algorithms can be applied to the data. This thesis will focus on techniques related to both these levels to maximise data transmission.

The following section will outline the specific areas that this thesis will examine.

1.1 Objectives of This Thesis

This thesis will focus on two main parts of a data communication system: the physical layer techniques, including modulation, multiplexing and channel effects as well as data compression techniques.

Orthogonal Frequency Division Multiplexing (OFDM) is one data transmission technique that has been the topic of much research since the 1960s [7]. OFDM is a parallel transmission scheme that can maximise data throughput by using many spectrally overlapping subcarriers to modulate data on. This ability to allow spectral overlap in the transmission is one of the main features that makes OFDM ideal for the transmission of large amounts of data. In a normal frequency division multiplexing (FDM) system, data streams are transmitted on spectrally non-overlapping channels so as to avoid interference between neigh-

bouring channels, with OFDM though, the data is able to be transmitted in very closely spaced and even overlapping channels by ensuring orthogonality between the separate subcarriers used to modulate the data as well as orthogonality of the data itself being transmitted on the individual channels [8], [9].

Because of this OFDM has proven over the years to be the ideal transmission technique for large amounts of multimedia data and has become the standard in digital television broadcasting (DVB-T), digital audio broadcasting (DAB), ADSL modems and wireless LANs [10]. It is because of this that this thesis will consider it as the transmission technique of choice and will consider the main variants of OFDM, Fourier and wavelet based OFDM.

OFDM may be a good method of transmitting large amounts of data wirelessly but data compression is also essential in these types of systems to improve system efficiency further. As raw data can contain large amounts of redundant information compression can be used to reduce the data size and allow for shorter transmission times [11].

This thesis will consider the two major transforms used in compression: the discrete cosine transform (DCT) commonly used in JPEG and MPEG compression and the discrete wavelet transform (DWT) used in subband coding and the JPEG2000 compression standard.

Another major objective of this thesis is to propose a new method of merging the efficient transmission technique of OFDM together with a data compression method. These two aspects of a communication system are major contributors to developing a highly efficient transmission system for large quantities of multimedia data, the idea of being able to compress and transmit data at the same time would be a very desirable attribute in a communication system as it would

simplify the system and reduce its computational complexity.

1.2 Contributions

The work from this thesis has provided the following contributions to the digital communication and signal processing fields:

1. The research from this thesis has proposed a new type of OFDM transmission system which reduces computational complexity of an OFDM system by combining transmission and compression blocks into one. (Chapter 5 and chapter 6)

2. The new method uses a combination of wavelet subband filtering and compression and wavelet OFDM to compress the data at the time of multiplexing and modulation. (Chapter 5)

3. This research has also extensively examined wavelet compression techniques including subband filtering and coefficient thresholding techniques. This work on wavelet compression has also led to work being published on the use of wavelet compression in OFDM systems and the optimal wavelet filters and compression methods to be used in both the proposed compressive OFDM system as well as traditional DFT-OFDM transmission systems. (Chapter 4 and [12])

4. This work also examined in detail the effect these different wavelet compression methods have from a data perspective. The data types being transmitted in wireless systems are very diverse, therefore an indication

on how different compression methods affect different data types is invaluable information when designing a compression method that works for the system being designed.

Work has been published on how the classification features in both speech and images are affected by different wavelet compression techniques and different wavelet filters. This has led to research being conducted on the perceptual quality of compressed data. Looking at data error alone may not give a perfect indication of how much degradation has occurred to images and audio since the human eye and ear have less sensitivity to some changes than to others, therefore perceived quality was examined after images and audio had been compressed and reconstructed. (Chapter 6 and [13] and [14])

1.3 Thesis Organisation

This thesis is organised in the following manner:

Chapter 2 - Wireless Data Transmission and Modulation Techniques presents a literature survey on the development of wireless transmission techniques. The first part of the chapter contains a fundamental review on common digital modulation techniques such as phase shift keying (PSK), amplitude shift keying (ASK), etc which have been used in many digital communication applications from modems to digital wireless data transmission.

This chapter continues by introducing the concept of parallel data transmission and discusses how this idea has developed from the purely theoretical

introduction in the 1960s, through the advancements in the technology that enabled it to be practically implemented, through to how it is used today in almost all wireless communication systems. This section considers the main orthogonal frequency division multiplexing (OFDM) techniques based on the discrete Fourier transform as well as the wavelet based version touted as a candidate for use in powerline communications.

Thirdly, compression techniques are considered with a look at the discrete cosine transform (DCT) used in standard JPEG compression and the discrete wavelet transform (DWT) used in the JPEG2000 standard. This section will look at lossy and lossless compression and how these can be achieved using the DCT and DWT.

Lastly this chapter will describe the importance of channel modelling when simulating a wireless transmission system. Common channel effects are discussed and the causes of these are also examined.

Chapter 3 - Orthogonal Frequency Division Multiplexing Systems considers the practical applications of OFDM technology. This chapter will look at the two main types of OFDM transmission: discrete fourier (DFT)- and discrete wavelet (DWT)- OFDM and look at the standards that utilise these in real life data transmission applications. The main applications that will be covered include the European digital television and audio broadcasting standards (DVB-T and DAB respectively), the IEEE 802.11a wireless LAN standard and the IEEE power line communication draft standard.

The second part of this chapter will then look at the problems associated with OFDM systems and consider the options available to mitigate these prob-

lems. OFDM systems have a few known issues, some examples covered in this chapter include the high peak-to-average power ratio exhibited in these systems as well as inter-channel interference and the need for a cyclic prefix.

Chapter 4 - OFDM for Multimedia Data Transmission presents results from simulations using the traditional DFT-OFDM transmission method with and without a separate compression block. This chapter will consider the effects the compression technique has on performance as well as the effects different baseband modulation mapping schemes have on the resulting data.

The data considered in these results are images and video so as to consider the effectiveness of wavelet compression and OFDM transmission on different multimedia data types. A quantitative analysis of the data error rate will be presented as well as a qualitative analysis considering the perceived error in the data.

Chapter 5 - A Compressive OFDM System for Multimedia Data Transmission examines a novel compressive OFDM transceiver system that is designed to combine compression and transmission into one block. This system is proposed as most OFDM systems consist of a compression block separate to the OFDM transmission block which increases the complexity of the system.

With wavelet transforms being both orthogonal and able to compress data, a system can be produced that combines these properties into one. This chapter will examine how this technique can be used for multimedia data transmission and compression and how it promises to reduce the computational complexity of a wireless transmission system.

Chapter 6 - System Analysis performs an in-depth analysis of the systematic operations of the proposed OFDM technique. All communication systems have a basic structure including source and channel encoding, synchronisation and specifically for OFDM systems, formation of the OFDM data block so as to mitigate unwanted channel effects from the data.

This chapter will consider all these aspects and look at common techniques that are used in communication systems to perform these tasks. Each technique will be evaluated for their relevance and performance in systems such as the proposed system. These blocks are essential for communication systems to work properly and need to be addressed for their practical effectiveness in any new system.

Chapter 7 - Performance Analysis of the Compressive Transceiver analyses the performance of the proposed compressive OFDM system. This chapter will again look at both image and video data transmission using the proposed method and compare the results obtained from this method with those obtained from the traditional methods presented in chapter 4.

As in chapter 4 a quantitative analysis of the error rate as well as a qualitative analysis looking at the perceived error in the data will both be presented.

Chapter 8 - Conclusions This chapter will summarise the main conclusions gained from this research, it will look at the comparisons between the two methods and contrast the strengths and weaknesses of these methods. Finally the future directions for this research will be presented.

Chapter 2

Wireless Data Transmission and Modulation Techniques

2.1 Introduction

Digital modulation techniques are an extension of the ideas associated with analogue modulation used commonly in radio and television transmission and reception.

In analogue modulation the aim is to take a baseband signal containing the information needed to be transmitted and by using a high frequency sinusoidal carrier and altering some aspect of it (amplitude, phase or frequency) the information signal can be effectively encapsulated and encoded in the high frequency region of the spectra and easily transmitted via an antenna [15]. Since the information signal has been shifted up in the frequency spectra from baseband the antenna used for transmission can be relatively short since antenna length is proportional to a quarter wavelength of the signal being transmitted. This

concept is shown in figure 2.1.

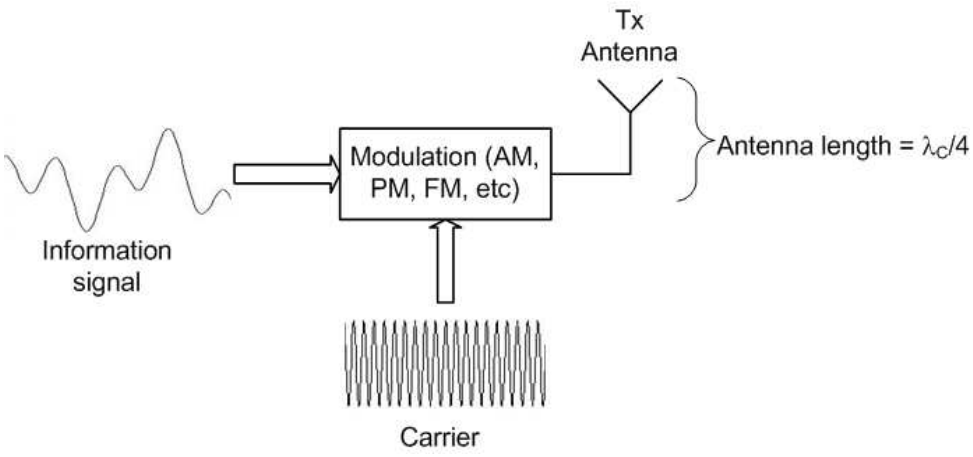

Figure 2.1: Diagram of a basic analogue modulation system

This technique of modulating analogue signals has been widely used since the late 1800s with the advent of the radio transmitter and receiver which gained much commercial popularity during the first and second world wars and later the transmission of television signals in the 1940s and 1950s where the modulation of image as well as audio signals became a reality. Of more recent times these same techniques have been developed and effectively adapted to the digital world and the transmission of digital data, which has opened the door to incorporating computer systems and digital signal processors (DSPs) into the wireless domain [10].

Digital television, digital radio, wireless internet transmission and multimedia applications on mobile telephones are some of the many areas that digital modulation has impacted on of recent times and improvements to the transmission of this data are constantly being sought.

This chapter will start by reviewing some of the most commonly used mod-

ulation schemes which have been used in digital data transmission and will build upon this by looking at the development of more complex digital modulation schemes such as M-PSK and M-QAM. Constellation diagrams will be examined for these schemes and an explanation of baseband data encoding will be presented. This chapter will also discuss the more recent development of parallel transmission schemes with Orthogonal Frequency Division Multiplexing (OFDM) being presented as an example of this type of scheme. Technical details about this technique will be presented and a brief summary will be given of how OFDM is being used today in wireless data transmission.

The second part of this chapter will consider data compression techniques and discuss why it is necessary to use data compression when developing an efficient transmission system. Particular emphasis will be placed on the types of compression used most commonly with multimedia data, particularly images.

Lastly channel modelling will be examined with a look at how the attributes of a wireless channel can affect the data being transmitted. This section will consider the importance of accurate channel modelling in the case of communication system simulations and what steps should be taken to ensure effective data transmission can occur in these channel environments.

2.2 Digital Modulation

The theories behind digital modulation are analogous to the way modulation is used in analogue systems. In analogue modulation a signal is used to modulate a carrier by changing some aspect of that carrier, be it amplitude, phase, frequency, or a combination of these [15].

The most well known analogue modulation schemes used in radio transmission are: amplitude modulation (AM) where the carrier's amplitude is varied proportionally to the amplitude of the analogue message being transmitted ($m(t)$), frequency modulation (FM), where the frequency is varied in relation to the amplitude of $m(t)$ and phase modulation (PM) where, again, the phase is varied according to the behaviour of $m(t)$.

Digital modulation uses these same techniques but where previously $m(t)$ was an analogue signal this time the message is replaced by binary encoded digital information (figure 2.2).

The following subsections give a brief summary of the common types of digital modulation used.

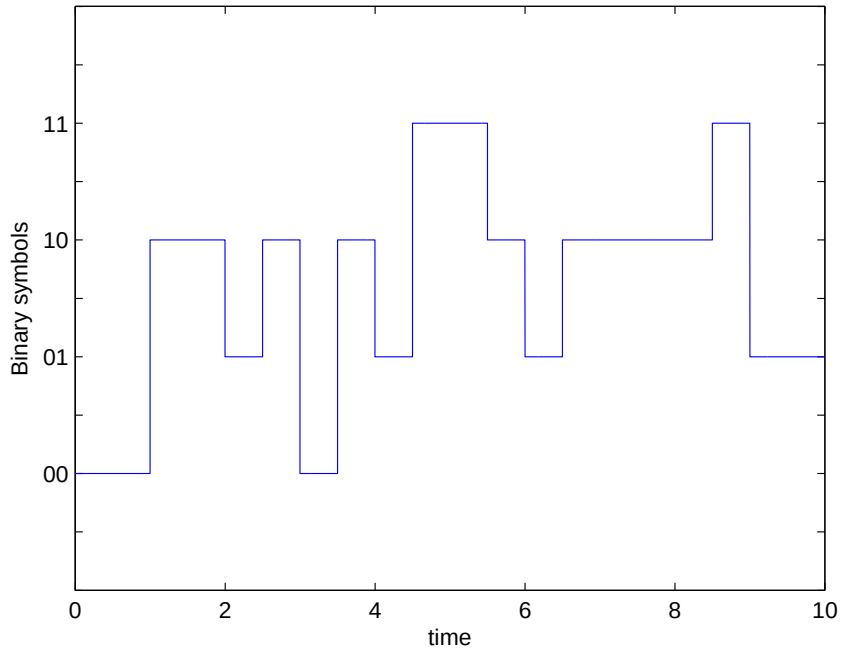

Figure 2.2: Example of binary encoded data used to digitally modulate a carrier

2.2.1 Amplitude Shift Keying (ASK)

Amplitude shift keying (ASK) behaves in virtually an identical manner to the analogue amplitude modulation (AM) scheme where a high frequency carrier's amplitude is altered depending on the incoming message signal. The simplest and earliest implementation of ASK is also known as On-Off Keying (OOK) where the sinusoidal carrier is transmitted only during the symbol period for a binary 1, for a binary 0 a zero amplitude signal is transmitted (figure 2.3). This equates to the function in equation (2.1) [16].

$$s(t) = \begin{cases} A_c \Pi(t/T_0) \cos \omega_c t, & \text{for binary 1} \\ 0, & \text{for binary 0} \end{cases} \tag{2.1}$$

where A_c is the carrier amplitude, Π is the rectangular pulse function, T_0 is the ASK symbol duration and ω_c is the angular frequency of the carrier wave. This type of ASK is very similar to DSB/SC AM in the analogue domain.

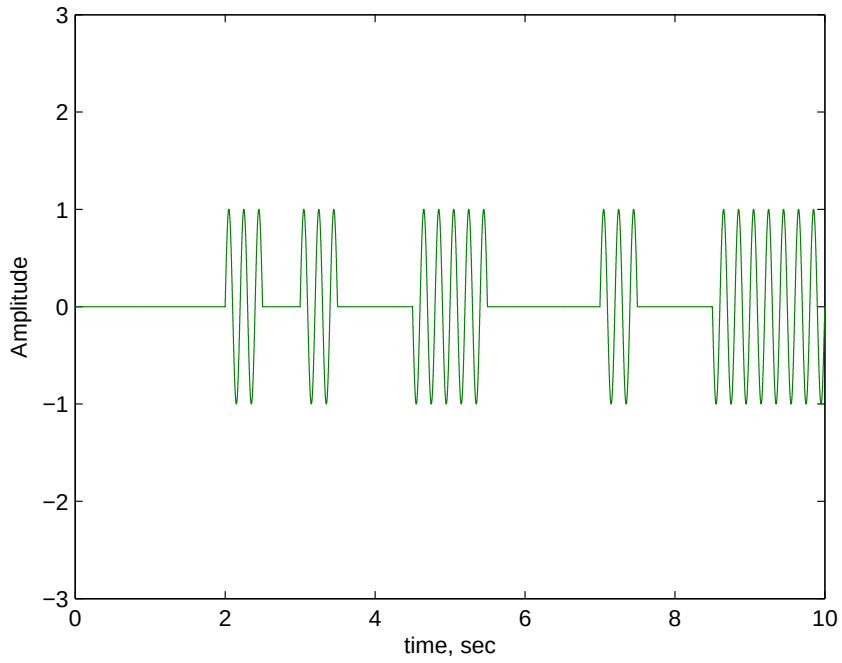

Figure 2.3: Example of an OOK signal

A more sophisticated implementation of ASK involves firstly quantising the binary message so as to achieve M discrete levels each representing a different binary string combination. This will in turn produce an M-level signal, $m(t)$, which modulates the amplitude of the high frequency carrier, $c(t)$. This results in an output signal more like that of the conventional AM analogue equivalent and is shown in figure 2.4 and mathematically in equation (2.2) [10]:

$$s(t) = A_c[1 + m(t)] \cos \omega_c t \tag{2.2}$$

where $m(t)$ is the M-level digital message, A_c is the amplitude of the carrier and ω_c is the angular frequency of the carrier.

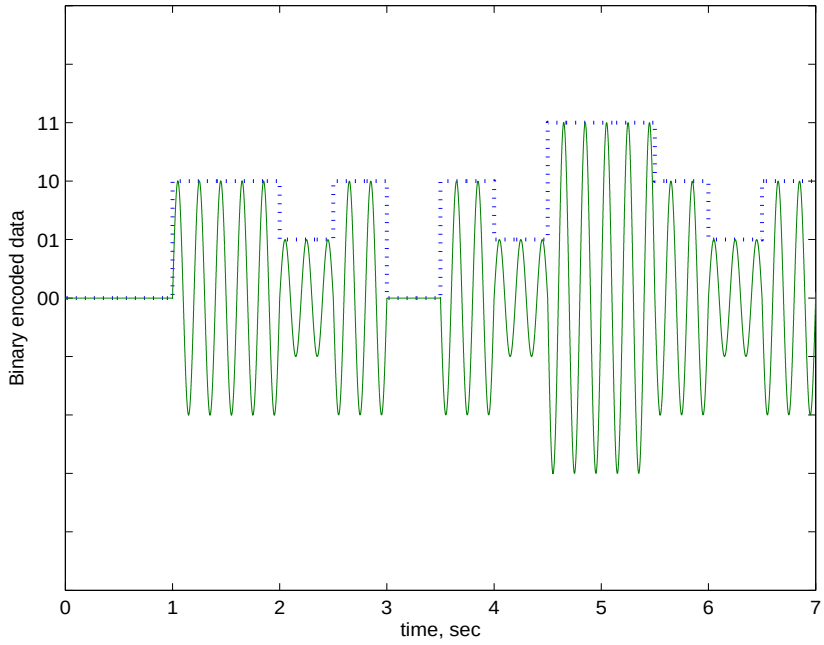

Figure 2.4: Example of a 4-level ASK signal

Figure 2.4 shows the result of this type of modulation; The dotted line shows the original encoded message while the solid line shows the modulated carrier.

2.2.2 Frequency Shift Keying (FSK)

FSK as in analogue Frequency Modulation (FM) alters the carrier's frequency in relation to the amplitude of the digital message being modulated. The simplest FSK scheme is binary FSK where two discrete frequencies define a binary 1 and 0. This simple FSK method is described in equation (2.3) [10].

$$s(t) = \begin{cases} A_c \cos(\omega_1 t + \theta_1), & \text{for binary 1} \\ A_c \cos(\omega_2 t + \theta_2), & \text{for binary 0} \end{cases} \tag{2.3}$$

where A_c is the amplitude of the carrier, ω_1 and ω_2 are the carrier's angular frequencies for a binary 1 and 0 being modulated respectively and θ_1 and θ_2 are the carrier's phases when a binary 1 and 0 are modulated.

As with ASK, FSK can also be used to modulate multi-level binary coded messages, therefore for an M-level encoded message there will be M discrete frequencies describing each level. Equation (2.4) mathematically describes this M-FSK modulation, this equation shows that FSK is virtually identical to analogue FM except where the the message is replaced with a binary encoded signal [10].

$$s(t) = A_c cos[\omega_c t + \Delta_f \int_{-\infty}^{t} m(\lambda) d\lambda] \tag{2.4}$$

where A_c is the amplitude of the carrier, ω_c is the angular frequency of the carrier's centre frequency, Δ_f is the frequency sensitivity of the system and $m(\lambda)$ is the binary encoded message being modulated.

This modulation scheme results in the waveform shown in figure 2.5.

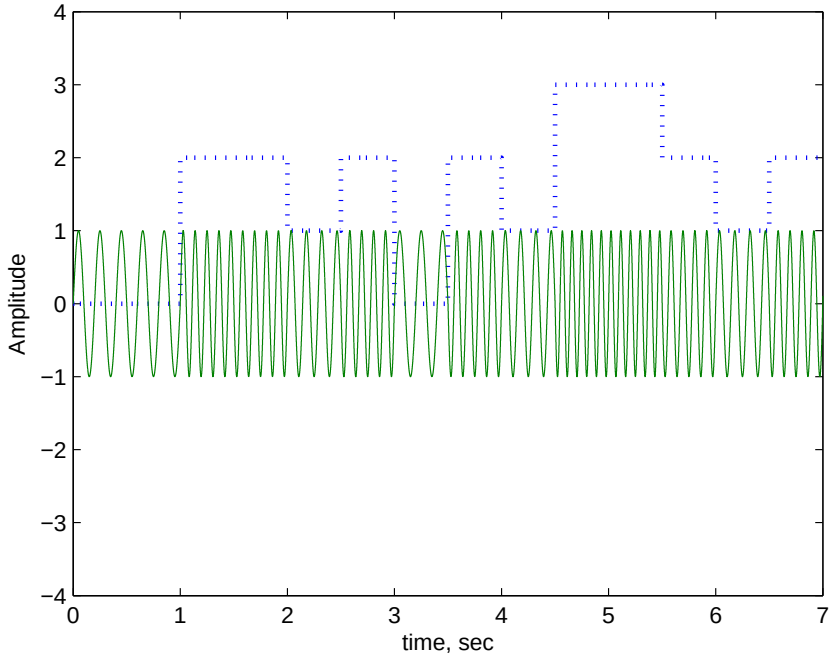

Figure 2.5: Example of a 4-FSK signal

2.2.3 Phase Shift Keying (PSK)

Analogous to Phase Modulation (PM) used in analogue communications, Phase Shift Keying changes the phase of a carrier depending on the encoding levels of a binary message. A general equation for PSK is in equation (2.5).

$$s(t) = A_c \cos[\omega_c t + \Delta_p m(t)] \tag{2.5}$$

where A_c is the amplitude of the carrier, ω_c is the angular frequency of the carrier's centre frequency and Δ_p is the phase sensitivity of the system.

PSK modulation is one of the most widely used digital modulation schemes

around and has proven to be one of the most versatile and simplest schemes to implement. In its simplest form PSK takes the form of Binary-PSK (BPSK) where only two different phases are used to encode and transmit a binary 1 and a binary 0; one symbol transmitted on a carrier with a 0^o phase-shift and the second symbol transmitted on a 180^o phase-shifted carrier [10], [17]. To visualise this, constellation diagrams are used, figure 2.6 shows the above scenario on its respective constellation diagram.

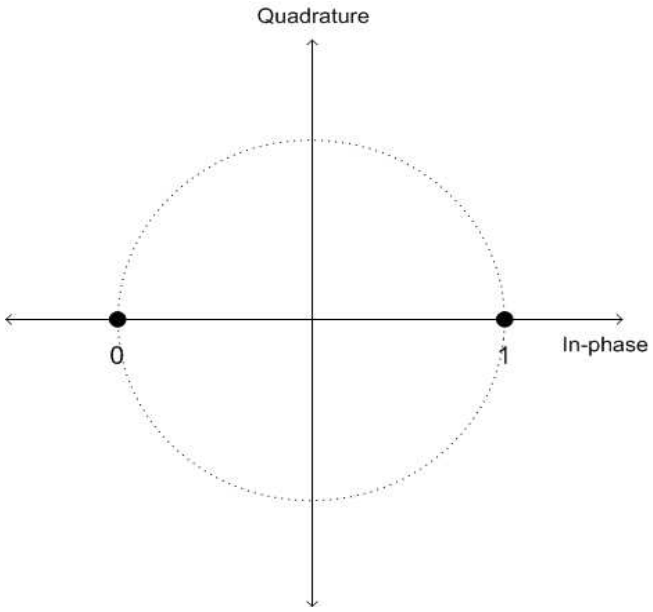

Figure 2.6: Constellation diagram for the BPSK digital modulation scheme

Other variants of the PSK scheme include: Quadrature-PSK (QPSK), Offset-QPSK (OQPSK) and higher order PSKs (M-PSK).

The QPSK scheme is an interesting case as it can be implemented either using the traditional PSK method, where a single carrier is modulated by the binary data onto four discrete phases (45^o, 135^o, 225^o, 315^o), or it can be imple-

mented with the same result in the IQ (In-phase, Quadrature) modulation style where two carriers with 90^o phase differences are amplitude modulated by the data and the superposition of these modulated carriers is what is transmitted [15]. Either way this method allows two bits to be modulated and transmitted per PSK symbol period as opposed to the single bit per PSK symbol period that standard BPSK can achieve, therefore increasing bandwidth efficiency [15], [10], [16]. The constellation diagram and waveform diagram for this style of QPSK modulation is shown in figures 2.7 and 2.8 respectively.

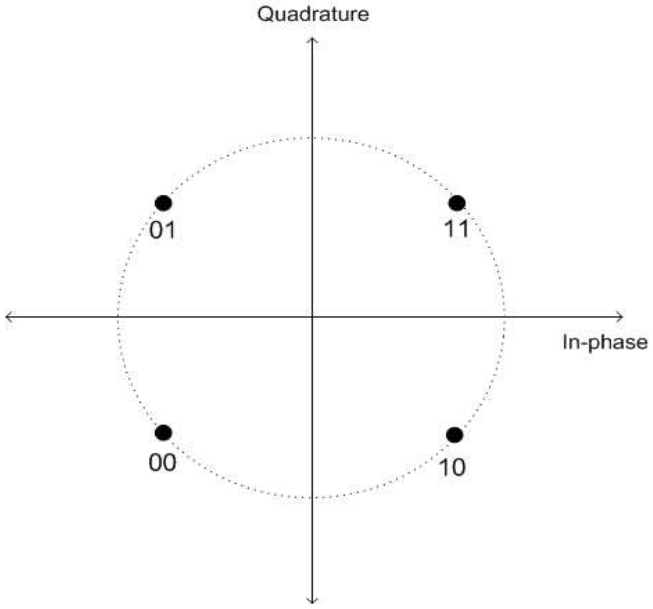

Figure 2.7: Constellation diagram for the QPSK digital modulation scheme

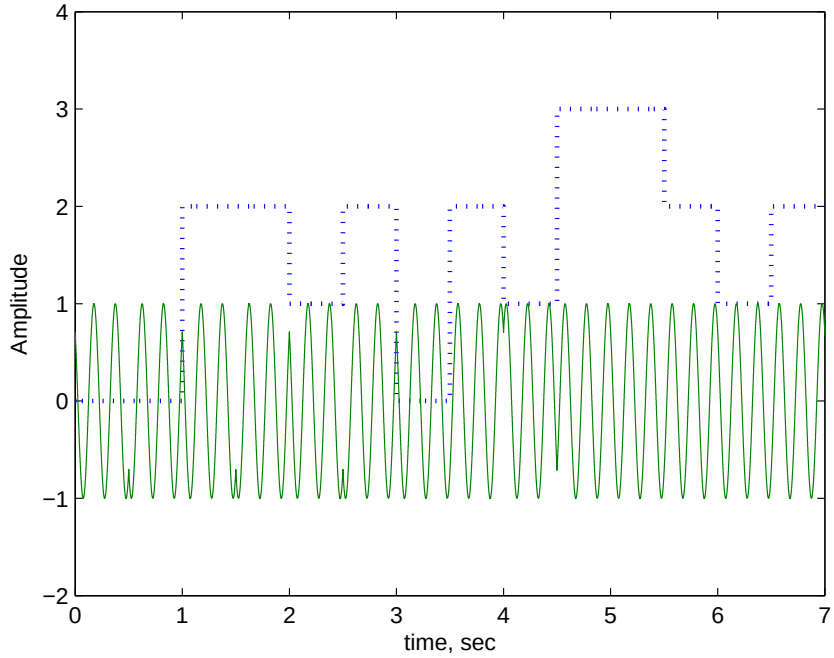

Figure 2.8: Example of a 4-PSK (QPSK) signal

The OQPSK modulation scheme is often used to improve on error performance of the QPSK system. This modulation scheme is almost identical to QPSK except this method offsets the data stream modulating the quadrature carrier component by half a QPSK symbol period. By allowing this offset to occur before modulating the carrier, harsh transitions in the amplitude of the modulating signal (and hence the phase of the modulated signal) can be eliminated, (i.e. on the constellation diagram there will only be transitions occurring between adjacent constellation points) [16].

Another variant of PSK is the higher order PSKs (M-PSK) where extra points (phases) are added to the constellation diagram so as to enable the simultaneous modulation of three (8-PSK), four (16-PSK) or more bits per

symbol period. Figure 2.9 shows this for an 8-PSK modulation system.

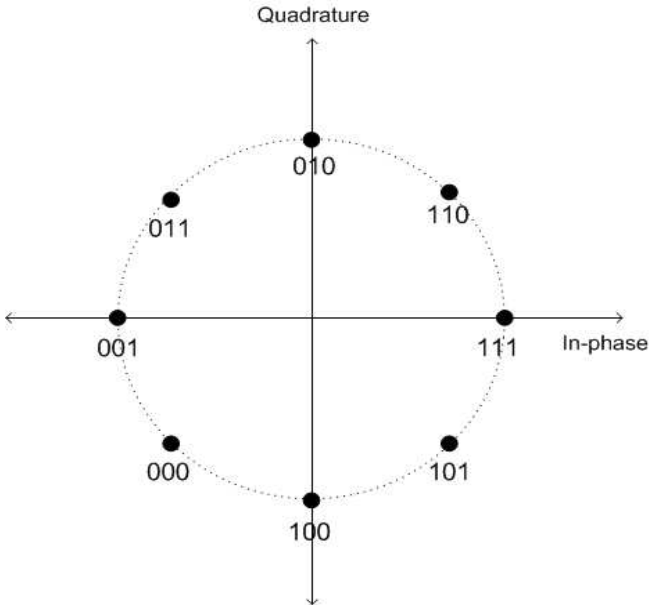

Figure 2.9: Constellation diagram for the 8-PSK digital modulation scheme

2.2.4 Quadrature Amplitude Modulation (QAM)

QAM modulation developed from hybrid combinations of the ASK and PSK digital modulation schemes. By using the summation of two Double Sideband Suppressed Carrier (DSB/SC) modulated signals, this digital modulation scheme can conserve a great deal of bandwidth and improve bandwidth efficiency [10], [17], [18]. The general formula for QAM modulation is in equation (2.6).

$$s(t) = A_c x(t) \cos \omega_c t - A_c y(t) \sin \omega_c t \tag{2.6}$$

where $x(t)$ and $y(t)$ are the two independent messages being modulated.

Again constellation diagrams can be used for QAM modulation to visualise

the modulation scheme. Unlike M-PSK modulation though the constellation diagram need not be circular, square/rectangular constellations are actually the most commonly implemented constellations for QAM. A constellation that can be used in 16-QAM is shown in figure 2.10.

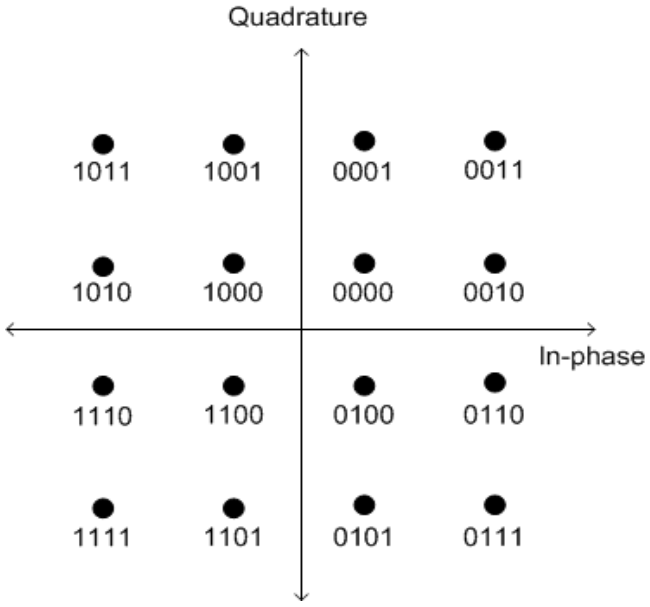

Figure 2.10: Constellation diagram for the 16-QAM digital modulation scheme

From figure 2.10 it can be seen in this case that each point on the constellation diagram represents an encoded 4 bits of a binary string. The phases and amplitudes, A_c, of the two quadrature and in-phase carriers are therefore dependent on the 4-bit binary string being encoded and modulated [16].

2.3 Parallel Frequency Division Multiplexing Methods

During the mid-to-late 1960s research into the areas of digital modulation and transmission began to consider parallel transmission techniques as opposed to the traditional serial transmission methods. By taking parallel streams of data and modulating these on closely spaced (and overlapping) orthogonal carriers, transmission could become much more efficient when compared to serially modulating and transmitting the data. Some of the pioneers in this area of research during this time include: R. Chang [7],[19], B. Saltzberg [20], and S. Weinstein [21] who all began to consider the efficiency of parallel transmission schemes and how this theory could begin to be applied in practice.

In the works by Chang and Saltzberg in 1966 and 1967 respectively ([7],[20]), the concept of using spectrally overlapping subchannels to multiplex the data stream on was explored. This method opposed the traditional notion where Frequency Division Multiplexed (FDM) data channels were confined to non-overlapping regions of the spectra. The reasoning behind the new suggestion stemmed from the fact that this method allowed for a more efficient use of channel resources and maximised the data rate without compromising on data quality (potential inter-symbol and inter-channel interferences).

The block diagram of the transmission method proposed in [7] is shown in figure 2.11 and worked by ensuring signal orthogonality occurred within each subchannel as well as between adjacent subchannels by carefully designing transmitting filters that would fulfil certain criteria.

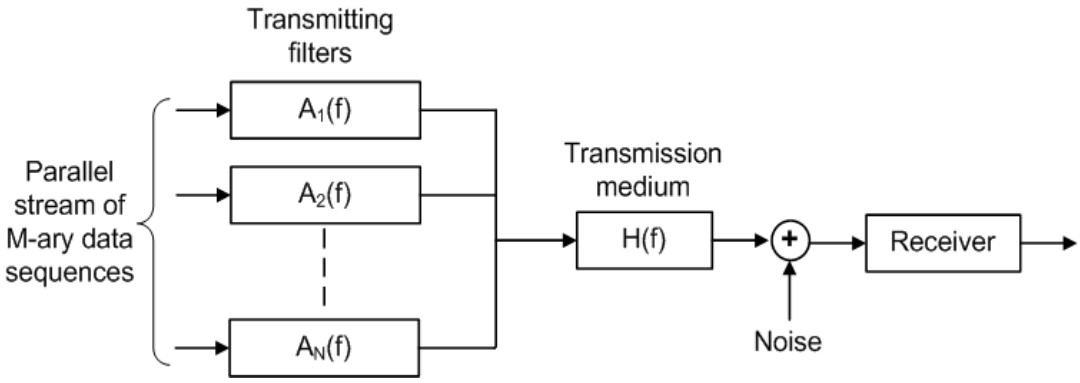

Figure 2.11: Parallel data transmission system proposed by R. Chang (1966)

Within a single subchannel (the i^{th} subchannel) orthogonality between consecutive symbols being transmitted was achieved by satisfying the orthogonality condition in equation (2.7)

$$\int_{-\infty}^{\infty} u_i(t)u_i(t-kT)dt = 0, \;\; \mathrm{k} = 0, \pm 1, \pm 2, \ldots \tag{2.7}$$

where $u_i(t)$ is the convolution between the i^{th} transmitting filter's impulse response and the transmission medium's impulse response and T is the symbol period.

Between adjacent subchannels (e.g. the i^{th} subchannel and the j^{th} subchannel) orthogonality between the two transmission streams was similarly achieved by satisfying equation (2.8)

$$\int_{-\infty}^{\infty} u_i(t)u_j(t-kT)dt = 0, \;\; \mathrm{k} = 0, \pm 1, \pm 2, \ldots \tag{2.8}$$

where $u_j(t-kT)$ is the convolution between the j^{th} transmitting filter's impulse response and the transmission medium's impulse response for all symbol

periods.

Satisfying these conditions meant that Chang's system could withstand both inter-symbol and inter-channel interference and allow the data rate to approach the theoretical limit of the transmission channel, while at the same time ensuring the data can still be received and decoded accurately at the receiver.

Works by S. Weinstein in 1971 developed this idea further, Weinstein noted that a multitone data signal was in effect the same as the Fourier transform of the original data stream and that a bank of coherent detectors at the receiver acted like an inverse Fourier transform. From this observation Weinstein proposed the idea of transmitting the data in the form of a Discrete Fourier Transform (DFT), this new techniques simplified the parallel transmission system by reducing the number of complex sinusoidal generators and coherent demodulators needed in the system and allowed the system to become more realisable in practice [21],[8].

This same work also confronted the issue of inter-block and inter-channel interference caused by the truncation of the DFT symbols and the need for a guard interval (or cyclic prefix) to be used to mitigate the effect of this. The guard interval was deemed necessary since fading channels can cause delay spreads to occur to the OFDM symbols causing both inter-block interference where delayed versions of the previously transmitted OFDM block can overlap with the current block as well as inter-channel interference where spectral leakage can occur between each of the N sub-carriers in one OFDM block [22],[23]. This guard interval concept is still widely used today and is considered the standard in such systems as digital television broadcasting [24], [9].

From these significant works the way was paved for the development and

deployment of Orthogonal Frequency Division Multiplexing (OFDM) as is currently used in digital television broadcasting, wireless local area networks and ADSL communication.

2.3.1 Fourier Based OFDM

A Fourier based OFDM transmission block is shown in figure 2.12. This figure shows the OFDM system takes in a serial stream of binary data, this data can be in the form of raw binary data or a multi-level binary data stream [10]. This data stream is then input into a baseband constellation mapper such as the BPSK, QPSK or M-QAM schemes. From this process a stream of baseband encoded symbols are produced in the form of complex numbers: $D(k) = A(k) + jB(k)$.

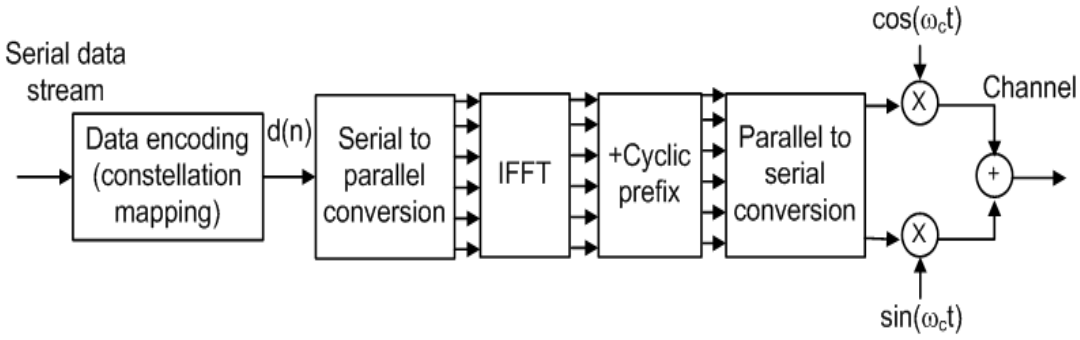

Figure 2.12: FFT-OFDM transmitter block diagram

At this point a serial to parallel conversion takes place on the data stream to convert the data into blocks of N data symbols (where N represents the number of subcarriers used in the OFDM system). These blocks of data are then passed into an Inverse Fourier Transform block, the output of which is shown in equation (2.9) [9], [25].

$$d(n) = \frac{1}{\sqrt{N}} \sum_{k=-N/2}^{k=N/2-1} D(k) e^{j2\pi \frac{k}{N} n} \tag{2.9}$$

where $n \in [-N/2, N/2]$ and N is the number of subcarriers.

The inverse fourier transform was determined to be an ideal transform to use in OFDM transmission as it was able to replicate the transmitting filters described in [7] perfectly without the excess in hardware, this allowed orthogonality of the channels to be achieved in an extremely efficient manner. In [9] it is described how the N analogue filters could be replaced with one inverse discrete Fourier transform. It is stated that by examining the orthogonal analogue filters used to process the OFDM symbols, as described in equation (2.10), it could be seen that the filterbank could be reduced to an inverse Fourier transform with the window function, $u(t)$ ($u(t)$ being a rectangular function as described in equation (2.11)).

$$g_k(t) = u(t) e^{-2j\pi f_k t}, \tag{2.10}$$

where $u(t)$ is the window function, $f_k = f_0 + \frac{k}{NT_s}$ and $0 \leq k \leq N-1$

$$u(t) = \begin{cases} 1/\sqrt{NT_s}, & 0 \leq t \leq NT_s \\ 0, & \text{otherwise} \end{cases} \tag{2.11}$$

While using the rectangular window function for $u(t)$ ensures the necessary orthogonality of the data occurs, it also causes a truncation in the resulting OFDM symbol which gives a $\sin(x)/x$ shape to the overall spectra of the modulated symbol. This symbol truncation has the effect of causing inter-channel

interference (ICI) to occur between transmitted OFDM blocks. This phenomena led to the need to introduce a guard interval to the OFDM symbols to reduce this interference [21]. These guard intervals often take the form of a cyclic prefix appended to the transmitted OFDM symbol blocks in many practical OFDM systems.

To ensure further preservation of orthogonality in the transmitted signal, the N subcarriers being used to modulate $d(n)$ needs to be precisely spaced in the frequency spectra. If the duration of one OFDM symbol being transmitted is T_s seconds then the spacing of the subcarriers needs to be $\frac{1}{T_s}$Hz apart.

Fourier OFDM has been widely accepted in industry and has now become the standard in systems such as terrestrial digital television transmission (DVB-T), ADSL broadband internet and wireless LANs. even so Fourier OFDM does have some drawbacks, these will be discussed in more detail in chapter 3 but briefly they include the previously mentioned cyclic prefix and, most notably, the large peak-to-average power ratio (PAPR) OFDM exhibits.

A large PAPR is an effect caused by the multiplexing of the DFT filtered QAM symbols produced in OFDM. As figure 2.13 shows the OFDM symbol is characterised by having mostly relatively low power peaks but interspersed with the occasional large magnitude power spikes. This gives an overall low average power but a very large peak power which results in needing to use inefficient linear amplifiers in transmission systems to avoid distortion of the signal [26],[27].

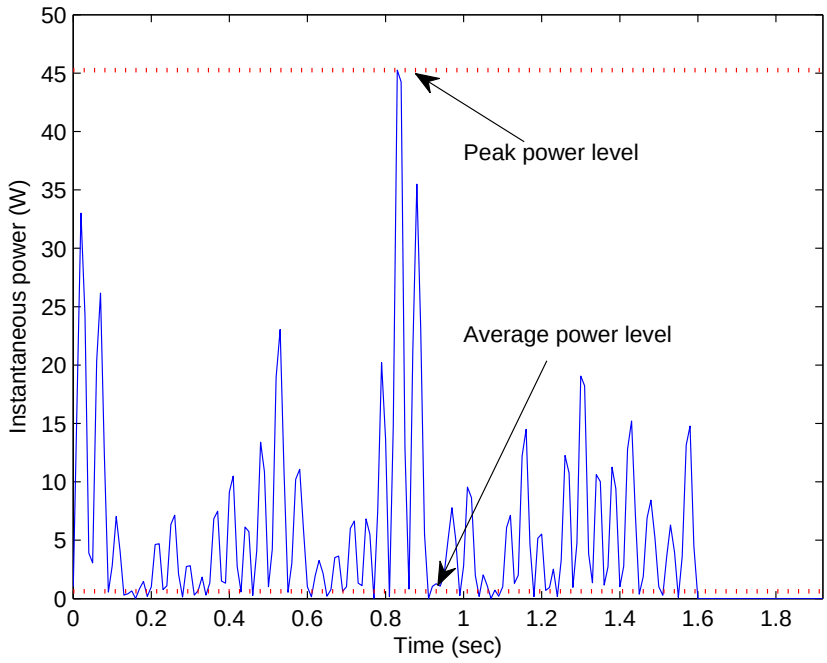

Figure 2.13: Power of an OFDM symbol with 16 carriers showing the large peak-to-average power ratio

This issue has been widely discussed and work has been done to develop methods to reduce the PAPR of OFDM signals including the use of block codes, phase rotation and clipping and filtering the signal [28]. This topic is covered in more detail in section 3.4.1.

2.3.2 Wavelet Based OFDM

Power line communications has been around in a very primitive form since the early 1900s and was used mainly for very basic, low frequency, signalling by electricity companies to control load on their system and to remotely read meters [29], [30]. Works started to appear in the 1970s and 1980s into the

possibility of expanding this communication technique to wider ranges of data and to increase the data rate through the channel. Some of the earlier works into this were published in [31] and [32] where the characteristics of power lines were thoroughly investigated and the types of modulation techniques needed to combat harsh power line channels were considered.

Research into the power line communication (PLC) field considered the types of modulation schemes that would be appropriate to be used in the harsh channel environments of a power line. Since the primary purpose of power lines is to provide electricity to households, and not for communications, they tend to be very noisy and lack the desired shielding to prevent interference from external sources. The basic equipment attached to the power grid such as circuit breakers and capacitor banks as well as household electricity use (i.e turning appliances on and off, using light dimmers, etc) is enough to cause both impulsive as well as coloured noise to effect the channel [30]. Transmission schemes that were robust to these conditions needed to be considered for PLC to be an effective method of data transmission.

One of the earlier work in this specific area was published in [31] where a pseudonoise modulation technique using the 60 Hz zero-crossing of the AC power frequency as synchronisation was proposed. This work considered the tendency for frequency selective fading to occur on power lines and proposed the pseudonoise code PSK modulated with a square wave carrier to help spread the spectrum of a narrowband signal over a large range to mitigate this effect.

Other modulations techniques considered include the basic ASK and FSK digital modulation techniques as well as more complex spread spectrum modulation methods [30]. One other modulation option proposed was OFDM as

it had been a successful technique in wireless communications, proving itself effective in fading channel environments [33], [34]. The Open PLC European Research Alliance (OPERA) is one organisation that has looked at the standardisation of PLCs. In their technology standard DFT-based OFDM is the transmission technique used [35].

As discussed in section 2.3.1 Fourier based OFDM has its drawbacks, it was found to lack good performance in harsh channel environments particularly channels with the characteristics of power lines. It also lacked efficiency by needing guard intervals to prevent ISI, it had large spectral leakage and lacked the ability to reject narrowband interference [36], [37].

A solution to these issues appeared in the form of wavelet OFDM. In [36] and [38] it was noted that in conventional DFT-OFDM transmultiplexing system that the DFT filterbanks with their harsh rectangular symbol filtering gave the data the required orthogonality but also contributed strongly to the ICI and IBI problem that plagues OFDM. [36] and [38] realised that this harsh rectangular filtering effect could in fact be replaced with wavelet filters, wavelets are orthonormal functions which meant filterbanks designed on this principle still possessed the necessary orthogonality properties needed for OFDM transmission but would also increase the spectral efficiency of the signals and allow for the removal of the guard interval / cyclic prefix from the data blocks.

As shown in figure 2.14 wavelet OFDM basically replaces the IDFT / DFT blocks of the conventional OFDM system with wavelet transform blocks (IDWT / DWT), while the cyclic prefix blocks of the OFDM system can also be effectively removed.

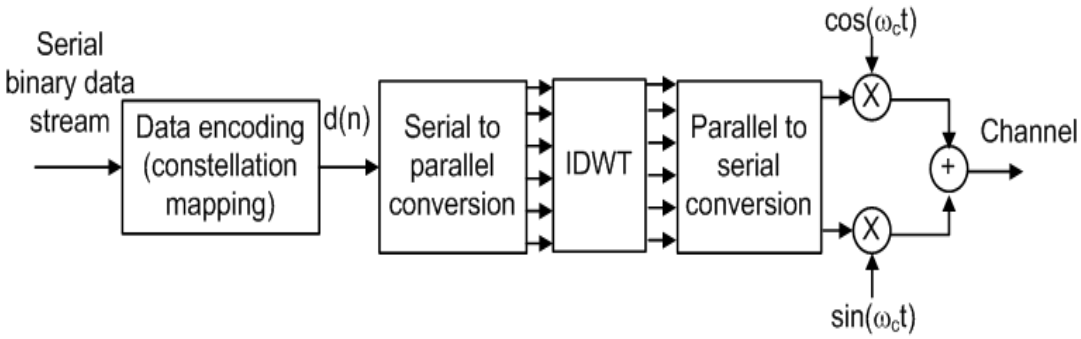

Figure 2.14: Transmit block diagram for a wavelet OFDM transmission system

The discrete wavelet transform block in this type of OFDM system can be considered as behaving in the same manner as a bank of N orthogonal wavelet filter functions [36]. By considering this equivalency the system behaves in the same manner as that shown in figure 2.15 [37], [39].

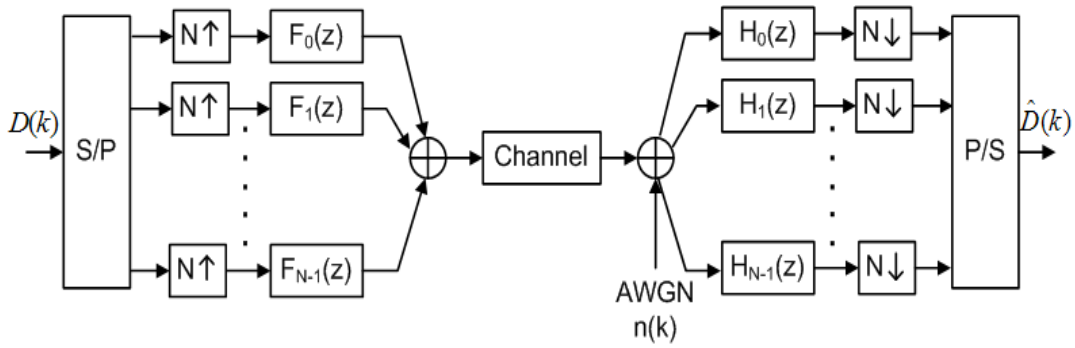

Figure 2.15: Block diagram of a transmultiplexing system

This wavelet-based transmultiplexing system consists of an interpolation (or up-sampling) process where the data is zero-padded before being input into a bank of inverse wavelet synthesis filters, $F_n(z)$, (i.e. IDWT), at the transmitter. The receiver on the other hand consists of a forward wavelet analysis filterbank,

$H_n(z)$, (i.e. DWT), with a downsampling process where the zeros padding the data stream are removed [40]. Equations (2.12) and (2.13) show respectively the general expressions for the synthesis and analysis filterbanks.

$$F_n(z) = \sum_{k=0}^{L-1} f_n(k) z^{-k}, \;\; 0 \leq n < N \tag{2.12}$$

$$H_n(z) = \sum_{k=0}^{L-1} h_n(k) z^{-k}, \;\; 0 \leq n < N \tag{2.13}$$

where N is the number of subchannels and L is the length of each filter.

For wavelet-based OFDM these synthesis and analysis filterbanks are obtained from an appropriate wavelet basis function. These wavelet-based filters then effectively replace the inverse DFT at the transmitter and the DFT at the receiver in DFT-based OFDM giving the output at the transmitter of [38], [41]:

$$d(n) = \sum_{a=0}^{\infty} \sum_{b=0}^{\infty} D(k) 2^{a/2} \psi(2^a k - b) \tag{2.14}$$

where a is the scaling factor, b is the shift factor, $\psi(n)$ is the wavelet basis function and $D(k)$ is the data for the k^{th} sub-carrier, $0 \leq k \leq N-1$, where N is the total number of OFDM subcarriers.

These wavelet filters are of larger length than the rectangular DFT filters used in standard OFDM and because of this the resulting sidelobes of the OFDM symbols are smaller, reducing inter-channel and narrow-band interferences in the transmitted symbol [37], [33].

Comparative studies on DFT-OFDM and wavelet-OFDM have shown that wavelet-based OFDM has greater spectral containment from the pulse shaping

attributes the wavelet transform imposes on the data and that wavelet based OFDM systems are more efficient due to the removal of the guard interval [37], [38].

2.3.3 Wavelet Packet OFDM

A variant on wavelet-based OFDM is the wavelet packet OFDM technique. This technique is very similar to wavelet OFDM but utilises the discrete wavelet packet transform in the OFDM modulation block described in section 2.3.2.

The main difference between the wavelet-based OFDM and the wavelet packet-based OFDM is the way the synthesis and analysis filters in the trans-multiplexer process the incoming data. In a wavelet-based analysis filter the data is filtered to produce a decomposition of the incoming signal consisting of a low-pass signal of low resolution and a number of high-pass signals containing the detail information of the data(the number of these high-pass signals depends on the level of decomposition used) of varying resolutions [42]. Figure 2.16 shows this for a three level decomposition.

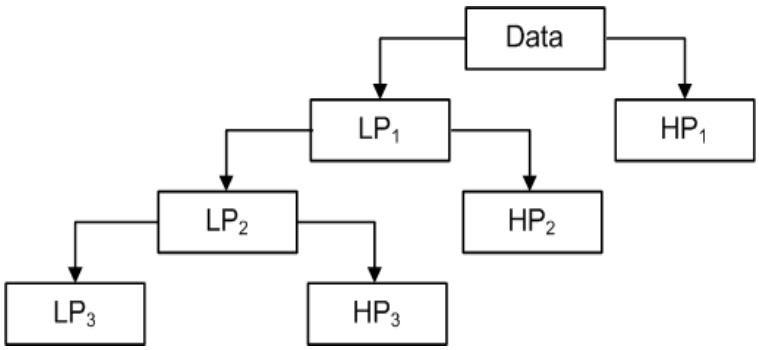

Figure 2.16: A 3-level wavelet decomposition

This figure shows the decomposition performed on the data produces both low-pass coefficients, produced from downsampling and filtering the data using a wavelet low-pass filter, and high-pass coefficients, produced from downsampling and filtering the data with a wavelet high-pass filter. From the initial decomposition each subsequent level of decomposition is then only applied to the previous low-pass coefficients while the high-pass coefficients are left unaltered.

After the desired number of levels have been reached in the decomposition the resulting signal consists of grouping together the final low-pass coefficients with all the high-pass coefficients calculated for the previous levels. The result of this is that for a J-level decomposition there will be $J+1$ blocks of coefficients of increasing resolutions, the ultimate length of the coefficients will also be the same length as the original data. This is shown in figure 2.17.

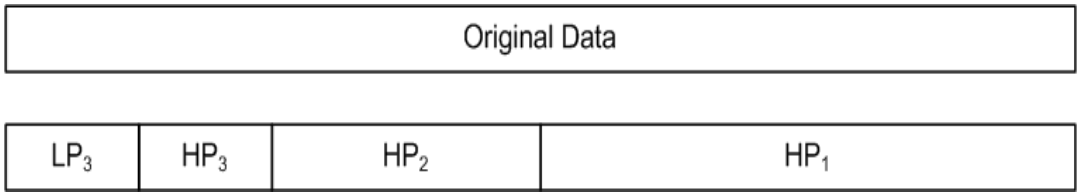

Figure 2.17: Length of original data (top) compared to the length of the wavelet decomposed coefficients for $J = 3$ (bottom)

The filters in a wavelet packet decomposition on the other hand applies the wavelet filtering to both high- and low-pass coefficients. The decomposition tree for this type of wavelet transform is shown in figure 2.18.

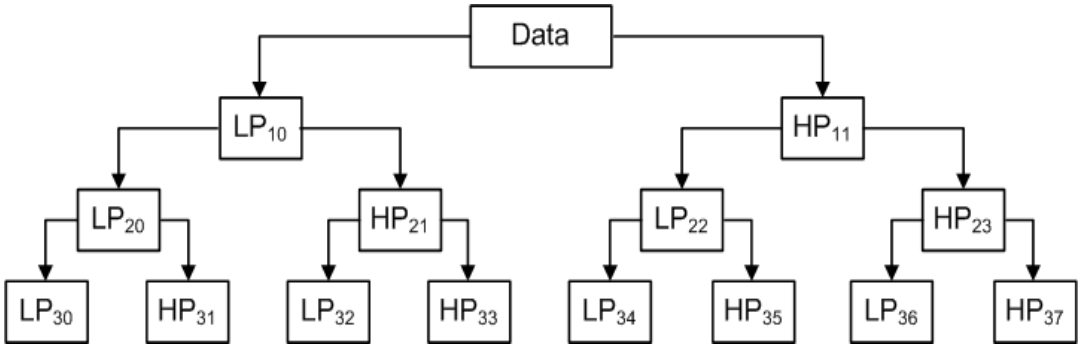

Figure 2.18: A 3-level wavelet packet decomposition

This type of wavelet decomposition results in 2^J blocks of coefficients, each of the same length. Again the length of the total resulting coefficients will equal the length of the original data as shown in figure 2.19.

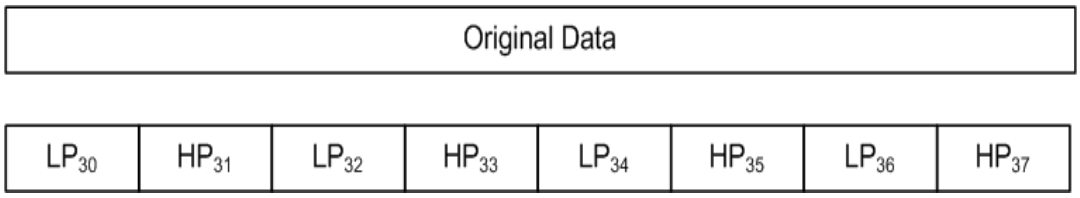

Figure 2.19: Length of original data (top) compared to the length of the wavelet packet decomposed coefficients for $J = 3$ (bottom)

By replacing the synthesis and analysis filters in the traditional OFDM system shown in figure 2.15 with this wavelet packet transform, the wavelet packet-based OFDM system is produced. Similar to the output of the wavelet OFDM system the transmitted data is given by equation (2.15) [45].

$$d[k] = \sum_{s} \sum_{n=0}^{N-1} D_{s,n} \psi_n[k - sN] \tag{2.15}$$

where $D_{s,n}$ is the s-th encoded data symbol modulating the n-th subcarrier and $\psi_n[k]$ is the wavelet packet filtering operation given as:

$$\psi_{j,2n}[k] = F_{low}[k] * \psi_{j-1,n}[k/2] \tag{2.16}$$

$$\psi_{j,2n+1}[k] = F_{high}[k] * \psi_{j-1,n}[k/2] \tag{2.17}$$

where j is the iteration number of the wavelet decomposition resolution, $1 \leq j \leq J$ and $F_{low}[k]$ and $F_{high}[k]$ are the low-pass and high-pass wavelet packet synthesis filters respectively. These equations also assume that the data is being upsampled by two as shown by the term $\psi_{j,n}[k/2]$.

As with wavelet OFDM the length of these wavelet packet filters are longer than the DFT filters, this allows the spectral leakage of the resulting signal to be reduced, allowing for the removal of the cyclic prefix extension.

2.4 Data Compression

In data storage systems, data compression is the concept of taking large amounts of information and reducing its size by removing redundancies within that information hence enabling more data to be stored in less space [46]. In the ideal world data compression would reduce the size of the information so it can be efficiently stored but not alter the semantic content or quality of the information, this is called lossless compression. In practice though lossless compression is not always achievable so a loss of data is always a possibility when applying compression to data.

In the world of data transmission, compression is also a critical element of

the transmission system. In any form of data transmission the more data you need to transmit the longer the process is going to take and in today's world with e-mail effectively replacing the "snail mail" postal service and instant messages being part of every facet of society, instantaneous is what people want.

With that in mind, research into data compression is never-ending with techniques developing from the earliest and simplest methods of compression such as run-length encoding, (which is often used in image compression where a run of repeated symbols in a stream of data is replaced by a single symbol representative of the length of the run) [47] all the way to more complex compression schemes such as linear predictive algorithms often used video compression (e.g. MPEG encoded video).

For multimedia data several compression schemes can be applied before transmission occurs, these compression schemes are often dependent on the data type being transmitted and often a scheme which works well for one data type may not work well for another data type. The following gives some examples of data compression schemes often used in multimedia data transmission.

MPEG is one commonly used encoding and compression scheme aimed at video streaming, it is based on a type of linear predictive coding which works by encoding the predicted motion of objects in a video into frames, these prediction frames are called P-frames and B-frames in an MPEG stream. P-frames contain predictions of expected locations of moving objects by using previous reference frames to make a prediction while B-frames use a bi-directional predictive algorithm to predict the motion from previous as well as future frames. These predictive frames are used in conjunction with reference frames known as I-frames to reduce redundancy in the data. These I-frames are refreshed pe-

riodically and act as a reference for the decoder's predictive algorithm. These frames are of higher quality (hence lower compression) than the P- and B-frames [11].

For the transmission of image data, compression can be achieved by using cosine and wavelet transforms to alter the data, JPEG and JPEG2000 are two well known methods which utilise these transforms for compression. The remainder of this section is dedicated to these transforms and the way they can be used to compress data in preparation for transmission.

2.4.1 Discrete Cosine Transform

The DCT proposed in [48] is most commonly known for its use in the JPEG (Joint Photographic Experts Group) still image compression standard [49]. In this type of compression an image is segmented into 8×8 pixel segments and a 2-dimensional DCT is applied independently to each of these segments.

The discrete cosine transform (DCT) is a transform used in signal analysis which can be used to give information about the frequency content of a signal. The DCT uses a cosine basis function to decompose a signal into a finite sum of weighted cosines. The transform pair equations for a 1-dimensional discrete cosine decomposition and recomposition of a signal, $x(n)$, is given in equations (2.18) and (2.19) respectively [48].

$$\begin{aligned} X(0) &= \frac{\sqrt{2}}{N} \sum_{n=0}^{N-1} x(n) \\ X(k) &= \frac{2}{N} \sum_{n=0}^{N-1} x(n) \cos \frac{\pi k(2n+1)}{2N}, \;\; k = 1, 2..., (N-1) \end{aligned} \tag{2.18}$$

$$x(n) = \frac{1}{\sqrt{2}}X(0) + \sum_{k=1}^{N-1} X(k) \cos \frac{\pi k(2n+1)}{2N} \tag{2.19}$$

The 2-D DCT is similar to this method but instead of applying the transform in one dimension it is applied twice; once in the horizontal direction and once in the vertical direction and then multiplying the resulting terms together. Mathematically this operation is shown in equation (2.20) using x and y for horizontal and vertical space respectively and u and v for horizontal and vertical frequency respectively [50]

$$S(v,u) = \frac{C(v)}{2}\frac{C(u)}{2} \sum_{y=0}^{7}\sum_{x=0}^{7} s(y,x) \cos[\frac{(2x+1)u\pi}{16}] \cos[\frac{(2y+1)v\pi}{16}] \tag{2.20}$$

where u=0,1,2,...,7, v=0,1,2,...,7, $C(u) = \frac{1}{\sqrt{2}}$ for u=0, $C(u) = 1$ for u>0, $C(v) = \frac{1}{\sqrt{2}}$ for v=0, $C(v) = 1$ for v>0, $s(y,x)$ is a 2-D sample value and $S(v,u)$ are the 2-D DCT coefficients.

Using this DCT algorithm in the JPEG compression standard in effect calculates a correlation value between an 8×8 pixel segment of an image and a set of 2-D cosine basis functions representing different spatial frequencies. These basis functions are given in figure 2.20 and show cosine basis functions of increasing spatial frequency in horizonal space (from left to right of the figure) as well as increasing frequency in vertical space (from top to bottom of the figure).

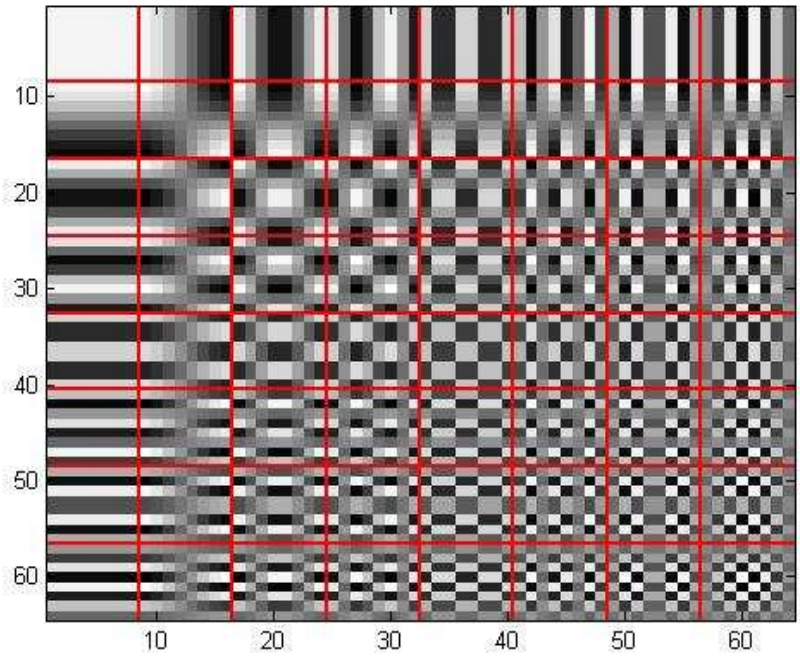

Figure 2.20: Basis functions for a 2-D DCT decomposition

The benefits of using the DCT to extract coefficients from an image is that the DCT tends to concentrate most of its energy in very few coefficients, giving a sparse distribution of coefficients compared to the original data [46], [51]. The DCT also produces larger coefficient values for regions of an image with high spatial frequencies (or low correlation between neighbouring pixels) [46]. These effects can be seen in figure 2.21 where it can be seen the largest coefficient values are concentrated in the upper left hand corners of the 8×8 coefficient maps and that there are larger coefficient values in regions of the image where there is higher spatial frequencies.

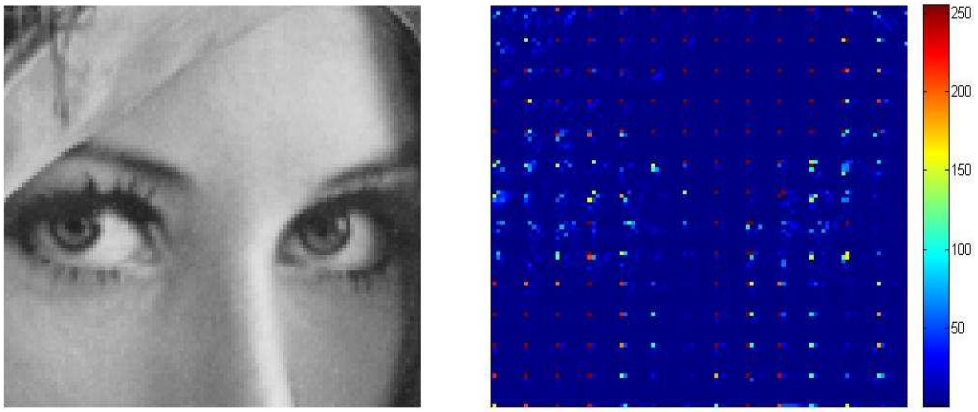

Figure 2.21: Segment of Lena image and its corresponding DCT coefficient map

All these factors make the DCT an ideal transform from a compression point of view as now encoding can be applied to the image to remove redundant information such as the long runs of zero coefficients in the resulting coefficient map.

JPEG compression utilises quantisation tables to weight each coefficient before applying run-length encoding and then entropy encoding [50]. All of this allows for variable compression rates and quality in JPEG images as shown in figure 2.22.

Figure 2.22: Lena JPEG image with increasing compression ratios

2.4.2 Discrete Wavelet Transform

The wavelet transform, as used in signal processing, was pioneered in the works of Ingrid Daubechies [52], [53], [54] and Stephane Mallet [55]. As with the Fourier transform the wavelet transform proved to be an important analysis tool in signal processing with its ability to extract time-frequency information about a signal.

The theory behind the wavelet transform is that any signal/waveform can be represented by a series of wavelet basis functions with varying translations and dilations. This is known as the continuous wavelet transform (CWT) and

can be defined as [56], [57]:

$$CWT_f^{\psi}(a,b) = \frac{1}{\sqrt{a}} \int_{\mathbf{R}} \psi^*(\frac{t-b}{a}) f(t) dt \tag{2.21}$$

where a is the dilation factor ($a \in \mathbf{R}^+$) and b is the translation factor ($b \in \mathbf{R}$).

For the analysis of digital signals and in particularly the coding of images, the discrete wavelet transform (DWT) was found to be an appropriate tool. The DWT took the equation in (2.21) and converted it into discrete time where wavelet and scaling coefficients can be extracted from a digital signal [58]. Equations (2.22) and (2.23) show this discrete time wavelet transform.

$$DWT_x(j,k) = c_{j,k} = \sum_n x[n] h_j^*[n - 2^j k] \tag{2.22}$$

$$b_{j,k} = \sum_n x[n] g_J^*[n - 2^J k] \tag{2.23}$$

where J is the desired resolution of the decomposition, $j = 1, 2, ..., J$; k is the discrete time shift; $h_j[n - 2^j]$ is the discrete wavelet function; $g_J[n - 2^J]$ is the scaling sequence; $c_{j,k}$ are the wavelet coefficients, and $b_{j,k}$ are the scaling coefficients.

The use of the wavelet transform in audio applications was first proposed in [59] where a 1-dimensional DWT was used to filter sounds (the sounds used in this work included samples of speech and clarinet notes). The focus of this work was on aiding in the composition of synthesised music since, while the sound was decomposed, it could be processed and modified to cause interesting effects to occur when the sound is reconstructed. In works in [60] and [61] the wavelet transform was extended to include the compression of speech.

Works in [62] and [63] introduced the concept of using the DWT in the coding of images. The attraction to using the discrete wavelet transforms in both image processing and in audio processing is the DWT's ability to concentrate its energy into several subbands. In speech and audio processing this is useful since voiced and un-voiced speech can be detected as well as the pitch of audio [64]. Similarly in image processing the subband decomposition can be utilised in pattern recognition and in compression applications.

The most common wavelet subband decomposition of an image is shown in figure 2.23 and shows a low resolution version of the original image in the upper left hand corner with increasing resolution coefficients towards the lower right hand corner. These subbands are classified as low and high pass and consist of the low pass approximation and vertical detail coefficients (LL and LH coefficients) and the high pass horizontal and diagonal detail coefficients (HH and HL coefficients) [46].

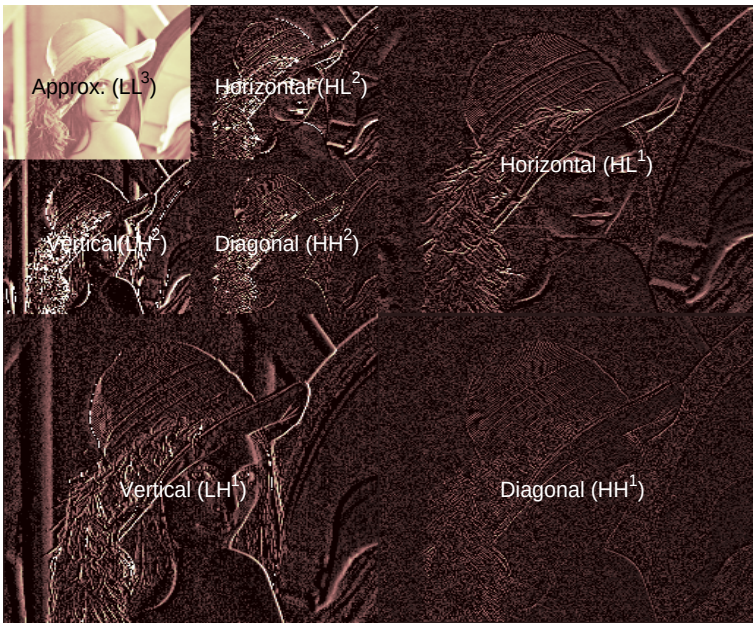

Figure 2.23: A three level wavelet decomposition of the Lena image

Two common techniques can be applied to the resulting wavelet decomposition of images to achieve compression. Since the energy of the decomposition is concentrated in certain regions of the decomposition, thresholding can be applied to compress the data. In this method all values below a certain threshold are set to zero so run-length and entropy encoding algorithms can be applied to compress the data (similar to what occurs in JPEG compression explained in section 2.4.1) [46].

The second method is subband filtering. Subband filtering relies on the theory that the human eye is most sensitive to low spatial frequencies. Since the wavelet decomposition is made up of high and low frequency subbands the-

oretically entire subbands can be removed (or coarsely quantised) to achieve compression. Applying this method and then reconstructing the image theoretically causes little impact on the perceived quality of an image since only high frequency subbands are affected [46].

2.5 Wireless Channel Modelling

Wireless communication channels are particularly complex structures to model and work with. To accurately assess the viability of any new transmission method for wireless channels it is necessary to be able to accurately model this type of environment. It is therefore essential that accurate mathematical models of wireless channels be used in simulations to achieve the best possible sense of the viability of any proposed system.

Some of the main complications in modelling wireless communication channels are the many environmental factors that constantly impact on the quality of the channel at any given point in time. These include obstacles such as buildings, trees and geological structures in the path between the transmitter and receiver, transmitter/receiver movement such as mobile phones being used in a vehicle and interference due to constantly changing atmospheric conditions.

The following section will cover some of the main features of wireless communication channels and some of the mathematical models used to simulate these conditions in experiments.

2.5.1 Multipath Channels

One of the most common problems in wireless communication channels is multipath effects on a signal. In an ideal world electromagnetic waves would be sent from a transmitter in a spherical pattern outwards towards the receiver. At the receiver the same signal would be received, with slight propagation loss and delay but otherwise unchanged. In reality though, most wireless channels will contain a number of obstacles between a transmitter and a receiver which will scatter the transmitted signal and cause multipath delays and superposition effects to the received signal [65]. An example of this is shown in figure 2.24, the scatterers in this case could be buildings, trees, hills or any other geological or man made object standing between a transmitter and receiver.

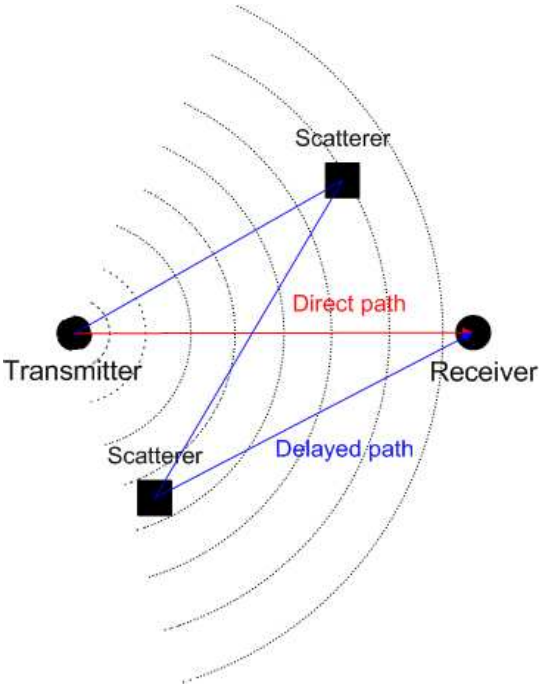

Figure 2.24: An example of a two-path multipath channel environment

Mathematically the result of this effect in a multipath channel is an impulse response as shown in equation (2.24) [65], [66].

$$h_0(t) = \sum_{n=1}^{m_p} H_n \delta(t - \tau_n) \tag{2.24}$$

where m_p is the total number of multipaths, H_n is the attenuation factor and τ_n is the delay factor for the n^{th} multipath. Something to note is that H_n is not a constant value, the attenuation values change randomly over time making it impossible to accurately predict the response of the channel.

In OFDM systems, this type of channel distortion can cause severe inter-block interference (IBI) where the delays to the previous OFDM block, caused by the multipaths, interfere with the current OFDM block being received [67]. To combat this type of channel distortion OFDM uses a guard interval in the form of a cyclic prefix to mitigate the effects of multipath interference. A more in-depth analysis of the cyclic prefix and its use in combatting IBI and ICI is in section 3.4.2.

2.5.2 Doppler Spread

The doppler effect is a type of signal distortion caused by motion affecting the perceived frequency of a received signal. The most common cause of this is if either the signal transmitter or the receiver is in motion. An obvious example of this is in the case of mobile telephones where a person could be speaking on the telephone while travelling in a moving car or train [68]. Figure 2.25 shows what happens to a signal when this occurs.

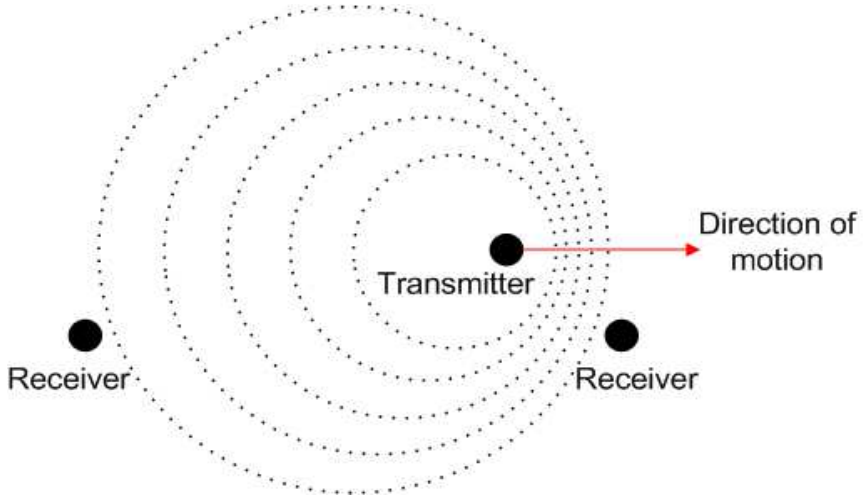

Figure 2.25: An example of the Doppler effect

The doppler effect can be explained in the following way: if an object transmitting a signal is in motion, any receiver located behind the motion of the transmitter (such as the receiver on the left of figure 2.25) is going to perceive that signal at a lower frequency than a receiver located in front of the same transmitter (on the right of figure 2.25). This same concept occurs at audio frequency as well as RF and gives rise to the effect of hearing an ambulance or police siren at a higher or lower pitch as the vehicle passes by on the road. This relationship also applies when a receiver, as opposed to the transmitter, is is motion. This relationship can be mathematically given by equation (2.25) [69].

$$f_d = f_c v/c \tag{2.25}$$

where v is the velocity of the moving receiver, c is the speed of signal propagation, f_d is the perceived carrier frequency and f_c is the actual carrier frequency.

It is clear that doppler spread is an undesirable distortion if a communica-

tion system is relying on knowledge of a signal's transmit carrier frequency to accurately receive data. It is for this reason that a large amount of research has been conducted on estimating the doppler frequency spread in communication systems.

A common method of estimating the doppler spread of communication channels is using the auto-correlation of the channel. A relatively simple algorithm using this approach to estimate the doppler spread is given in [69]. This work considers the digital television broadcasting standard which consists of transmitting OFDM symbols with pseudo-random sequences appended as a guard interval prefix to each symbol. It was stated that the received data is given as [68], [69]:

$$r(k) = s(k)h(k) + w(k) \tag{2.26}$$

where $s(k)$ is the data block, $h(k)$ is the channel which is a complex Gaussian process with an auto-correlation function dependent on the doppler spread and $w(k)$ is complex AWGN with zero mean. In [69] it is assumed that the channel exhibits the same behaviour as the Jakes channel model and would have the spectral characteristics, $S(f)$, of:

$$S(f) = \begin{cases} \frac{P}{\pi f_d \sqrt{1-(f/f_d)^2}}, & |f| < f_d \\ 0, & \text{otherwise} \end{cases} \tag{2.27}$$

where P is the average power of all received signals. From this the auto-correlation function (ρ_{h_k}) of the channel is given by:

$$\rho_{h_k}(\tau) = J_0(2\pi f_d \tau) \tag{2.28}$$

where $J_0(\tau)$ is the 0^{th} order Bessel function. Rearranging this equation gives the estimate of the doppler spread as:

$$f_d = J_0^{-1}(\rho(\tau)) \tag{2.29}$$

Since a pseudo-random sequence known to both the transmitter and receiver is used as an OFDM symbol prefix for each OFDM block, a reasonable channel estimate is available to the transmitter and receiver. Therefore the doppler spread can be reasonably estimated by using the process in equations (2.27) to (2.29).

Other methods based on the channel auto-correlation have also been proposed, some of which can be found in [68] and [70].

2.5.3 Selective Fading Channels

Selective fading in communication channels can be viewed as an extension to the effects discussed in sections 2.5.1 and 2.5.2. Wireless channels are frequency, spatially and time selective. Frequency selectivity occurs when the response of a channel varies for different frequencies being transmitted, spatial selectivity occurs when the channel response changes depending on the distance between the transmitter and receiver and time selectivity is caused by motion of the transmitter or receiver giving a different channel response over time [65].

These fading effects can all be caused by combinations of multi-path scattering and doppler spread and many models have been created to model these

types of channels. The following subsections cover a few fading channel models used in transmitter systems.

Rayleigh Fading Model

The Rayleigh fading channel is a statistical model for a time-variant multipath channel. The Rayleigh fading model assumes there is no dominant signal component being received therefore the channel response can be modelled using a Rayleigh statistical distribution [71]. This definition implies that the received signal from a Rayleigh fading channel is due wholly to randomly scattered components and can therefore be modelled using a 2-dimensional, random, Gaussian process with zero-mean. If there did happen to be a dominant signal component being received (i.e. from line-of-sight or signal reflectors), the channel response would no longer follow the Rayleigh distribution making it more appropriate to model the channel using the Rician statistical model instead [71].

Mathematically Rayleigh fading is an extension to equation (2.24) and defines a much stricter rule for what the attenuation factor, H_n should be. As its name suggests this attenuation factor follows the Rayleigh distribution criteria. This criteria states that a Rayleigh distribution consists of two zero-mean, statistically independent random variables, X_1 and X_2 each with a Gaussian PDF as shown in equation (2.30) [71], [72].

$$p(y) = \frac{1}{2\sigma^2} e^{-y/2\sigma^2} \tag{2.30}$$

where σ^2 is the variance of the Gaussian random variables and x relates to the Gaussian random processes $X_1(t)$ and $X_2(t)$.

By defining the random variable R as:

$$R = \sqrt{X_1^2 + X_2^2} = \sqrt{Y} \tag{2.31}$$

And substituting this into equation (2.30), the Rayleigh probability density function can be defined as:

$$p(r) = \frac{r}{\sigma^2} e^{-r^2/2\sigma^2} \tag{2.32}$$

Using this statistical knowledge of the Rayleigh distribution of fades a more accurate definition of the time-variant attenuation factor, H_n in equation (2.24) can be defined as follows [71]:

$$H_n(\tau; t) = \alpha(\tau; t) e^{-j2\pi f_c \tau} \tag{2.33}$$

where $H_n(\tau; t)$ is the channel impulse response at delay time τ and time instant t, $\alpha(\tau; t)$ is the attenuation factor also at delay time τ and time instant t and f_c is the carrier frequency.

Figure 2.26 shows what can occur to a sinusoidal signal when it is passed through a multipath Rayleigh fading channel, it can be seen that the multipath effects cause constructive and destructive superposition to occur to the signal.

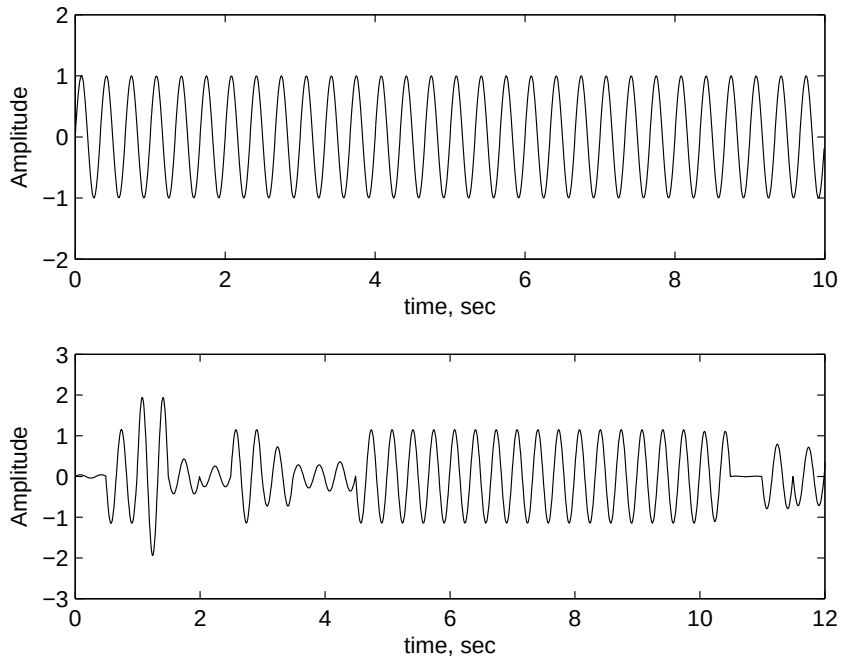

Figure 2.26: A signal (top) and received signal (bottom) after transmission through a Multipath Rayleigh fading channel

Rician Fading Model

The Rician fading model is similar to the Rayleigh model but instead of the fading envelope following a Rayleigh distribution it follows a Rician distribution instead. This distribution assumes there is a dominant component to the received signal which could be attributed to line-of-site to the transmitter, fixed scatterers and/or reflectors in the channel medium [71].

The main difference between the Rayleigh distribution and the Rician distribution is the means of the two Gaussian random processes, in the Rayleigh model the mean of X_1 and X_2 are both zero while the Rician model has a com-

mon variance but differing means for X_1 and X_2. By following the same process as in section 2.5.3 the PDF for a Rician distribution is given as [71]:

$$p(r) = \frac{r}{\sigma^2} e^{(-r^2+s^2)/2\sigma^2} J_0(\frac{r.s}{\sigma^2}), \quad r \geq 0 \tag{2.34}$$

where s^2 is the non-centrality parameter due to the unequal mean values of X_1 and X_2 and is defined as $s^2 = m_1^2 + m_2^2$ and J_0 is the zero-th order bessel function of the first kind.

From this statistical knowledge of the channel, equation 2.24 can be re-written as:

$$h_0(\tau; t) = \alpha\delta(t) + \sum_{n=1}^{m_p} H_n \delta(t - \tau_n) \tag{2.35}$$

where $\alpha\delta(t)$ represents the line-of-sight component of the received signal with attenuation α while $H_n\delta(t-\tau_n)$ represents the multipath scattered components with the time-variant Rayleigh distributed attenuation H_n.

2.6 Conclusions

In this chapter a summary has been presented of digital modulation, parallel transmultiplexers, data compression and channel modelling techniques. The development of digital transmission technology has been outlined from the earliest digital modulation techniques based on early analogue methods such as FSK, PSK and ASK through to the orthogonal transmultiplexing schemes used in wireless communications, digital television broadcasting and powerline communications.

This chapter also presented methods of data compression looking particularly at the compression of multimedia data including images, video and audio to improve transmission efficiency. The DCT and DWT were both presented as useful transforms for compression schemes.

Channel modelling was finally discussed and the importance of accurate channel models was emphasised. Not taking into account the charcteristics of a realistic channel can be highly detrimental when attempting to develop new and effective transmission techniques. A technique that has only been tested in an ideal environment under certain circumstances is sure to fail when tested in the complex environment of a real channel. Therefore any experiment that is performed needs to consider what can happen under non-ideal channel conditions before accurate conclusions can be formed about a certain technique.

Chapter 3

Orthogonal Frequency Division Multiplexing Systems

3.1 Introduction

Orthogonal Frequency Division Multiplexing has become one of the transmission standards in many wireless applications. Digital television broadcasting as well as wireless internet and ADSL are some of the applications utilising the DFT-based OFDM transmission schemes while standards are also being developed for the use of DFT and/or wavelet-based OFDM in possible power line communication systems.

In the previous chapter the development of orthogonal data transmission systems were discussed and a brief analysis of the three main OFDM systems, DFT-based, wavelet-based and wavelet packet-based OFDM, was presented. In this chapter practical OFDM transmission systems utilising these techniques will be covered in more detail with emphasis on the technical information from

many of the common standards currently being employed. The systems presented in this chapter include the European digital video broadcasting (DVB-T) standard, the European digital radio standard (DAB), the IEEE 802.11a wireless LAN standard and finally the relatively new IEEE standard being developed for powerline communications.

Finally in this chapter the common problems associated with OFDM transmission will be discussed. These include the common high peak-to-average power ratio multicarrier systems tend to suffer from as well as the inter-symbol and inter-channel interference problems DFT-OFDM has. This section will also look at the methods being utilised to try and mitigate these effects.

3.2 DFT-OFDM Transmission Systems

DFT-based OFDM is the most commonly used OFDM scheme for wireless transmission, this type of scheme was first proposed in 1966 in [7] where complex orthogonal filterbanks were used in the synthesis and analysis phases of the system. This system was further developed in 1971 in [21] where a DFT operation was first proposed to simplify the complexity of the system and make it more practical as a wireless transmission scheme.

Currently this technology is being employed in digital television and radio broadcasting, wireless LANs and ADSL systems. The following sections will cover this type of OFDM transmission, the practical systems employing this method and the standards for these systems explaining how OFDM is utilised.

3.2.1 Digital Video Broadcasting-Terrestrial (DVB-T)

From the European standard for digital terrestrial television broadcasting [24] a typical block diagram of the system is shown in figure 3.1

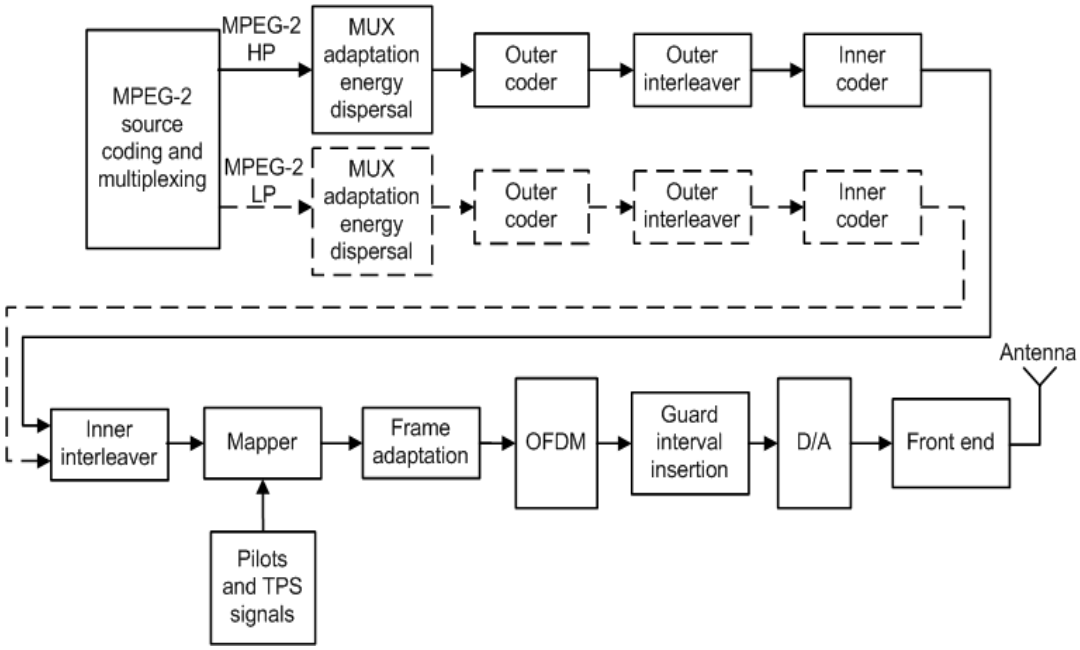

Figure 3.1: Block diagram of the European digital video broadcasting transmitter system

In digital television broadcasting the raw audio and video data stream is encoded using the MPEG-2 encoding method where compression of the data takes place before the transmit block. The DVB-T standard states that the MPEG-2 data should be organised into packets of 188 bytes in length before being scrambled, encoded using the Reed-Solomon encoding algorithm, convolutionally encoded and sent on to the transmitter stage.

The specifications for the transmitter stage of the DVB-T system depends on whether the standard being employed is the 2K or the 8K transmit modes.

DVB-T can consist of either of these methods depending on the network size and defines the number of subcarriers and the spacing between the subcarriers used for transmission.

The interleaving block of the DVB-T system consists of two types of interleaving, a bit-wise interleaver and a symbol-wise interleaver. The bit-wise interleaver groups bits into appropriate length segments for baseband modulation mapping while the symbol wise interleaver takes the mapped symbols and interleaves them into parallel blocks for the IDFT process. The baseband modulation mapping of a DVB-T system can be either QPSK, 16-QAM or 64-QAM, therefore the bit-wise interleaving will either arrange the bits into groups of 2 (for QPSK), 4 (for 16-QAM) or 6 (for 64-QAM).

The symbol-wise interleaving then converts this data to a parallel stream of $N - N_c$ symbols per block, where N in this case is the number of subcarriers used to modulate the OFDM block and N_c is the guard interval/cyclic prefix length. in the 2K DVB-T case this value is equal to interleaving the symbols into 1512 parallel streams and in the 8K case it is 6048 parallel streams.

These parallel streams are then processed using a IDFT operation to create the OFDM symbols to be transmitted. Table 3.1 shows the standards from [24] for the OFDM symbol transmission parameters for both the 2K and 8K DVB-T modes.

As with all DFT-based OFDM systems a guard interval is necessary to avoid ICI and ISI in multi-path fading channels, the DVB-T standard defines a guard interval consisting of a cyclic extension made up of some of the useful data from the end of the OFDM block appended to the start of the OFDM block. The standard states that the cyclic extension should be 1/4, 1/8, 1/16 or 1/32 of

Table 3.1: OFDM transmission parameters for DVB-T.

Parameter	**2K**	**8K**
Number of carriers (N)	1705	6817
OFDM symbol duration T_U (prior to cyclic extension)	$224\mu s$	$896\mu s$
Carrier spacing ($1/T_U$)	4464 Hz	1116 Hz
Spacing between max and min carriers ($(N-1)/T_U$)	7.61 MHz	7.61 MHz

the length of the overall OFDM symbol duration.

The DVB-T standard is designed to operate on the UHF frequency band with 6, 7 and 8 MHz channels.

3.2.2 Digital Audio Broadcasting (DAB)

Another common application that utilises OFDM for the transmission of information is the European Digital Audio Broadcasting (DAB) standard (digital radio) [73]. Digital radio, as with digital television, is being seen as an eventual replacement for the old analogue AM and FM radio transmission technology. The block diagram for the DAB system is shown in figure 3.2.

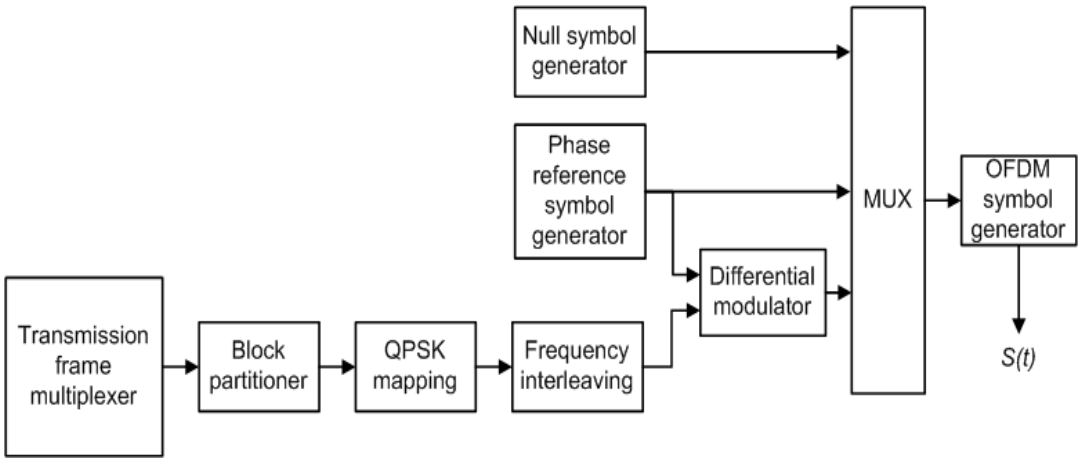

Figure 3.2: Block diagram of the European digital audio broadcasting transmitter system

The ETSI standard [73] for digital radio takes a stream of PCM encoded audio data sampled at a rate of 24 or 48 kHz and uses the MPEG audio coding layer II to encode this data. This data is then arranged into data packets containing information about the type of data being transmitted, dynamic labels, the actual data as well as service flags. At this point the data is then convolutionally encoded, scrambled and interleaved before being passed to the OFDM transmission block.

The input of the OFDM block in this diagram consists of: the data which has been baseband modulation mapped using differential-QPSK (D-QPSK) modulation, the null symbol generator - this block makes sure the first OFDM symbol is zero and lastly the phase reference symbol generator - this acts as a reference for the differential modulation block.

This multiplexed data is then processed using the IDFT operation to create the OFDM symbols to be transmitted. The DAB standard consists of four

different transmission modes each used for different purposes. Each of these modes have different parameters for the OFDM transmission which are shown in table 3.2 [73].

Table 3.2: OFDM transmission parameters for DAB.

Parameter	**Mode I**	**Mode II**	**Mode III**	**Mode IV**
Number of carriers (N)	1536	384	192	768
OFDM symbol duration T_U (prior to cyclic extension)	$1246ms$	$312\mu s$	$156\mu s$	$623\mu s$
Carrier spacing ($1/T_U$)	1000 Hz	4000 Hz	8000 Hz	2000 Hz

The four different modes DAB can operate in are: mode I - used for single frequency networks and local-area broadcasting in bands I, II and III, modes II and IV - which are used for local broadcasting in bands I - V as well as satellite and hybrid satellite terrestrial broadcasting in the L-band and, lastly, mode III - which is also intended for local broadcasting, satellite and hybrid satellite broadcasting as well as cable distribution in frequency bands below $3,000$ MHz [73].

This DAB standard can be implemented by either using the frequency bands currently assigned to analogue AM and FM radio or by using a new bandwidth region, in many countries implementing DAB these new bandwidths are what is being used for their digital radio broadcasts. In the USA, however, this has been problematic since this new bandwidth region falls within a restricted RF region primarily used by the US military. The US also had problems using the current AM and FM bands since the analogue and digital radio signals cannot co-exist together in the same band when using the DAB standard. Due to these issues the US utilise an in-band on-channel (IBOC) system to allow both analogue and

digital radio signals to co-exist on the same bands to reduce analogue/digital receiver compatibility issues [74], [75].

3.2.3 Wireless LAN (IEEE 802.11a standard)

From the IEEE wireless LAN specifications standard [76] a typical block diagram of the system is shown in figure 3.3

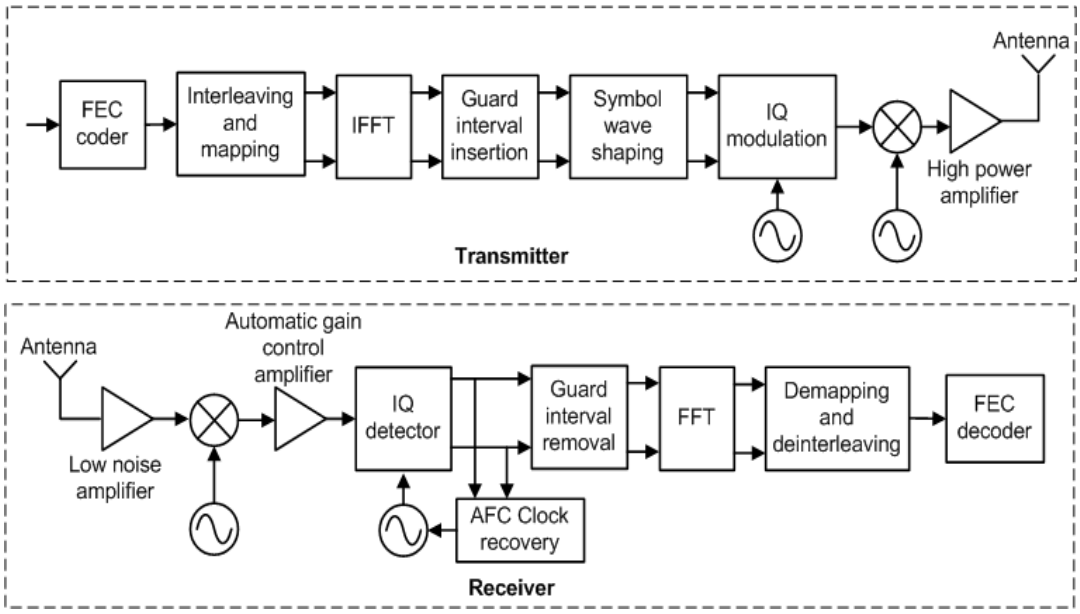

Figure 3.3: Block diagram of the IEEE 802.11a transmit and receive system

The 802.11a Wireless LAN standard firstly scrambles the data and encodes it using a $K = 7$ convolutional code (FEC block) before the data is interleaved and mapped onto a baseband modulation constellation in preparation to being processed in the IDFT block.

The modulation mapping schemes used in the Wireless LAN standard consist of BPSK, QPSK, 16-QAM or 64-QAM encoding, the encoding scheme is

selected depending on the required transmission rate.

These interleaved streams of BPSK/QPSK/QAM encoded data are then processed using an IDFT operation to create the OFDM symbols to be transmitted. Table 3.3 shows the standards from [76] for the OFDM symbol transmission parameters for the 802.11a Wireless LAN standard.

Table 3.3: OFDM transmission parameters for the 802.11a Wireless LAN standard.

Parameter	**Value**
Number of subcarriers (N)	52
OFDM symbol duration T_U (prior to cyclic extension)	$4\mu s$
Carrier spacing ($1/T_U$)	250 kHz
Spacing between max and min subcarriers ($(N-1)/T_U$)	16.6 MHz

As with the DVB-T case a guard interval is necessary for the 802.11a standard. The guard interval is defined similarly to that of the DVB-T case where the cyclic extension is made up of some of the useful data from the end of the OFDM block. This standard states that the cyclic extension should be $0.8\mu s$ in duration. At transmission the structure of the data should be as shown in figure 3.4

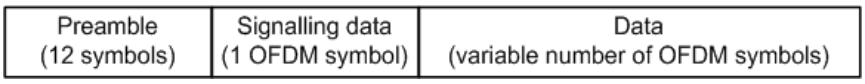

Figure 3.4: Structure of transmitted data for the 802.11a standard

The preamble consists of 12 symbols (10 short symbols and 2 long symbols) used as a training and synchronisation sequence at the beginning of the transmit sequence. The signalling data is a single OFDM symbol consisting of BPSK

constellation encoded data. This signalling data gives details to the receiver about the rate of the incoming data (and hence which baseband constellation encoding is used for the data), length of the incoming data as well as parity bits. The data block is where the incoming data is transmitted and is a variable number of OFDM symbols.

The 802.11a standard operates in the super high frequency (SHF) range in the 5 GHz frequency band.

3.3 DWT and DWPT OFDM Systems

The discrete wavelet and wavelet packet transforms are a relatively new development in OFDM transmission. By using the same general structure of the DFT-based OFDM but replacing the DFT operation block with a discrete wavelet/wavelet packet transform block an orthogonal signal can be produced which fulfils the requirements for OFDM transmission.

Because of how new this type of technique is, standards are still in the development stage for many of the potential applications that could utilise this type of OFDM. One of these applications is power line broadband communications where standard residential power lines are utilised in the transmission of broadband data, this standard is being developed by the IEEE and is currently in its draft stages [29], [77].

The following section will talk in some detail about how power line communication techniques are developing and particularly some of the research conducted in the use of wavelet-based OFDM for PLC transmission.

3.3.1 Power line Communications

Power line communications is a concept that's been around since the early 1900s where they were used for low frequency signaling by electricity companies. In the late 1970s power line communications became the topic of more research into the transmission of more complex data. Over the years since this was first proposed there have been numerous studies into the best types of modulation and transmission techniques to use on the harsh channels that are power lines, some of the early work into this field were discussed in section 2.3.2.

One of the more recent developments in this area is to use wavelet-based OFDM as the transmission technique for PLCs. The IEEE standard for Broadband over Power Line Networks which is currently in its draft phase specifies the use of wavelet-based OFDM in conjunction with DFT-OFDM in the standard. In [29] a description of the current progress of the IEEE P1901 Corporate Standards Working Group was outlined. From this work the following progress has been made in the standardisation of PLC communications.

The IEEE PLC transmission standard intends to employ both wavelet-based OFDM with DFT-based OFDM in its transmission standard. The reason behind this decision is that power lines have a much narrower bandwidth than standard transmission mediums (coax, wireless, etc) to work with, this aspect has the disadvantage of causing all devices on the PLC network to have to share a common frequency band (between 2 - 30 MHz), this causes self-interference on the communication medium, particularly if there are many users within close proximity to each other using the same medium. A way to allow efficient sharing of this medium is to allocate the two different transmission techniques (DFT-

based OFDM or DWT-based OFDM) depending on the type of transmission devices and data being transmitted.

The P1901 draft standard uses the power frequency and phases as a synchronising technique to allow shared devices to detect the usage of the medium. Each device accesses the medium using a time slot allocation method called Time Division Multiple Access (TDMA).

Since both DFT-based and DWT-based OFDM are proposed as being used in this standard different parameters apply to the baseband modulation mapping, number of subcarriers and OFDM symbol length for both methods. The OFDM parameters given in [29] for the draft IEEE PLC standard proposal are given in table 3.4, some parameters are yet to be finalised but these give a base indication of the intended implementation of OFDM in these systems.

Table 3.4: OFDM transmission parameters for PLC.

Parameter	**DFT-based**	**DWT-based**
Number of carriers (N)	3072, 6144	512, 1026
OFDM symbol duration T_U	$40.96\mu s$	$8.192\mu s$
Guard Interval duration	5.56, 7.56, $47.12\mu s$	N/A
Baseband modulation mapping	BPSK, QPSK, 8, 16, 32, 64, 256, 1024 or 4096-QAM	BPSK, 4, 8, 16, or 32 PAM
Frequency band	2 - 30 MHz	2 - 28 MHz

3.4 Problems Associated with OFDM Systems

While standard DFT-based OFDM has been widely accepted in many mainstream wireless transmission applications (e.g. digital television broadcasting (DVB-T) and wireless transmission) and DWT-OFDM is being seriously con-

sidered in the power line communications field, there are still some negative aspects to using OFDM. The following sections will summarise the most common problems with OFDM transmission systems and look at ways that have been attempted to try and alleviate these problems.

3.4.1 High Peak to Average Power Ratio

Peak-to-average power ratio (PAPR) is a well known issue with many communication systems that use the sum of many (N) unmodulated or identically modulated sinusoids in transmission [78].

One particular system that employs this method in its transmission is OFDM with its N orthogonal subcarriers used to multiplex together one OFDM symbol. The resulting high peak-to-average power ratio caused by this method is of particular concern when the signal needs to be passed through a high power amplifier for transmission [79], [80]. Generally speaking the high power amplifiers used in wireless transmission systems have a linear response when used at low amplitude but for large amplitude input signals a non-linear response occurs in the amplifier, this means that for the amplification of OFDM symbols the occurrence of the high amplitude peaks will cause in-band and out-of-band distortion to occur from the amplifier's response [80].

Some of the work that has been performed to attempt to reduce the effect of high PAPR in OFDM include the use of clipping and filtering of the signal, block coding methods and clever constellation mapping techniques. The following subsections give a brief summary of some of these techniques.

Clipping and Filtering

Clipping the high peaks of the OFDM signal is one of the easiest techniques employed to reduce the effect of a high peak-to-average power ratio, basically the amplitude peaks of the signal are clipped to a predetermined amplitude level using this method. This method does have the drawback of causing distortion to the signal due to clipping, this distortion can be considered as noise and affects both in- and out-of-band regions of the signal. While the in-band distortion cannot be remedied it is possible to correct the out-of-band distortion by passing the clipped signal through a filter. This filtering process causes some peak growth to occur so usually this process is repeated several times to ensure the peak amplitudes stay under the clipping level before being amplified [79], [80], [81].

Block Coding

Block coding is another way to reduce the PAPR in OFDM systems. It was found in the works in [26] and [27] that the peak envelope power (PEP) in OFDM transmitted data symbols was higher for certain transmitted symbols than for others. Figure 3.5 shows the results obtained from modulating 16 BPSK encoded values (ranging from decimal zero to decimal 15) onto 4 orthogonal carriers. The works of [26] and [27] showed that a PEP of 16.00W occurred in the modulated OFDM symbols for decimal zero, 5, 10 and 15, they also showed that for decimal 3, 6, 9 and 12 a PEP of 9.45 occurred.

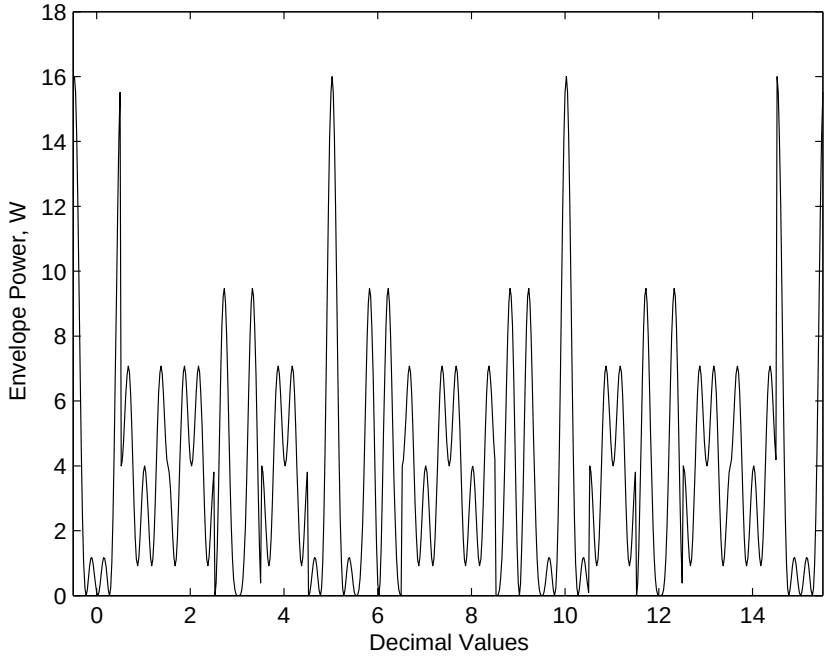

Figure 3.5: The envelope power of 16 BPSK encoded symbols transmitted on four orthogonal carriers. Reproduced from [26]

It was therefore proposed in this work that if data can be block encoded in such a way as to avoid using the codes that would produce a large PEP then some headway could be made in reducing the PAPR problem in OFDM.

The solution proposed was to map a 4-bit codeword onto 3-bit encoded data symbols making sure codewords that produce a high PEP were avoided. This method decreased the data rate so was a trade off between data rate and reducing the PAPR. In simple cases with few subcarriers to deal with and small M-PSK constellations this is an effective solution, but in larger systems complex searches for effective codewords and complex decoding methods make this technique somewhat prohibitive [79].

Active Constellation Extension

Active constellation extension (ACE) is one method of reducing PAPR by altering the constellation map the data is being encoded onto. The concept behind this is presented in [82] and describes a method of extending the outer constellation points in M-PSK and QAM constellations and mapping the data onto these extended points. The theory behind this is that by extending the constellation points outward in an intelligent manner, the magnitude of the sinusoidal and cosinusoidal carrier components can be actively controlled to cancel out large peaks from the modulated data.

Two iterative methods were presented in [82] to achieve this constellation extension, the first method was the 'projection onto convex sets' method (POCS) and the second method was an approximate gradient-project method. The POCS method starts with a block of data symbols, an IDFT is applied to this block and the resulting signal is clipped at a certain amplitude threshold (A) as shown in equation (3.1)

$$\bar{x}[n] = \begin{cases} x[n], & |x[n]| \leq A \\ Ae^{j\theta[n]}, & |x[n]| > A \end{cases} \tag{3.1}$$

where $x[n] = |x[n]|e^{j\theta[n]}$

A DFT is applied to the result of this process. After this the algorithm forces all of the interior constellation points back to their original values while the exterior points are projected into the region of increased margin. This algorithm is iterative therefore this process is repeated several times until no clipping occurs to the signal.

The second method is similar but initially takes note of the allowable constellation extensions before applying the iterations to the data block. Similarly the data block ($|x^i[n]$) is clipped as in equation (3.1). The difference between the methods occurs when a DFT is then applied to the clipped signal portion and the clips are then analysed to determine which parts of the clip to keep to allow only acceptable constellation extensions, clips that would cause unacceptable constellation extensions are set back to zero. Using this clip data and equation (3.2) the constellation points can be set using an iteration of this method.

$$\mathbf{x}^{i+1} = \mathbf{x}^i + \mu\mathbf{c} \tag{3.2}$$

where μ is a step size determined by some criterion and $\mathbf{c}$ is the IDFT of the clipped portion of the signal.

3.4.2 Inter-channel Interference and the Guard Interval

Because of OFDM's proven robustness in frequency selective fading channels this type of transmission is what is primarily used in these situations, it is perfect for the conditions faced for wireless transmission. Unfortunately the way the DFT-OFDM symbols are filtered and the characteristics of frequency selective fading channels, inter-channel interference is an ever present problem in these types of OFDM systems [21], [23].

The ICI issue is a problem predominantly in DFT-based OFDM transmission, it is less of an issue in wavelet based OFDM and much of this interference is due to the effect the DFT filtering and symbol truncation operations have

on the resulting transmitted OFDM symbols. By performing an IDFT operation on the data and windowing this data, the output symbols are in effect the equivalent of a sum of sinusoids truncated to the length of the OFDM block. This gives the output in equation (3.3) [83].

$$d(n) = (\frac{1}{\sqrt{N}} \sum_{k=-N/2}^{k=N/2-1} D(k) e^{j2\pi \frac{k}{N} n}) \Pi_N(n) \tag{3.3}$$

where $-N/2 \leq n \leq N/2$, N is the number of orthogonal subcarriers and $\Pi_N(n)$ is the rectangular window used to truncate the OFDM symbols.

This truncation causes the OFDM blocks to exhibit a $\sin(x)/x$ frequency characteristic on each sub-channel, this shape causes each sub-channel to interfere with adjacent sub-channels and causes inter-channel interference [8]. On top of this, frequency selective fading and multi-path channels also cause delay spread to occur to the OFDM symbols. With frequency selective fading channels the frequency selectivity causes different amounts of delay to occur to the different sub-channel frequencies. By setting a guard interval longer than the maximum delay spread in the OFDM block inter-channel interference can be mitigated to some degree [67].

The accepted guard interval used in the case of OFDM is a cyclic prefix extension to each OFDM block. This cyclic prefix consists of a certain number of data symbols, longer than the delay spread from the channel, from the end of the OFDM block appended to the beginning of the OFDM block. This technique has the benefit of reducing inter-channel interference and at the same time the prefix data can be used at the receiver for synchronisation purposes [84].

Assuming the frequency selective fading channel behaves as a filter of length $L_h + 1$, the cyclic prefix should be long enough to account for the delay in this channel. The typical length of the cyclic prefix is thus determined to be [85]:

$$N_c \geq L_h \tag{3.4}$$

where N_c is the length of the cyclic prefix appended to the OFDM block, N and L_h is the length of the channel impulse response.

While it may appear the longer this extension is, the better the system performance will be, system efficiency does need to considered. The longer the cyclic prefix the less efficient the system becomes, this efficiency is measured by $N/(N + N_c)$ so the larger N_c is the less efficient the system becomes. So while we need a suitably long cyclic prefix it also needs to be short enough so as not to substantially reduce the efficiency of the transmission system.

3.5 Conclusions

In this chapter four practical systems were presented which utilise various forms of OFDM transmission. These systems were: digital television broadcasting, digital radio broadcasting, the 802.11a wireless LAN system and the relatively new OFDM application of power line communications. These four methods are all used in the transmission of large quantities of data and particularly multimedia data such as video, images and audio which appear in television data streams and internet traffic.

Also presented in this chapter were some common problems associated with traditional DFT and DWT-based OFDM systems. Included in these problems

were the high peak-to-average power ratio associated with all multicarrier transmission systems and the problem of inter-carrier interference (ICI) caused by spectral leakage between adjacent sub-carriers. Some methods were also presented which have been proposed and utilised to alleviate these problems.

Chapter 4

Using Wavelet Compression and Standard OFDM for Multimedia Data Transmission

4.1 Introduction

From chapter 3 a number of applications were introduced that use various OFDM transmission techniques. Systems such as digital television broadcasting and wireless LAN standards are common implementations of Fourier based OFDM and are often used in everyday life.

This chapter will look at DFT-based OFDM transmission and consider the performance these systems have in wireless multipath fading channels when transmitting compressed image and video data. The chapter will present results of experiments run to simulate the type of OFDM transmission implemented in the applications mentioned above and present relative mean squared error

(RMSE), structural similarity (SSIM) and PSNR values to quantify the amount of expected error in these types of systems.

This chapter will also look at DFT-based OFDM systems when wavelet subband compression is applied to the image and video data. RMSE, SSIM and PSNR values will also be presented for this compressed and transmitted data also.

4.2 Simulation Results for DFT-OFDM Transmission

The results in this section were obtained using MATLAB simulation software where image and video data has been used to assess the effects OFDM systems have on transmitted data. The image set used in the experiments was obtained from the USC-SIPI Image Database [86] and consisted of 69 random images of various sizes and subject matters. A full set of the images with their corresponding numbers are given in appendix A. The videos used in the experiments were obtained from the Arizona State University Trace Video Library [87], seven video segments each consisting of 100 frames were analysed and processed using the DFT-OFDM system.

These images and video frames were firstly converted to greyscale before being processed in the transceiver system, for colour images/video the same process would be applied in transmission but to the three red, green and blue (RGB) layers independently.

The system used in the experiments is shown in figure 4.1.

For an initial benchmark test this system was used without the compression

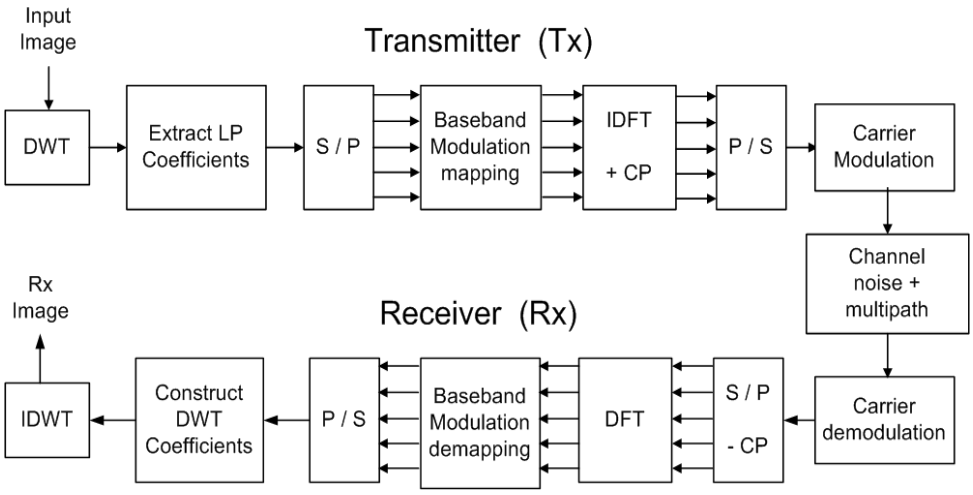

Figure 4.1: DFT-OFDM system block diagram with wavelet compression block

block, further results were then obtained by including this compression block in the system.

In the simulations involving the compression block the data was first input into a data compression block where a discrete wavelet transform is applied, the resulting low and high-pass subbands are then filtered so that only the low-pass subbands are left for transmission. The data is then converted to N parallel streams of data where N corresponds to the 16 subcarriers used in the OFDM transmission. The baseband mapping constellations used were the 16-, 32- and 64-QAM constellations which are common constellations used in DFT-based OFDM systems (see OFDM applications in chapter 3).

Since DFT-based OFDM is used there needed to be a cyclic prefix appended to the data after the IDFT process so as to reduce the inter-channel interference (ICI) in the received data symbols. The length of the cyclic prefix was determined from the simulated multipath channel impulse response length and

consisted of appending $L_h + 1$ symbols from the end of the OFDM block to the beginning of the block.

The channel used for the transmission was a multipath fading channel with 5 multipaths (i.e. $L_h = 5$) with AWGN, the signal-to-noise ratio of this noise was defined as the ratio of the average QAM-symbol energy over the noise energy per QAM-symbol.

4.2.1 Error Measures

For the experimental results the error measures used were relative mean squared error, structural similarity and peak signal-to-noise ratio. These error measures are outlined as follows.

Relative Mean Squared Error

To measure the error for data received from this system the relative mean squared error (RMSE) is calculated. RMSE is a method of calculating error that compares pixel-by-pixel or sample-by-sample between the sent data stream and the received data stream. RMSE is defined as:

$$\text{RMSE} = \sum_{i=1}^{M}\sum_{j=1}^{N}[x(i,j) - x_r(i,j)]^2 / \sum_{i=1}^{M}\sum_{j=1}^{N}[x(i,j)]^2 \tag{4.1}$$

where x and x_r are the original and reconstructed data stream respectively, N is the number of rows in the data stream (N is equal to 1 for a vector) and M is the number of columns in the data set.

Structural Similarity

The second error measure method, which is commonly used for images, is called structural similarity and was proposed in [88]. Structural similarity (SSIM) considers the perceived quality of an image, therefore rather than a pixel value by pixel value comparison (such as in the RMSE method) SSIM considers such things as a luminance, contrast and pixel structure comparisons.

Since the human eye perceives certain errors much more easily than other errors this measure is very useful when determining the quality of images. Figure 4.2 shows an example of a situation where the RMSE value of images can be almost identical but the eye perceives the error differently.

Figure 4.2: Clockwise: Original image, image corrupted with impulsive noise, lossy JPEG compressed image and image corrupted with AWGN.

In each of the cases in the above figure the RMSE value was calculated as $\simeq 0.185$, but structural similarity varied from 70% for the image corrupted with impulsive noise, 59% for the image corrupted with AWGN and 43% for the lossy JPEG compressed image. It's clear from this that not all errors are equal.

The algorithm for calculating structural similarity as defined in [88] is outlined as follows:

The luminance measure of the images is defined as:

$$l(\mathbf{x}, \mathbf{y}) = (2\mu_x\mu_y + C_1)/(\mu_x^2 + \mu_y^2 + C_1) \tag{4.2}$$

where μ_x and μ_y are the mean values of the images $\mathbf{x}$ and $\mathbf{y}$ respectively and C_1 is defined as:

$$C_1 = (K_1 L)^2 \tag{4.3}$$

where L is the dynamic range of the pixel values and $K_1 << 1$.

Similarly the contrast measure is defined as:

$$c(\mathbf{x}, \mathbf{y}) = (2\sigma_x\sigma_y + C_2)/(\sigma_x^2 + \sigma_y^2 + C_2) \tag{4.4}$$

where σ_x and σ_y are the standard deviations of the images $\mathbf{x}$ and $\mathbf{y}$ respectively and C_2 is defined as:

$$C_2 = (K_2 L)^2 \quad \text{where} \;\; K_2 << 1. \tag{4.5}$$

The structure measure is also defined as:

$$s(\mathbf{x}, \mathbf{y}) = (\sigma_{xy} + C_3)/(\sigma_x\sigma_y + C_3) \tag{4.6}$$

where $C_3 = C_2/2$ and σ_{xy} is defined as:

$$\sigma_{xy} = \frac{1}{N-1}\sum_{i=1}^{N}(x_i - \mu_x)(y_i - \mu_y) \tag{4.7}$$

Finally the structural similarity is defined as:

$$SSIM(\mathbf{x}, \mathbf{y}) = [l(\mathbf{x}, \mathbf{y})]^{\alpha}.[c(\mathbf{x}, \mathbf{y})]^{\beta}.[s(\mathbf{x}, \mathbf{y})]^{\gamma} \tag{4.8}$$

where α, β and γ are considered equal to 1.

Peak Signal to Noise Ratio (PSNR)

Peak signal-to-noise ratio (PSNR) is another error assessment metric often used in evaluating video and image codec performance [89].

PSNR is an objective quality assessment measure which is defined as the ratio of the peak signal and the noise corrupting the image or video [90]. PSNR is evaluated using the simple algorithm:

$$PSNR = 10\log_{10}(\frac{2^M - 1}{MSE}) \tag{4.9}$$

where $2^M - 1$ is the maximum value a pixel can take and MSE is the mean squared error.

The simplicity of this algorithm makes it popular in the field of multimedia quality assessment in determining the amount of error different compression algorithms and codecs apply to an image/video. This error measure does not give a precise indication of the quality of an image or video *as perceived by the human eye*, but it is still considered an important measure when considering

video and image manipulation algorithms [89], [90].

4.2.2 Image and Video Transmission with No Compression

Initially, image transmission will be considered in a DFT-OFDM system with no compression applied, this will be a good benchmark test for the amount of error caused by the transmission schemes and the amount of error caused by the compression techniques being applied to the data. These results were obtained by performing 100 simulations and averaging the results obtained.

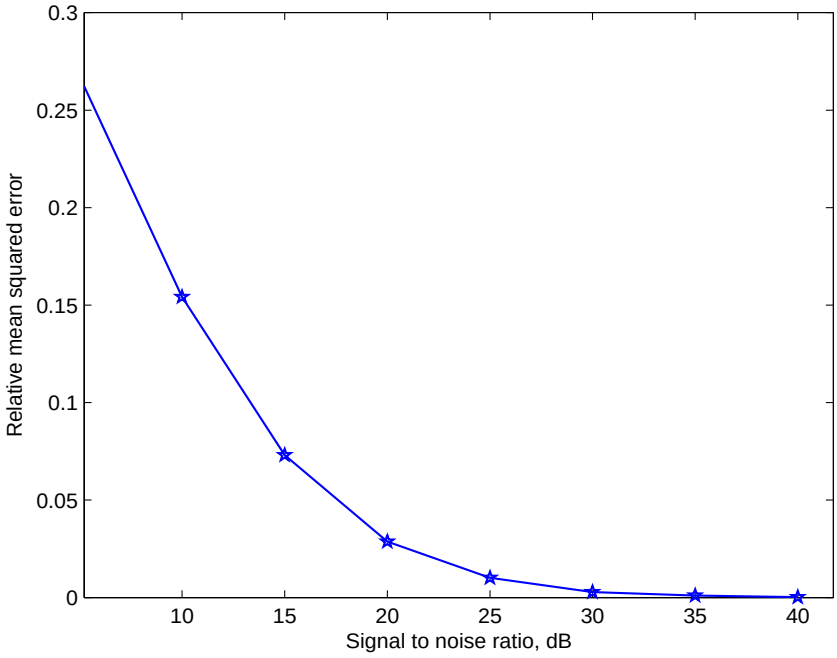

Figure 4.3: Relative mean squared error for images for eight different SNRs (no compression applied)

The system used to obtain these results is a typical DFT-based OFDM

system with 16-QAM baseband modulation mapping and 16 subchannels used for the OFDM transmission. Figure 4.3 shows the RMSE error obtained from the transmission of images for signal-to-noise ratios of 5 - 40 dB.

Figure 4.4 shows the structural similarity obtained from the same OFDM transmitted image data.

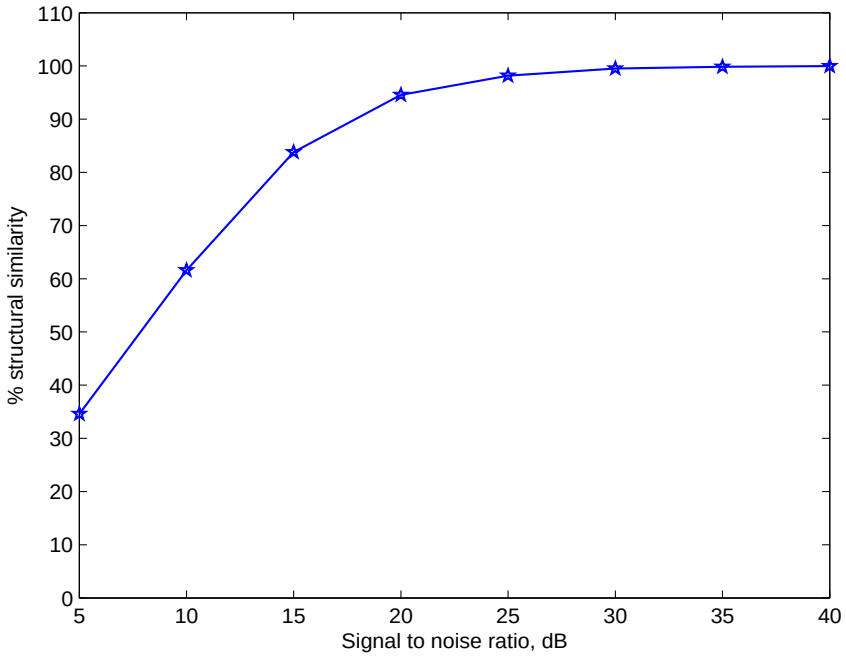

Figure 4.4: Structural similarity of images for eight different SNRs (no compression applied)

These results show that for signal-to-noise ratios above 25 dB error in this type of system tends to zero. The structural similarity in these cases is also nearly 100% showing very good quality is obtained at these SNRs. For SNRs below 25 dB there is some degradation in quality of the received image data with a decrease in the SSIM results (to 34.6% at SNR = 5dB) and an increase

in the RMSE value (to 0.27 at SNR = 5dB).

This high quality of received data is expected at these SNRs since there is very little channel noise to corrupt the data and no compression applied so no data loss can be attributed to a lossy compression schemes.

The same process as described above was also applied to a set of video frames. The error results from this are shown in figures 4.5 and 4.6.

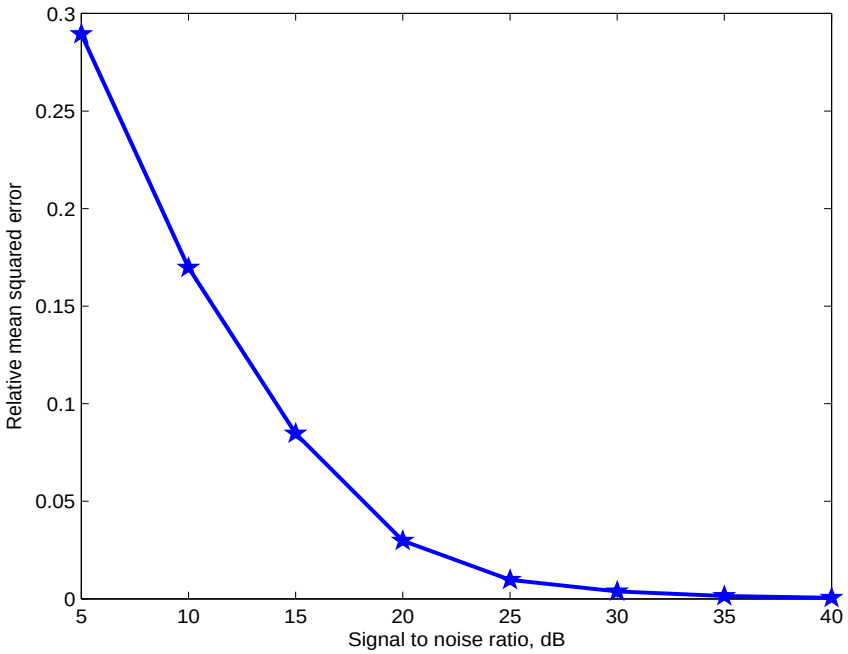

Figure 4.5: Relative mean squared error for video frames for eight different SNRs (no compression applied)

Figure 4.6 shows the structural similarity obtained from the same OFDM transmitted video frames.

Both figure 4.5 and 4.6 show the same result as that obtained from the image transmission. These results show that the behaviour of this system with

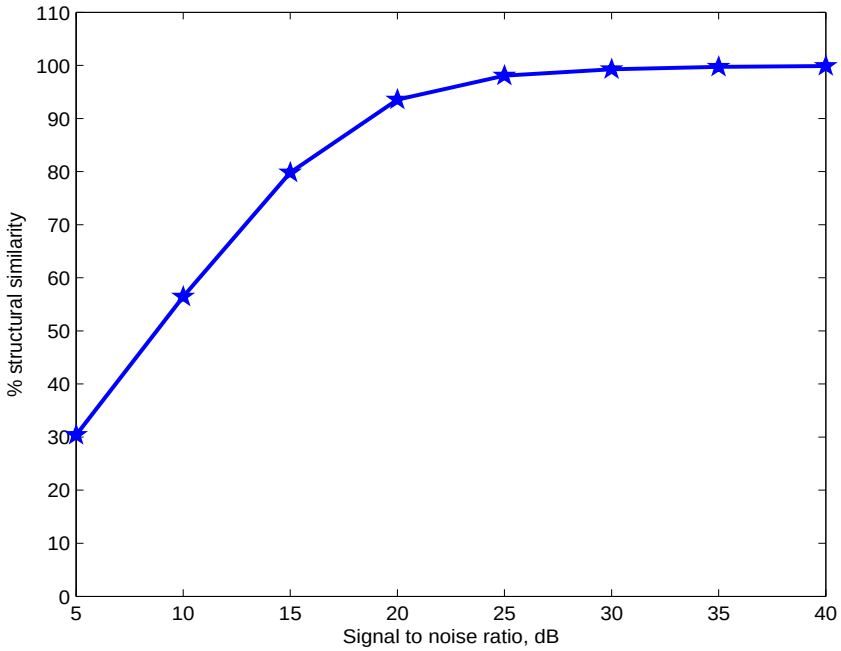

Figure 4.6: Structural similarity of video frames for eight different SNRs (no compression applied)

no compression is equivalent for both still images and video content.

4.2.3 Image Transmission with Wavelet Subband Compression

Knowing the benchmark result for DFT-OFDM transmission with no compression applied, the effect of wavelet subband compression with OFDM can be assessed. The following results show the error obtained from compressing and then transmitting image data. Each simulation was performed 100 times and averaged to give an indication of the results that would be expected in this type of system.

The type of compression used in this system was the wavelet subband compression method where the wavelet coefficients obtained from the decomposition of the original image were passed through a low-pass filter so as to remove the high frequency subband coefficients, for this compression block the wavelet used was the Daubechies 7 since, according to the literature, this wavelet works well for this type of compression [25]. The figure below shows the RMSE results for 16-, 32- and 64-QAM baseband modulation mapping.

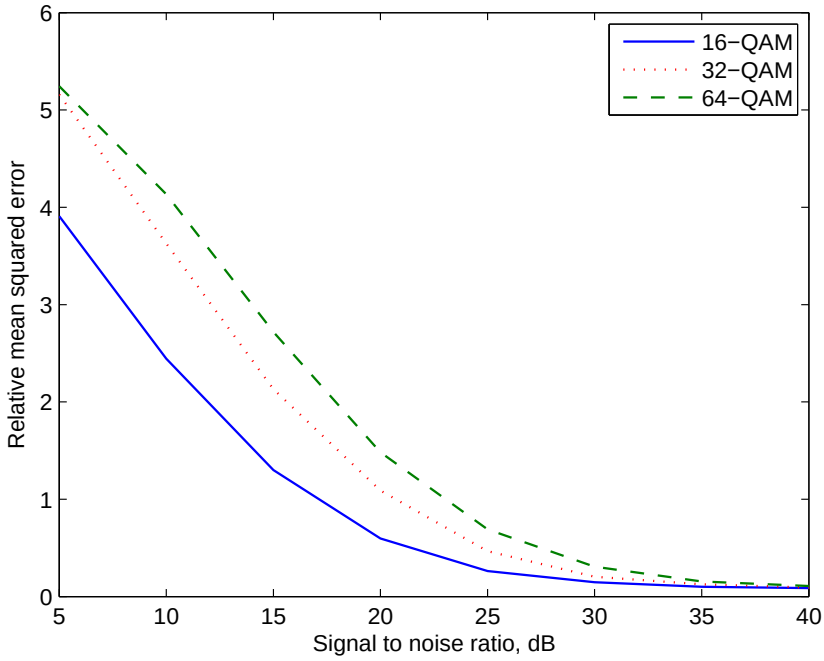

Figure 4.7: Relative mean squared error for images for eight different SNRs

Figure 4.8 shows the structural similarity obtained from the same wavelet compressed and transmitted image data. Again the results are for 16-, 32- and 64- QAM modulation mapping.

Figure 4.9 shows the PSNR values obtained from the compressed and trans-

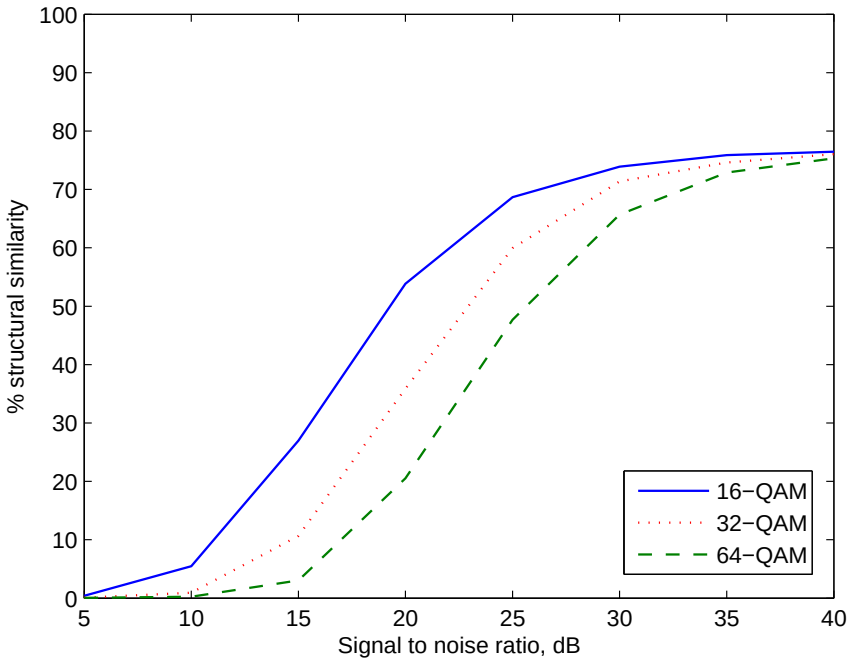

Figure 4.8: Structural similarity of images for eight different SNRs

mitted image data.

These results show that using a lower order QAM gives better performance in this type of system, this result is expected as the constellation points in lower order QAM maps have a greater Euclidean distance between them. In noisy channel situations this increased distance between points decreases the chance of the receiver making an incorrect decision on the constellation point selected [4]. This is shown by considering the probability of error formula for QAM in equation (4.10).

$$P_b = Q(\sqrt{\frac{d_{12}^2}{2N_0}}) \tag{4.10}$$

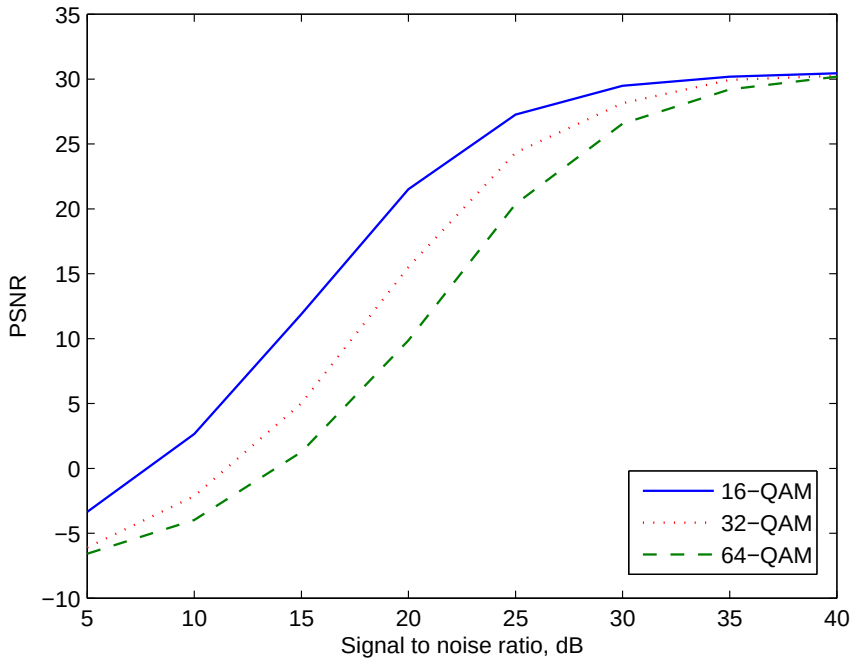

Figure 4.9: PSNR of images for eight different SNRs

where d_{12} is the Euclidean distance between points 1 and 2, N_0 is related to the gaussian noise power spectrum and:

$$Q(x) = 1 - \int_{-\infty}^{x} \frac{1}{\sqrt{2\pi}} e^{-t^2/2} dt \tag{4.11}$$

As well as the performance due to the QAM order it can also be seen in figure 4.8 that the structural similarity results also show that there is some loss of image quality due to the subband filtering process and that a maximum SSIM index of approximately 76% is achieved at a SNR of 40dB. When compared to the SSIM results obtained in section 4.2.2 where no compression was used, it is clear that this reduction in image quality is purely due to this subband

compression scheme as it is a lossy compression algorithm that will cause data loss. At high signal-to-noise ratios all QAM constellations perform comparably giving a RMSE value of approximately 0.1 at a SNR of 40dB for QAM orders 16 - 64.

By calculating the average RMSE obtained for each of the individual images at a signal to noise ratio of 35dB and using the Daubechies 7 wavelet figure 4.10 was obtained. This figure shows the dependence between the type of image being processed and the amount of error obtained using this transmission method.

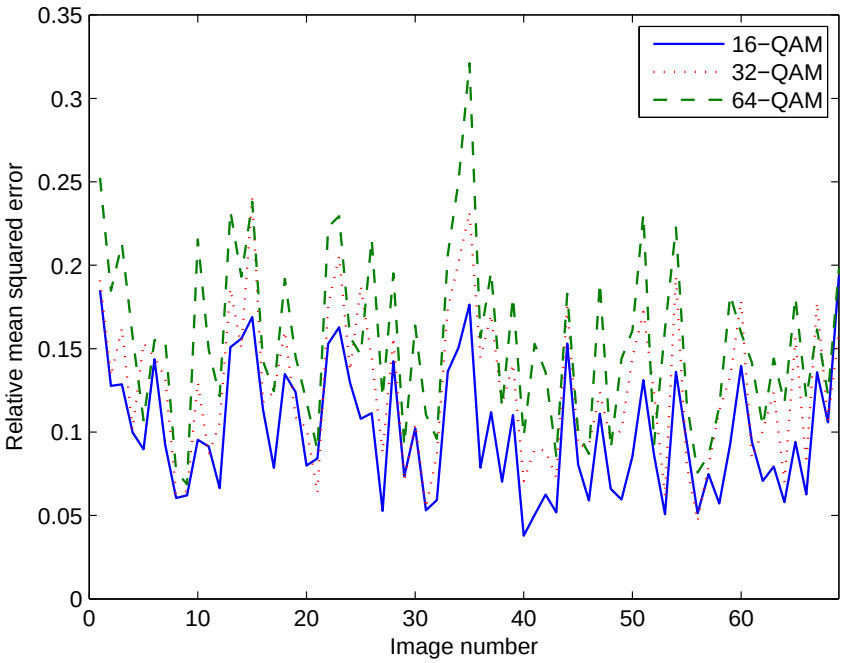

Figure 4.10: RMSE obtained for individual images for SNR = 35 dB

From these results it can be seen that error was not consistent between individual images, images 1, 14, and 35 had a noticeably higher error than the

other images while images 27, 31 and 40 had noticeably lower error (for the full sample of images used in these experiments please refer to appendix A for the images and their corresponding image numbers).

The images that compressed well in these experiments have very little detail contained within them and tend to consist of basic textures. This result is expected for these types of images since these tend to have low spatial frequencies therefore most of their wavelet coefficients would be confined to the low subband regions.

The images that did not compress well on the other hand tended to have a lot of detail in them and a lot of light/dark variations which would give them a generally higher spatial frequency. After wavelet decomposition and subband removal much of this information would also be removed.

4.2.4 Video Transmission with Wavelet Subband Compression

Again results were obtained for the compression and transmission of video frames. The following results were obtained when the frames were transmitted using DFT-OFDM with wavelet subband compression.

Figure 4.11 shows the RMSE obtained for these video frames. These results show a very similar result to the transmitted images with 16-QAM giving the least error while at high signal-to-noise ratios all QAM constellations perform similarly.

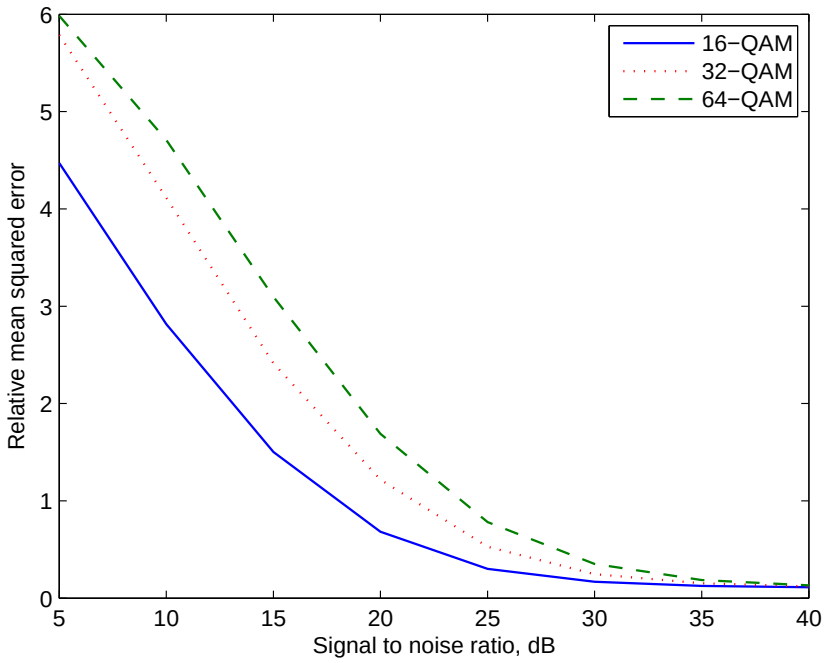

Figure 4.11: Relative mean squared error for video for eight different SNRs

Figure 4.12 shows the structural similarity obtained from the same wavelet compressed and transmitted video data. Again the results are for 16-, 32- and 64- QAM modulation mapping.

Figure 4.13 shows the PSNR values obtained from the compressed and transmitted video data.

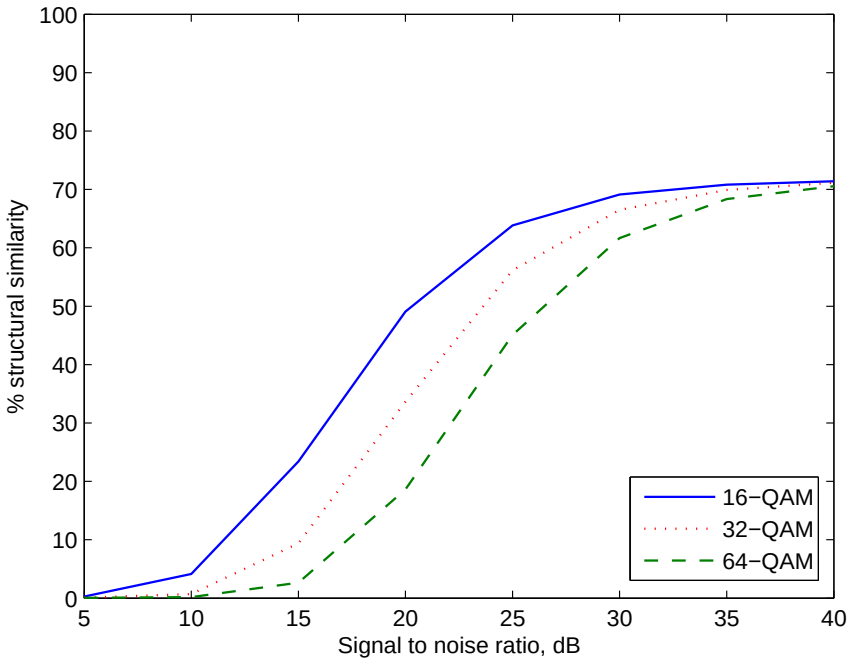

Figure 4.12: Structural similarity of video for eight different SNRs

Again the results show for videos a very similar result as that obtained for images. The structural similarity reflects the trend shown for images but a slightly smaller peak SSIM value of $\simeq 71\%$ shows a slight decrease in the maximum quality that could be obtained from video transmission.

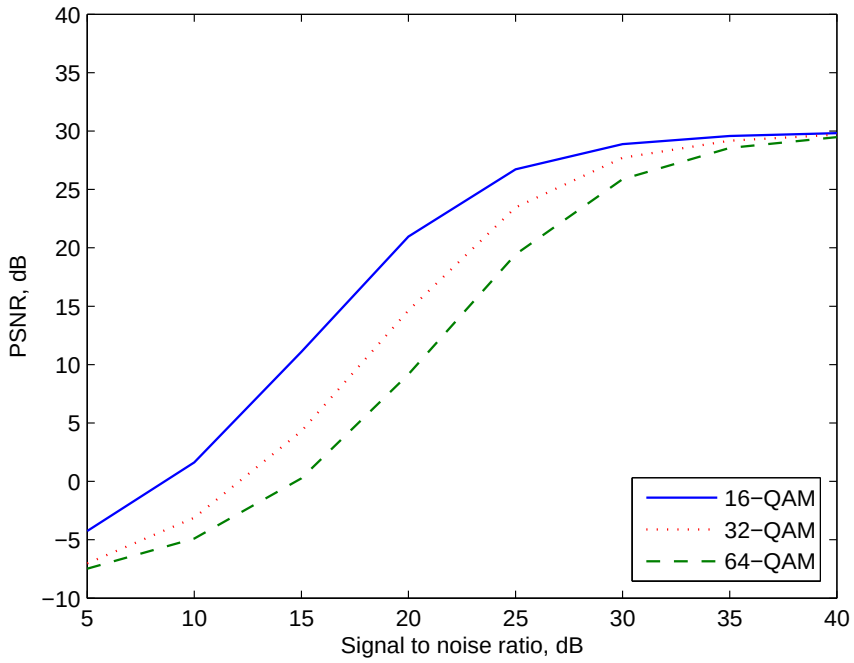

Figure 4.13: PSNR of video for eight different SNRs

4.3 Conclusions

This chapter has looked at the transmission of image and video data when using traditional DFT-based OFDM with and without a wavelet subband compression block. The compression used was a subband filtering method where the wavelet decomposition of images are passed through a low-pass filter to retain the approximation coefficients while discarding certain subbands containing the detail coefficients. This method is a useful method of compression as in many cases a wavelet decomposition concentrates the vast majority of a signal's energy in these low subbands.

Results from DFT-OFDM transmission with no compression applied to the data show that at signal-to-noise ratios above 30dB the error rates tended to zero while the structural similarity of the images and video frames tended to 100%. For SNRs below this there was the expected reduction in performance as the noise magnitude increased in the channel.

The results obtained from the DFT-OFDM process with wavelet compression included showed that this type of compression leads to some reduction in quality, with a maximum structural similarity of 71% being obtained for the highest SNR tested. Again this technique worked well for data transmission through a channel containing minimal noise to corrupt the signal (i.e. >30 dB).

It was also shown that the baseband modulation mapping has a strong influence on the error obtained. Using 16-QAM modulation gave better performance than both 32 and 64-QAM as the constellation points in 16-QAM have a larger Euclidean distance between them giving the receiver a better chance of correctly detecting the symbols transmitted [4].

These results also show video frames perform in a very similar manner to the images giving much the same results for the same SNRs and the same QAM constellation mappings.

Chapter 5

A New Compressive OFDM system for Multimedia Data Transmission

5.1 Introduction

This chapter will introduce a new method of improving upon the typical OFDM system by incorporating data compression in with the OFDM encoding and transmission block to reduce computational complexity of the transceiver.

With the sheer volume of data contained in multimedia information it is very inefficient if this data is transmitted in its raw, uncompressed form. For the vast majority of multimedia transmission and storage systems some form of compression needs to be applied to this raw data to reduce its size. The basic premise of data compression is to take the raw data containing redundant information and to remove this redundant information while still maintaining the integrity of information [46].

In dealing with data transmission and storage many compression schemes

have been developed. In data with high correlation between successive samples (whether the samples are pixel values in an image or other data) coding schemes such as run-length encoding (RLE) can be used. RLE encodes the lengths of data-runs (successive samples with the same values) and replaces the run with a symbol to represent its length and value. Entropy encoding is also another general compression scheme used in data compression. Entropy encoding is used when only a finite number of values occur in a data set, each of these set of values are assigned a probability of occurrence. Depending on how common each symbol is a variable length codeword is assigned to represent each symbol. In theory extremely common symbols will be replaced by a single (or very short) codeword while rare symbols will be assigned longer codewords, hence achieving compression [11],[46].

More specific compression standards used in multimedia compression include; the MPEG1 layer III compression standard (also known as MP3) which has been widely adopted in audio data compression, MPEG video-layer standards (MPEG1, 2 and 4) for video data compression and discrete cosine and wavelet based compression schemes (JPEG and JPEG2000) which have been adopted in still image compression.

One of the main aspects associated with including compression in a data transmission system is the processing time added to the system. Figure 5.1 shows a general framework for a transmission system with a preliminary compressive block before processing occurs for modulation.

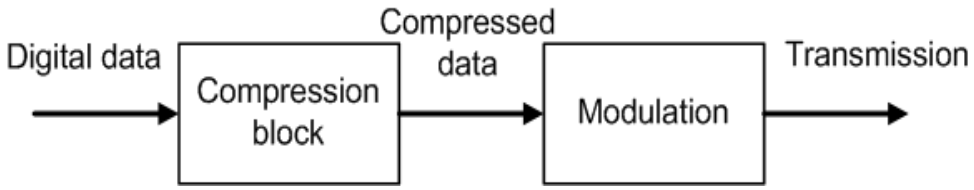

Figure 5.1: Block diagram of a general transmission system with compression block

5.2 The Proposed System

In the works in [91] it was noted that by replacing the IDFT block of an OFDM transmission system with a wavelet transform that inter-symbol as well as inter-channel interference (ISI and ICI) could be substantially reduced in wireless OFDM as compared to that obtained in a traditional DFT-OFDM transmission system. It was also noted in [33] that wavelet-based OFDM has such a robustness to ISI and ICI due to the spectral containment properties of the discrete wavelet transform that a cyclic prefix needn't be applied to the transmitted data at all. This discovery meant that the efficiency of an OFDM system could be substantially increased by replacing the DFT block with a DWT block allowing this removal of redundant cyclic extension data.

To alleviate some of the problems associated with traditional DFT-based OFDM, most notably the reduced efficiency due to the need for a cyclic prefix as well as the time consuming compression block, a system is proposed that will improve the transmission scheme. This proposed scheme improves the system efficiency by combining data compression using the discrete wavelet transform (DWT) with OFDM transmission as used in wavelet-based OFDM transmission. By combining the two operations into one block, computation

time can theoretically be decreased. A block diagram of this proposed system is shown in figure 5.2.

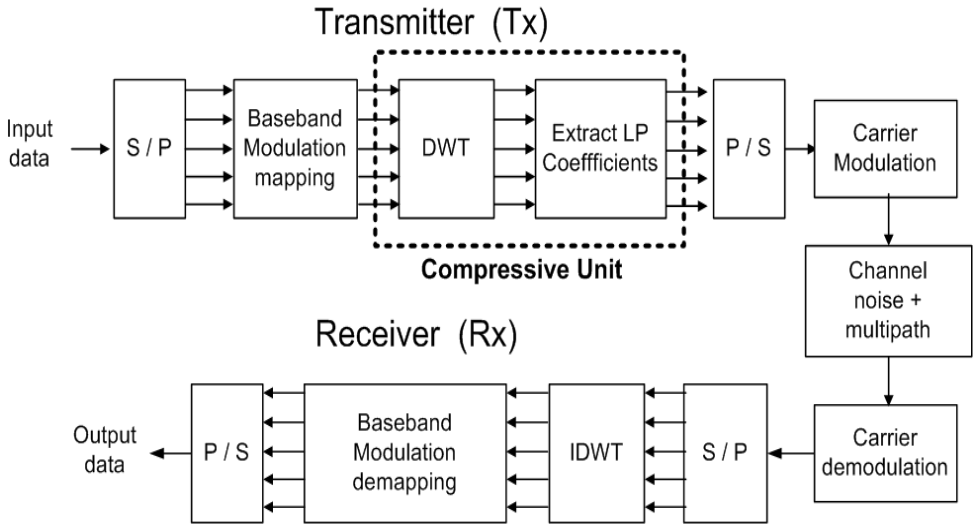

Figure 5.2: Block diagram of the Proposed Compressive OFDM Transceiver

The following sections look at the break-down of each individual block in this system.

5.2.1 Baseband Modulation Mapping

In this system a serial to parallel conversion takes place immediately on a sequence of binary symbols. These N parallel data streams are then input into an M-QAM constellation encoder where the baseband modulation mapping process takes place, this process converts the binary data into the form of M-level encoded complex values. As in traditional OFDM these symbols take the form of $d_n^{(m)} = (d_0^{(m)}, d_1^{(m)}, ...d_{N-1}^{(m)})$ where m is the OFDM block number and N is the number of subcarriers used in the modulation. The indi-

vidual elements ($d(n,m)$) of this matrix are complex numbers of the form: $d(n,m) = a(n,m) + ib(n,m)$.

5.2.2 Compressive Unit

Where the proposed scheme varies from traditional OFDM systems is in the compressive unit where compression, modulation and parallel multiplexing all take place together.

The data from the previous baseband encoding block has a 2-dimensional DWT applied to it. Since the M-QAM encoded data is in the form of complex numbers the DWT process is applied to both the real and imaginary components of $d_n^{(m)}$. The result of this wavelet transform process is still a parallel stream of complex numbers $D_n^{(m)}$.

The general equation for a 1-dimensional DWT process is shown in equations (5.1) and (5.2). This process consists of a multi-resolution decomposition of an original series of data samples ($x[n]$).

$$DWT_x(j,k) = c_{j,k} = \sum_n x[n] h_j^*[n - 2^j k] \tag{5.1}$$

$$b_{j,k} = \sum_n x[n] g_J^*[n - 2^J k] \tag{5.2}$$

where J is the desired resolution of the decomposition, $j = 1, 2, ..., J$; k is the discrete time shift; $h_j[n - 2^j]$ is the discrete wavelet function; $g_J[n - 2^J]$ is the scaling sequence; $c_{j,k}$ are the wavelet coefficients, and $b_{j,k}$ are the scaling coefficients.

By inserting the data ($d_n^{(m)}$) from the proposed system in for $x[n]$ in equations

(5.1) and (5.2) the parallel data stream ($D_n^{(m)}$) out of the DWT block for the proposed system can be derived. In one-dimension the wavelet and scaling coefficients obtained from the m^{th} OFDM block will be:

$$c_{j,k}^{(m)} = \sum_n \Re(d^{(m)}[n]) h_j^*[n - 2^j k] + i \sum_n \Im(d^{(m)}[n]) h_j^*[n - 2^j k] \tag{5.3}$$

$$b_{j,k}^{(m)} = \sum_n \Re(d^{(m)}[n]) g_J^*[n - 2^J k] + i \sum_n \Im(d^{(m)}[n]) g_J^*[n - 2^J k] \tag{5.4}$$

This process is then repeated in the horizontal direction to obtain the 2-dimensional DWT of the data. The result of this entire process is the creation of an approximation subband, which is simply a downsampled version of the original data, as well as additional subbands, these being the horizontal, vertical and diagonal detail coefficients. The number of these additional subbands is dependant on the desired resolution (J).

In the proposed system the output of this transform block consists of complex numbers representing these subband coefficients of the signal. To achieve compression low-pass filtering is applied to the coefficients to eliminate the high frequency coefficients. The low-pass filtering ensures only the approximation and horizontal subband components are retained for transmission.

In the case of image compression this wavelet subband compression process is traditionally performed on the raw image data (with pixel values consisting of integers between 0 and 255) in a separate compressive block before performing

an OFDM multiplexing operation on the data. A potential issue that needed to be considered when altering this traditional method and performing the wavelet subband compression on QAM encoded symbols was whether this method would degrade the reconstructed data more than when using the traditional compression method. Figures 5.3 and 5.4 show the reconstruction of the Lena image after a wavelet subband compression operation is performed on raw pixel values (figure 5.3) and QAM encoded data (figure 5.4). These results are purely from considering compression and reconstruction using the two different methods, at this point no OFDM transmission or channel effects have been introduced.

Figure 5.3: Original image (left) and reconstructed image (right) after image is wavelet subband compressed

Figure 5.4: Original image (left) and reconstructed image (right) after image is both baseband encoded and wavelet subband compressed

From these images it is clear that there is very little visible difference between the reconstructed images for both these methods. Since subbands have been removed in both cases there is some loss of data and hence errors occurring. To quantify this data loss the three error measures described in chapter 4 were used, these are: relative root-mean squared error (RMSE), structural similarity (SSIM) and peak signal-to-noise ratio (PSNR).

From these error measure algorithms a quantitative error analysis can be performed on the two compression techniques. Average RMSE and SSIM values were calculated over the 69 images, for wavelet subband compression on raw pixel values using a Daubechies order 6 wavelet filter (example shown in figure 5.3) an average RMSE value of 0.075 was achieved, this corresponded to an average structural similarity of 83.2% and a PSNR value of 32.7dB, compared to the wavelet compression of 256-QAM encoded symbols (example shown in

figure 5.4) where an average RMSE of 0.081, an average structural similarity of 81% and a PSNR value of 32.7dB was achieved.

These error measurements show a negligible increase in error for the proposed compression method. Looking deeper into the proposed method, the relationship between pixel values and the QAM values each of these pixels is mapped to is considered more closely.

Figure 5.5 shows two maps of the in-phase and quadrature QAM components that each pixel in the Lena image is mapped to. These two maps were produced by treating each amplitude component on the in-phase and quadrature axes of the QAM constellation as pixel values to produce a map of values between -15 and 15. These values were then mapped to colours varying from dark blue for the lowest value to dark red for the highest value. It's very interesting to note the strong visual correlation between the in-phase QAM component and the original Lena image, even the quadrature component has some weak visual correlation to the original image.

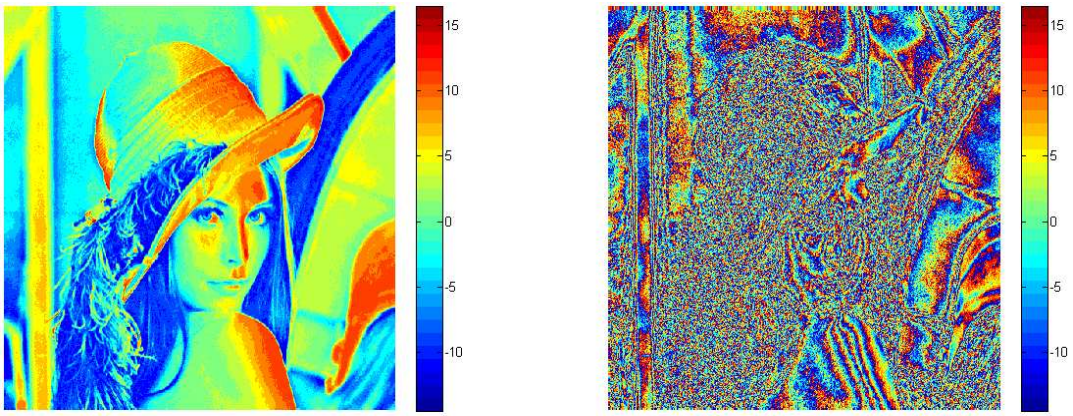

Figure 5.5: In-phase (left) and quadrature (right) components of the 256-QAM modulated Lena image

This relationship further confirms that the proposed method of modulating and wavelet compressing an image in one block is a viable method since the spatial frequencies of an image and the correlation between neighbouring pixels remains consistent even after modulation mapping. This is very important since the structure of a wavelet decomposition depends heavily on these properties of an image. The fact there is a very small increase in the RMSE for the two methods can be weighed up against the potential for reduction in computational complexity.

5.2.3 Carrier Modulation

Because wavelet OFDM does not require a guard interval these coefficients can then be passed to the carrier modulation block of the system as follows.

The parallel stream of subband filtered complex wavelet coefficients are then used to modulate the N orthogonal carriers before being multiplexed and transmitted via OFDM.

A diagram of typical carrier modulation is shown in figure 5.6.

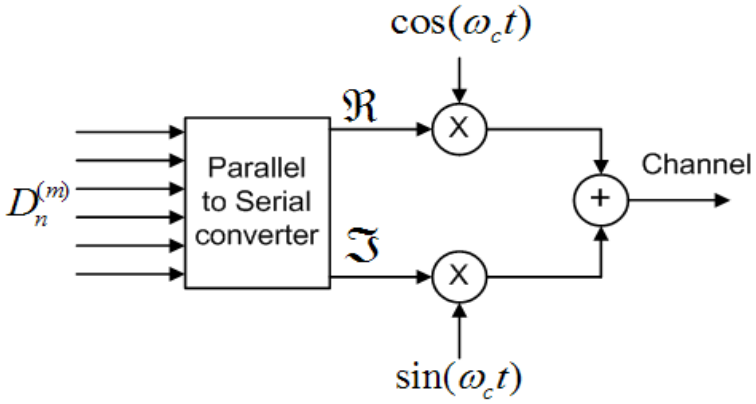

Figure 5.6: Carrier modulation of the wavelet filtered data

For the OFDM transmission N orthogonal subcarriers are used to modulate the data. To obtain orthogonality between OFDM symbols, and hence to be able to isolate the data at the receiver, the frequency spacing between the subcarriers needs to be multiples of $\frac{1}{T}$ where T is the OFDM symbol duration [8]. The result of this proceedure is shown in equation (5.5)

$$s_{transmit}(t) = \sum_{n=1}^{n=N} D_n^{(m)}(t) e^{j(2\pi(f_c + \frac{n}{T})t)} \tag{5.5}$$

where f_c is the initial carrier frequency, $f_c + \frac{n}{T}$ is the n^{th} carrier frequency offset and $D_n^{(m)}$ is the m^{th} OFDM data block.

The resulting RF modulated OFDM symbols are then transmitted on a channel. The receiver then performs channel equalisation and the inverse of the transmission operations on the received data to obtain the original data stream.

5.3 Conclusions

In this chapter a novel compressive wavelet filter based OFDM transmission scheme was introduced. The advantages of this system is its ability to reduce computational complexity and improve the efficiency of traditional OFDM by merging the compression and transmission operations into one block. This was achieved by incorporating both the compressive abilities of the wavelet transform as well at the orthogonal nature of wavelet basis functions to create a parallel transmission scheme based on OFDM.

By using wavelet transforms in this new multi-carrier multiplexing scheme the benefits of wavelet OFDM discussed in [33] and [91] can also be realised; namely the spectral containment of the OFDM symbols resulting in a reduction of ISI and ICI. This attribute also results in the removal of the cyclic prefix all of which adds up to efficient transmission system.

In the next chapter the systematic aspects of this system will be further examined with a look at how this system could be implemented in reality.

Chapter 6

System Analysis

6.1 Introduction

In chapter 5 a new OFDM system was introduced which could compress and modulate a signal simultaneously. While the techniques used to compress, modulate and multiplex a signal is important there are many other systematic considerations in an OFDM transmission system that need to be addressed and analysed.

Shown in figures 6.1 and 6.2 are block diagrams of the transmit and receive systems used in OFDM. These diagrams include the cyclic prefix extension blocks, synchronisation considerations and channel coding. These blocks are just as important in implementing an OFDM system as the compression and modulation components.

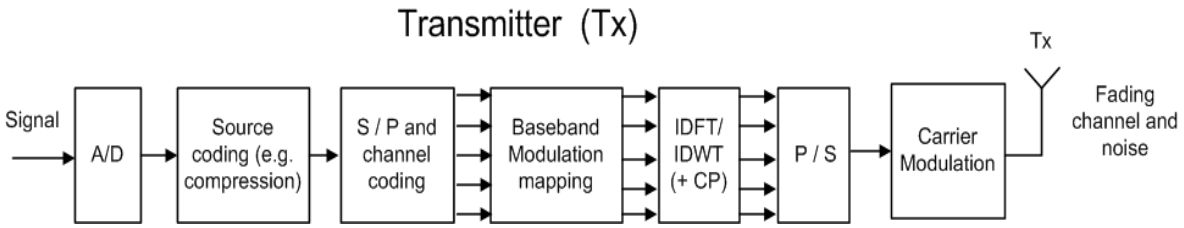

Figure 6.1: The transmit block of a general OFDM communication system.

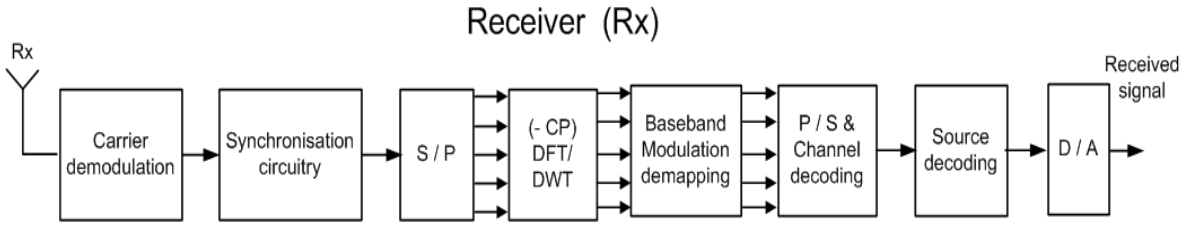

Figure 6.2: The receive block of a general OFDM communication system.

This chapter will look at the new compressive transceiver system and consider some of these practical implementation issues, the chapter will start by looking at channel coding and consider some of the common channel codes used in OFDM systems. The second section of this chapter will look at the cyclic prefix extension on OFDM blocks and examine the reasons DFT-OFDM needs this cyclic prefix, this section will also consider how and why the cyclic prefix issues differ for DWT-OFDM. Thirdly this chapter will consider the issues OFDM systems have with synchronisation, in this section different synchronisation methods will be discussed and considered for their appropriateness in the proposed system.

Lastly multiplexed multimedia data transmission will be considered. As this type of data stream is often used in multimedia transmission systems, such as

the DVB-T standard, it is important to consider how this type of data can be handled in the new compressive OFDM system.

6.2 Channel Coding in OFDM Systems

Channel coding is an important block in all communication systems. The purpose of channel coding is to reduce the amount of error, or to allow a receiver to detect and correct errors that have occurred due to noise and channel effects corrupting the signal that was transmitted [10].

In the DVB-T standard [24] the channel coding used in digital television broadcasting is outlined. In this standard the channel coding occurs over two phases; phase one is called the "outer coding and outer interleaving" phase and is performed using the Reed-Solomon code. The second channel coding phase is called the "inner coding and inner interleaving" phase which applies a convolutional code to the data.

In other works on coding in OFDM systems there has been interest in another type of channel coding called Turbo coding, this type of channel coding has been considered as a replacement for the inner convolutional coding phase of an OFDM system, [101]. This type of coding is attractive for this purpose for its ability to reduce bit-error rates and reduce ICI in OFDM systems [102], [103].

6.2.1 Reed-Solomon Coding

The Reed-Solomon code was originally outlined in [104], this work proposed an error correcting code that was based on Galois (or Finite) Field theory. This

code is a type of BCH code (Bose, Chaudhuri and Hocquenghem code) where the message symbols and code generator are represented using polynomials of finite fields [105].

In designing appropriate generator and field polynomials, finite fields need to be defined suitable to the type of data being transmitted via the communication system. Finite field theory states that for any prime number, p there is a finite field, $GF(p)$ associated with that prime number (where GF is the notation for a Galois field). For this finite field an extension field of size $q = p^m$ can then be defined as $GF(p^m)$ where m is any positive non-zero integer [105].

For Reed-Solomon coding the value of the prime number p used is 2 which can then be used to define fields for encoding binary data. Reed-Solomon coding is in itself a non-binary code but instead defines blocks of binary data and assigns each block a field element, α^i from the field $GF(2^m)$. An example of this type of field is given in equation 6.1.

$$GF(2^m) = \{0, \alpha^0, \alpha^1, \alpha^2, ..., \alpha^{2m-2}\} \tag{6.1}$$

Each of the field elements from this finite field is defined as shown in equation 6.2 [105].

$$\alpha^i = a_i(X) = a_{i,0} + a_{i,1}X + a_{i,2}X^2 + ... + a_{i,m-1}X^{m-1} \tag{6.2}$$

These fields can be represented by way of primitive polynomials. Therefore for each finite field used to represent a block of transmitted data a *field polynomial* can be used to define that field. In the case of DVB-T transmission the field polynomial associated with the Reed-Solomon coding of the transmitted

MPEG stream is: $p(x) = x^8 + x^4 + x^3 + x^2 + 1$ [24]. This polynomial has been derived from the primitive polynomial for a finite field of 8 elements (i.e each data block will consist of 8 bits mapped to a single finite field element, α^i).

The standard notation to define the Reed-Solomon code used for any application is given as $RS(n, k)$ this notation is used in encoding standards to define the total encoded block size, n for the code being used and the uncoded message block size, k before parity blocks are added. Clearly from this the length of the parity blocks can be found by subtracting k away from n. In the case of the DVB-T standard the Reed-Solomon code used is given in the standard as $RS(255, 239)$ which means a total encoded block of MPEG data is 255 symbols, the original, uncoded, MPEG block is 239 symbols therefore the length of the parity code added to the encoded block is 16 symbols ($2t = 16$).

The length of this parity block is directly related to the number of symbols the error correcting code can correct for at the receiver and the code generator polynomial is selected depending on this specific requirement. By having a parity block size of $2t = 16$ symbols, the DVB-T Reed-Solomon code can be used to correct up to $t = 8$ incorrect/corrupted symbols at the receiver. Depending on the application the code is being used for and/or the channel conditions of the communication system the number of parity symbols can be varied accordingly.

For a system that needs to correct for a potential t number of corrupted symbol blocks a code generator polynomial can be given as:

$$g(x) = (x + \alpha^0)(x + \alpha^1)(x + \alpha^2)...(x + \alpha^{2t}) \tag{6.3}$$

where α^i are the roots of the code generator polynomial.

Therefore using equation 6.3 the code generator polynomial used in DVB-T is: $g(x) = (x + \alpha^0)(x + \alpha^1)(x + \alpha^2)...(x + \alpha^{15})$ [24].

Once both the field generator polynomial and the code generator polynomial are defined the Reed-Solomon code can be applied using a linear feedback shift register circuit which in effect performs polynomial algebra on the data being encoded. This system works by moving the incoming block of data into the $(n - k)^{th}$ stage of a shift register which does the same thing as upshifting the message polynomial by x^{n-k}. This upshifted polynomial is then divided by the code generator polynomial which will give the parity polynomial. This parity polynomial is then appended to the upshifted data to complete the encoding [105].

At the receiver the received data is again translated to coefficients of a polynomial, the receiver then checks the parity data to make sure the parity symbols belong to the correct set of codewords. Finally the decoder can check whether the received polynomial coefficients are roots of the generator polynomial; if this check proves to be true then no error has occurred, if the check comes back false then an error can be detected, located and corrected. This technique is called Syndrome computation [105].

6.2.2 Turbo Codes

Another type of channel coding used in OFDM systems is turbo-coding which is a block coding technique first proposed in [102]. Turbo coding is a type of convolutional coding where two identical recursive systematic convolutional (RSC) coders are concatenated together using parallel concatenation. The output of these two RSC units are then interleaved together to create the turbo-coded

output.

Figure 6.3 shows the block diagram of the turbo coder given in [102].

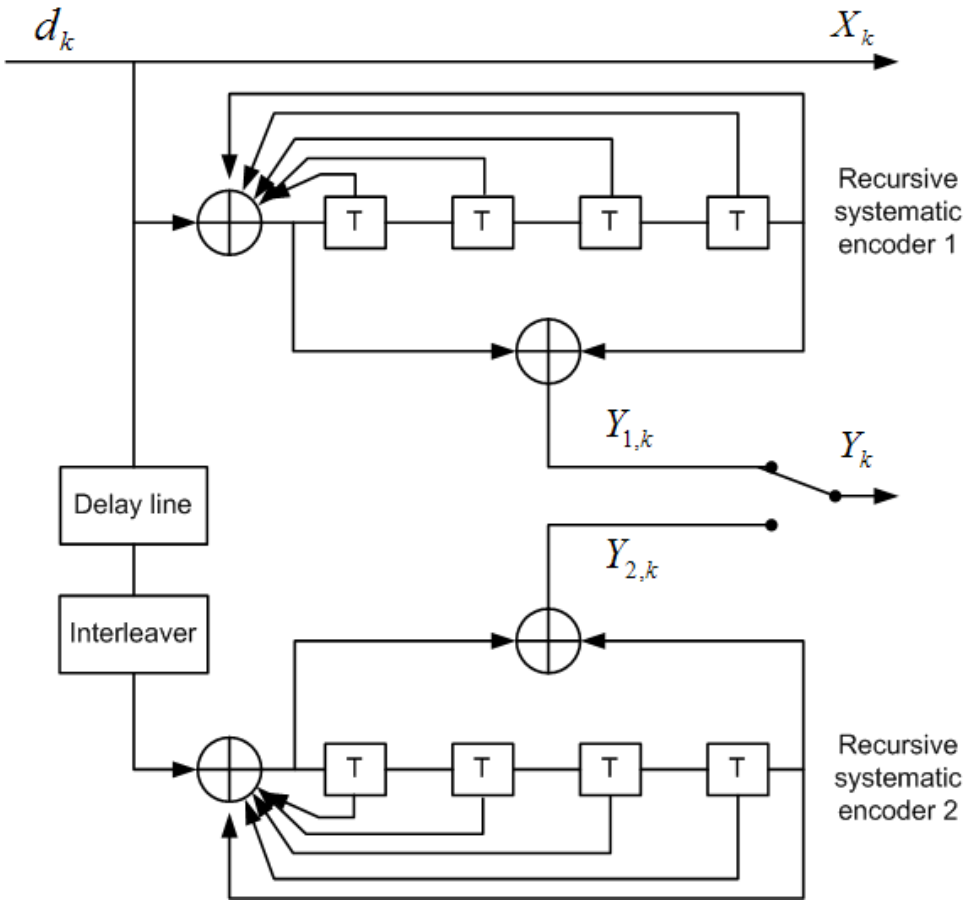

Figure 6.3: Block diagram of a turbo-coding system consisting of two concatenated RSC coders of memory = 4 [102].

In the block diagram d_k is the incoming bit sequence to be encoded. The outputs from this system are given by $X_k = d_k$ and Y_k (where Y_k is a multiplexed output of $Y_{1,k}$ and $Y_{2,k}$).

The unique thing about this encoding system is the use of two convolutional encoders to produce the encoded outputs, the only difference between the inputs

to the two RSC encoders is that the input to encoder 1 is the bit stream d_k while the input to encoder 2 is a delayed and interleaved version of d_k, this process changes the order of the bit sequence entering encoder two.

The behaviour of a turbo coding system is given in the following [102],[106]:

For a basic 1/2-rate convolutional encoder the output is a bit pair given by:

$$X_k = \sum_{i=0}^{K-1} g_{1i} d_{k-i} \mod 2 \quad g_{1i} = 0, 1 \tag{6.4}$$

$$Y_k = \sum_{i=0}^{K-1} g_{2i} d_{k-i} \mod 2 \quad g_{2i} = 0, 1 \tag{6.5}$$

where K is the encoder length, $K-1$ is the memory of the encoder and $G_1 = \{g_{1i}\}$ and $G_2 = \{g_{2i}\}$ are the code generators.

For a turbo coder 1/2-rate RSC coders are used, this type of code is closely related to the convolutional code but it uses a feedback loop to continuously feed back encoded information to the input. This type of coder also sets one of the output bits (X_k or Y_k) to the incoming bits, d_k. A recursive algorithm, shown in equation 6.6, is then used to determine a_k (the memory input) of the system [102], [106].

$$a_k = d_k + \sum_{i=1}^{K-1} g_i^{'} a_{k-i} \mod 2 \tag{6.6}$$

where $g_i^{'}$ is equal to g_{1i} if $X_k = d_k$ and g_{2i} if $Y_k = d_k$.

While this formula shows the output of a single RSC encoder, in a turbo-coding system two of these coders are concatenated together. In the turbo-coder case there will still be two outputs from the encoder, X_k which will be

the original data bits and Y_k which will be the parity bits appended to the data. Y_k though will consist of a combination of Y_{1k} and Y_{2k} (each of which make up half the parity bits to be transmitted), these two encoder outputs will be interleaved together and in some cases punctured according to a puncturing pattern [102].

To decode this type of code a log-likelihood ratio process at the receiver can be used. A turbo-decoder from [102] is shown in figure 6.4

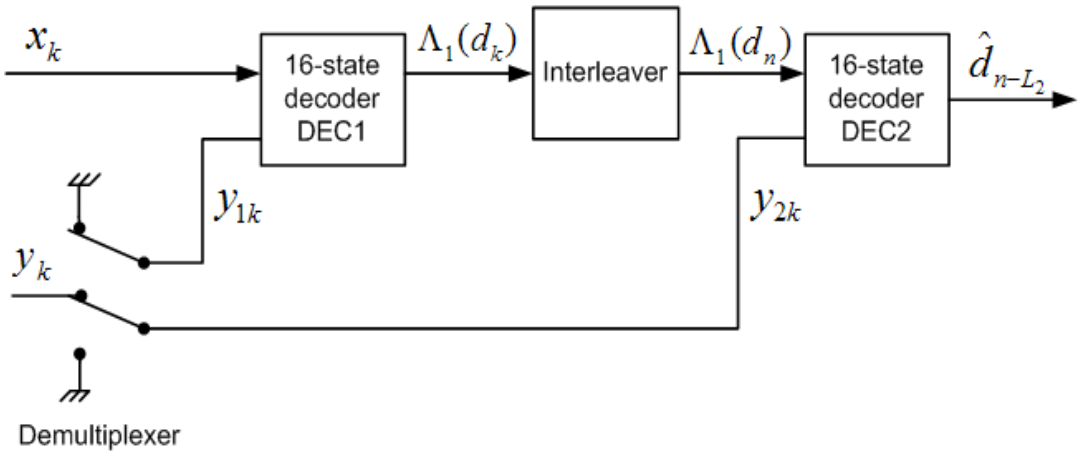

Figure 6.4: Block diagram of a turbo-decoding system from [102].

This diagram shows two separate decoding blocks, DEC1 and DEC2, that are used to decode the encoded information. The input to this decoding system is the data x_k and the redundant bits y_k these bits are the bits generated during the turbo-coding process with noise added from transmission.

In this system $\Lambda_1(d_k)$ is found using a log-likelihood detection algorithm given in equation 6.7:

$$\Lambda_1(d_k) = \log \frac{P_r\{d_k = 1/observation\}}{P_r\{d_k = 0/observation\}} \tag{6.7}$$

This turbo-coding technique has been shown to perform well in OFDM systems, this method has been proposed as a replacement to inner convolutional coding in the basic OFDM standard while still using a Reed-Solomon outer encoding block [101], [103].

6.3 Cyclic prefix

In standard DFT-based OFDM several considerations need to be made in the formation and transmission of an OFDM symbol, one of the main issues is the cyclic prefix addition to reduce inter-channel interferences. For wavelet-based OFDM it was found that this cyclic prefix was unnecessary due to the spectral characteristics of the OFDM symbols formed from wavelet filtering [33], [91]. This section will consider this in the proposed system and look at whether the same applies in this case.

For OFDM systems that employ the discrete Fourier transform in the formation of the symbols rectangularly filtered pulses are used in the modulation of the OFDM symbol, due to this type of filtering DFT-OFDM symbols have substantial spectral overlap [33]. In these cases as soon as multi-path channel distortion occurs to the symbols these overlapping subcarriers will start to interfere with each other causing inter-carrier interference (ICI). ICI is an undesirable effect that will increase the bit error rates of the data being received.

Work was produced by S. Weinstein in 1971, [21], on how this could be avoided and in it was proposed that a cyclic extension, or guard interval, could

be appended to the OFDM data to mitigate this effect. This cyclic extension should be long enough to span the length of the channel impulse response so subchannel isolation can be achieved at the receiver.

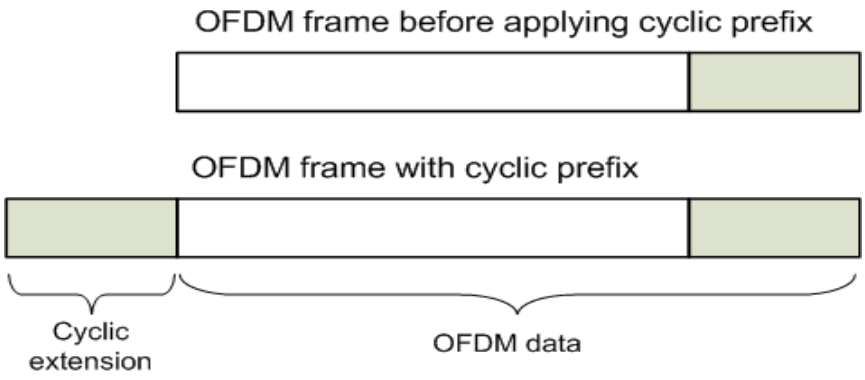

Figure 6.5: An OFDM symbol before cyclic prefix (above) and after adding cyclic prefix (bottom).

For all practical DFT-based OFDM systems this cyclic extension has become the standard [73]-[77]. As shown in figure 6.5 the accepted method for applying a cyclic extension to an OFDM symbol is to take a portion of the end of the OFDM symbol (with a length N_c) and append this portion to the start of the symbol [93]. This cyclic prefix length, N_c, is selected depending on the channel impulse response length, L_h, to assure its length is adequate.

6.3.1 Cyclic Prefix in Wavelet-Based OFDM

In the proposed system wavelet-based OFDM is used instead of DFT-based OFDM, this difference in symbol formation changes some of the characteristics of the system as the use of wavelet filters affects the spectral characteristics of a signal being transmitted.

In [33] an analysis of wavelet-based OFDM was performed and how the characteristics of this type of OFDM affect the need for a cyclic prefix extension. In this work it was found the spectral properties of an OFDM symbol filtered using a DFT process were substantially different to OFDM symbols filtered using wavelet based filters. An example of these contrasting spectral characteristics are shown in figures 6.6 and 6.7.

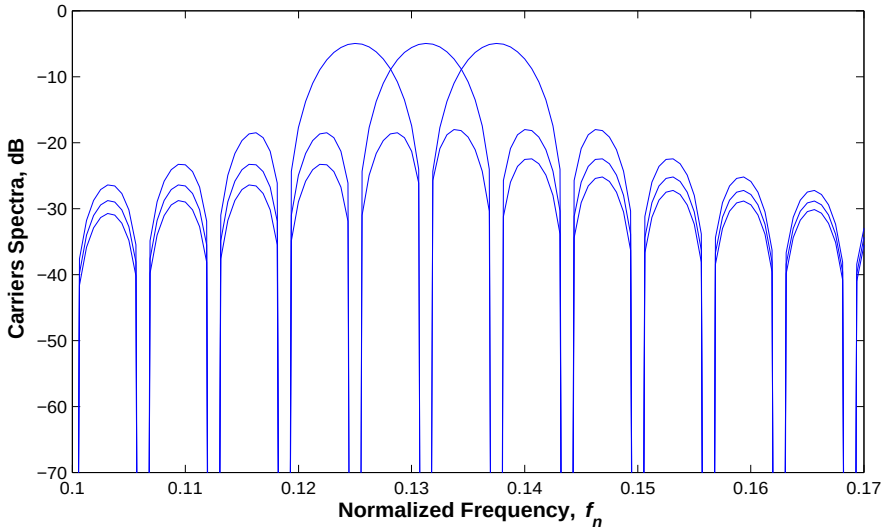

Figure 6.6: The magnitude spectrum of three subchannels of a DFT-OFDM transmitted symbol.

These figures show that the attenuation of the sidelobes for symbols transmitted using DWT-OFDM is much greater than the attenuation of the sidelobes for DFT-based OFDM, this means the amount of energy overlapping from neighbouring subchannels is substantially less for DWT-OFDM signals.

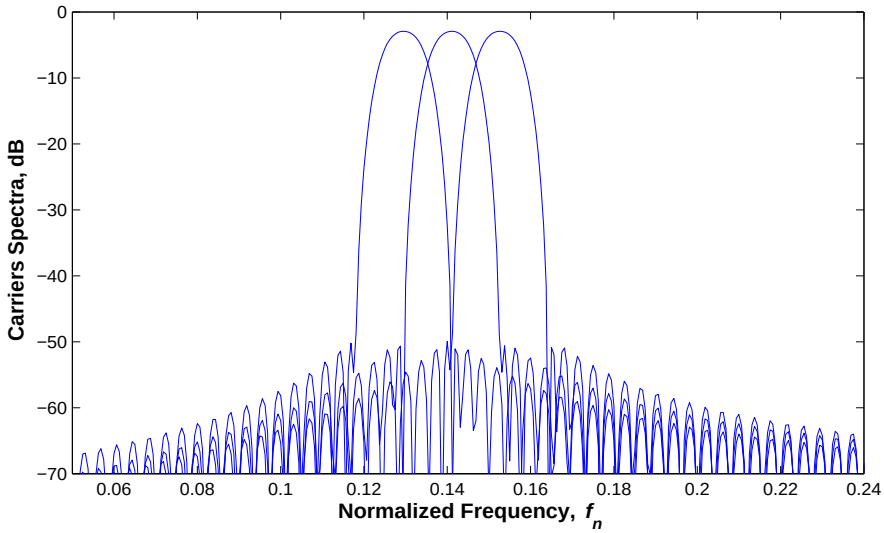

Figure 6.7: The magnitude spectrum of three subchannels of a DWT-OFDM transmitted symbol.

To maintain orthogonality of the OFDM symbols and to fulfil Nyquist's criterion for zero ISI, the choice of transmit filters is of utmost importance. In DFT-OFDM these filters are rectangular, effectively truncating the sinusoidally modulated symbols in time [21], [38], this harsh symbol truncation will result in an almost $[\sin(x)/x]^2$ shape of the spectra which leads to the high degree of spectral overlap as shown in figure 6.6.

Orthogonality of these transmitted symbols can be maintained if the transmit channel is perfect, distortionless and time invariant. In reality, though, time variant effects and multi-path fading channels can disrupt the shape of these symbols and hence the orthogonality of the incoming signals. In [21] it was noted that these truncated sinusoids can be delayed by differing amounts in a frequency selective and multi-path transmission medium and distortions from

the channel could also affect the on-off transitions of the modulated carriers. It is for these reasons that the use of guard intervals/cyclic prefixes were employed. By appending a guard period that is longer than the channel impulse response to the OFDM symbols ICI in the system could be reduced.

The filters used in DWT-OFDM, on the other hand, do not have the harsh rectangular response as that of the DFT-based filters, this contributes to the much higher attenuation of the sidelobes shown in figure 6.7. Wavelet filters still fulfil the orthogonality properties necessary to avoid distortions and they also fulfil the Nyquist criteria for zero ISI and by slightly extending the OFDM symbol in time they also give the OFDM symbols high spectral containment which makes this method attractive in multi-path fading channels and slowly time varying channels.

This high level of attenuation can reduce the amount of distortion when orthogonality is lost between the subchannels, this makes DWT-OFDM more robust than DFT-OFDM in multi-path fading channels. It is also for this reason that DWT-OFDM does not require a guard interval on the transmitted OFDM blocks [33], [36], [38].

6.4 Synchronisation

When receiving OFDM frames, synchronisation of the incoming symbols is extremely important to allow for the accurate reconstruction of the data. To achieve this data recovery at the OFDM receiver three main criteria must be considered to ensure the accurate reception of the data, these are: symbol timing synchronisation, carrier frequency synchronisation and sampling clock

synchronisation [94].

In the work in [95] both frequency and timing errors were considered and how these can affect the received OFDM symbols. In this work it was described that if a receiver's carrier is offset by a integer value of the subcarrier frequency spacing then the subcarriers will remain orthogonal relative to each other but the received data will not be accurate, resulting in a high bit error rate (BER). Also described was the case where the receiver carrier offset is a non-integer multiple of the subcarrier spacing, in this case there will be energy spilling over from adjacent subcarriers.

This concept can be explained visually in figure 6.8 [95].

If the case shown in the bottom plot of figure 6.8 occurred there will be a loss of orthogonality between the subcarriers and inter-carrier interference will occur. The figures show that the adjacent subcarriers will spill energy into their neighbouring subcarrier bands. The energy contributions from each subcarrier is shown with the overlaid symbols on the graphs.

Apart from frequency timing synchronisation, OFDM systems are also susceptible to symbol timing offset which causes inter-symbol or inter-block interference between incoming OFDM frames. If symbol timing is not correctly aligned to the incoming OFDM frames the receiver will apply the DFT window to the incorrect starting point for the symbols, therefore causing the window to span two consecutive OFDM frames, this will of course degrade the received data [94],[95].

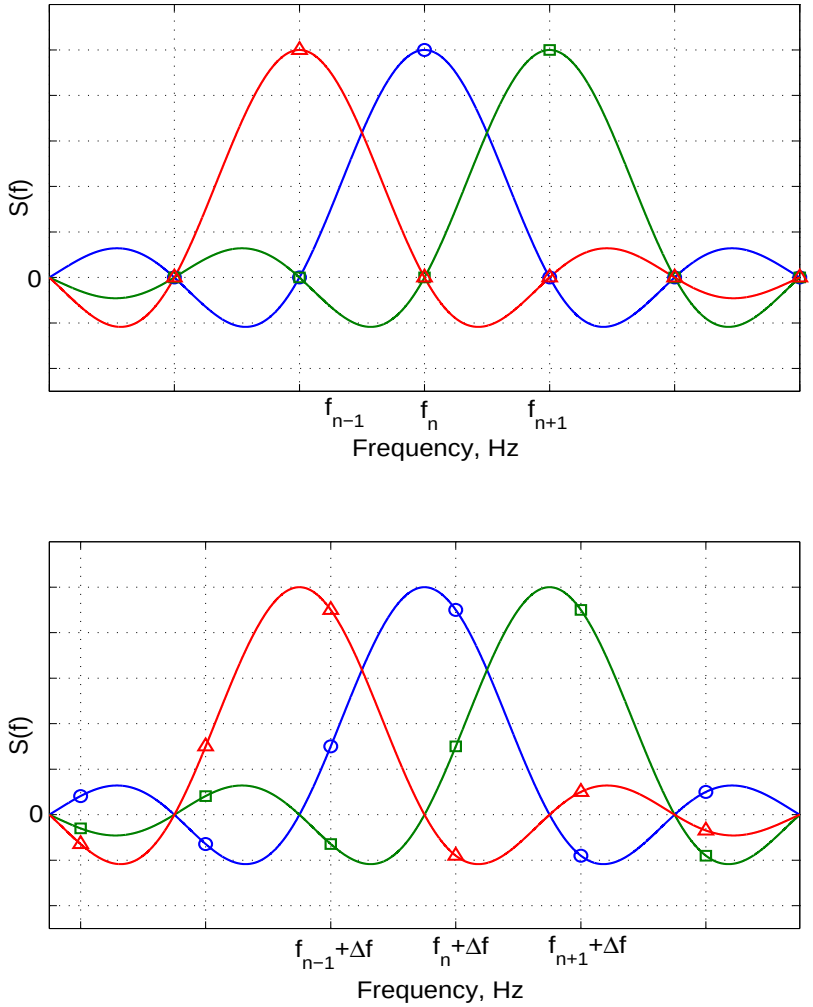

Figure 6.8: How frequency offset at a receiver (shown by the overlaid symbols) can affect a received OFDM symbol. Top figure: carrier frequencies are synchronised. Bottom figure: carriers with a frequency shift of Δf Hz.

To try to mitigate these effects OFDM receivers tend to use several frequency and symbol timing techniques to synchronise to an incoming OFDM frame. Generally a coarse frequency/timing synchronisation will occur first and then a

fine synchronisation process will follow to completely correct these issues.

6.4.1 Symbol Timing and Frequency Synchronisation

For many practical DFT-based OFDM systems, including the European digital television broadcasting system (DVB-T), the transmitted OFDM symbols contain a cyclic prefix and pilot carriers [24]. The cyclic prefix extension to the OFDM blocks is intended to reduce inter-symbol interference resulting from the harsh truncation of the IDFT process as well as the effects of multipath fading channel environments while the continuous pilot carriers are used in channel estimation in the system [96]. Both of these additional components can be utilised in symbol timing synchronisation algorithms [94] - [98].

In [97] a maximum likelihood (ML) estimator is given for the synchronisation of OFDM symbol timing and frequency offset, this method is based on using information about the cyclic prefix and the pilot carriers transmitted with OFDM data.

This ML estimator assumes there will be two parameters that are unknown to the OFDM receiver system, these two unknowns are: the timing of the incoming OFDM block as well as the precise carrier frequency, on top of these there is also noise from the channel corrupting the data. These effects will cause the received signal to be:

$$r(k) = s(k-\theta)e^{j2\pi(f_n+\Delta f)f} + n(k) \tag{6.8}$$

where θ is the symbol timing offset, Δf is the frequency offset of the receiver carriers and $n(k)$ is additive white Gaussian noise from the channel.

Normally with large amounts of data ($s(k)$) being transmitted, the probability distribution of the transmitted symbols would tend to be a Gaussian process with an independent Gaussian distribution representing the real and imaginary components of the transmitted data, but since in many applications a cyclic prefix is included in the transmitted symbols the distribution will actually be correlated within OFDM blocks [97], [98]. One accepted cyclic prefix method is to take the last N_c symbols from an OFDM data block and append that data to the start of the OFDM block. It is this property that is exploited in the maximum likelihood estimator algorithms used for frame timing synchronisation.

The maximum likelihood estimators are based on an observed interval of an OFDM stream, this interval is longer than one OFDM block since the precise timing of the incoming block is unknown; taking a longer observation interval will allow the synchronisation system to obtain enough information to observe the cyclic prefix of the incoming data block. An example of an observation interval used by the synchronisation system in shown in figure 6.9 [98].

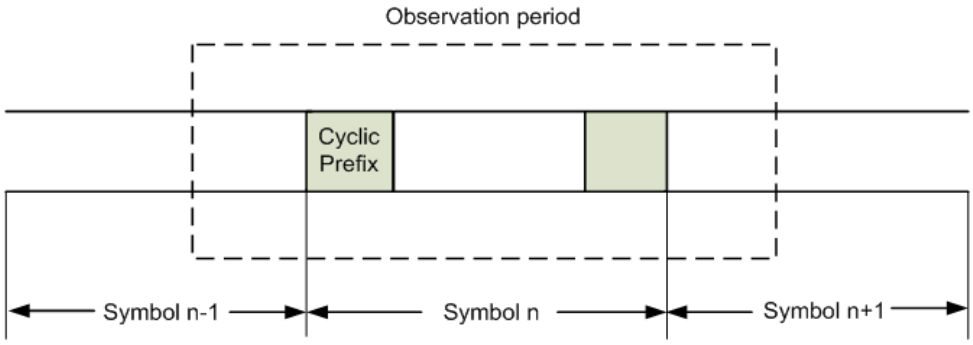

Figure 6.9: An observed portion of an OFDM signal with cyclic prefix shown.

The length of the observed signal in this type of synchronisation system is

$2N + N_c$ where N is the number of subcarriers and N_c is the length of the cyclic prefix extension. This observed signal is then passed to a system that can detect the correlation in the signal from time delayed versions of the observed signal. This system will give the most likely start point of the OFDM block and the most likely carrier frequency offset from this correlation data. The system used for this is described in [97].

The estimated timing offset, $\hat{\theta}_{ML}$ and the estimated frequency offset $\widehat{\Delta f}_{ML}$ can be calculated using the following algorithm:

Taking the observation period, $r(k)$, energy and correlation of the signal are both considered. The energy function used in this system is found by the addition of power from the observed signal sample and a sample of the observed signal with a delay of N. This energy term is defined as:

$$\Phi(m) = \frac{1}{2} \sum_{k=m}^{m+N_c-1} |r(k)|^2 + |r(k+N)|^2 \tag{6.9}$$

This energy term is subtracted from a correlation term given as:

$$\gamma(m) = \frac{1}{2} \sum_{k=m}^{m+N_c-1} r(k) r^*(k+N) \tag{6.10}$$

From this information both the frequency and timing offset can be calculated as:

$$\hat{\theta}_{ML} = \arg\max\{|\gamma(\theta)| - \rho\Phi(\theta)\} \tag{6.11}$$

where ρ is a term dependent on the signal to noise ratio in the channel and is given as $\rho = \frac{SNR}{SNR+1}$.

$$\widehat{\Delta f}_{ML} = -\frac{1}{2\pi}\angle\gamma(\hat{\theta}_{ML}) \tag{6.12}$$

where $\angle$ represents the angle of the complex number.

Synchronisation Without a Cyclic Prefix

While the method described above is possible for OFDM systems that use cyclic prefixes, the proposed system, as it is based on wavelet OFDM, need not have a cyclic prefix. Other synchronisation techniques have been proposed based on pseudo-random or known periodic preambles being appended to the OFDM frames [95], [99], [100]. These types of synchronisation methods would suit the proposed OFDM system for this reason.

In [99] a particularly practical synchronisation technique is described that consists of using a two-symbol training sequence placed at the start of an OFDM block. For the first training symbol symmetry in the time domain is required, this is ensured by transmitting a pseudo-random sequence on the even carrier frequencies while transmitting nothing on the odd carrier frequencies. This characteristic means the system relies on looking for the two identical halves of this time domain symbol to make a decision on timing synchronisation. The second training symbol is transmitted with a pseudo-random sequence on the odd carrier frequencies and another pseudo-random sequence on the even frequencies so frequency offset can be determined by the system.

The symbol timing estimation using this method is determined by creating a timing metric from correlative information in the received signal. For a received OFDM signal consisting of N subcarriers the receiver will use a sliding analysis

window of length N to take in samples of the incoming OFDM signal, d_m. A correlation value, $P(k)$ is then found from equation 6.13.

$$P(k) = \sum_{m=0}^{N/2-1} (d^*_{k+m} d_{k+m+(N/2)}) \tag{6.13}$$

where k is the time index of the first sample taken in the window of length N.

From here an energy metric, $R(k)$ is also defined as shown in equation 6.14.

$$R(k) = \sum_{m=0}^{N/2-1} |d_{k+m+(N/2)}|^2 \tag{6.14}$$

Finally the timing of the incoming symbols can be found using the timing metric, $M(k)$, found from these two correlation and energy metrics as shown in equation 6.15.

$$M(k) = \frac{|P(k)|^2}{(R(k))^2} \tag{6.15}$$

The result of this is a function where the timing of the incoming OFDM symbol can be found when the function is at a maximum. It is at this point the receiver system can assume the starting point of the OFDM symbol.

This training sequence method can also be used to determine the coarse and fine frequency offsets of the carrier frequencies. To perform a coarse frequency offset estimation the first training sequence is used where pseudo-random noise is only transmitted on the even carrier frequencies. Fine adjustments can then be made by using the second training sequence where pseudo-random noise is transmitted on both the even and odd carrier frequencies.

A coarse estimate of the frequency offset can be calculated by finding the

phase difference between the two halves of the first training sequence. This can be achieved by finding the angle information from the correlation metric, $\hat{\phi} = \angle(P(k))$. If $|\hat{\phi}|$ is less than π then the frequency offset can be found using just the first training sequence as shown in equation 6.17.

$$\widehat{\Delta f} = \hat{\phi}/(\pi T) \tag{6.16}$$

where T is the OFDM symbol period.

If the actual phase difference is greater than this, i.e. $|\hat{\phi}| > \pi$ then the actual frequency offset will be:

$$\Delta f = \frac{\phi}{\pi T} + \frac{2z}{T} \tag{6.17}$$

where z is an integer. In this case the second training sequence will be required to perform a fine frequency offset estimation on the OFDM carrier frequencies.

Since the value of z is unknown the extra phase shift is also unknown and will need to be found by maximising another metric, $B(g)$:

$$B(g) = \frac{|\sum_{k\epsilon X} x^*_{1,k+2g} v^*_k x_{2,k+2g}|^2}{2(\sum_{k\epsilon X} |x_{2,k}|^2)^2} \tag{6.18}$$

where $x_{1,k}$ and $x_{2,k}$ are the FFTs of the first and second training symbols (after coarse frequency correction has been applied), v_k is the pseudo-random sequence on the even frequencies of the second training sequence, g is an integer that has a range of all possible frequency offsets and X is a set of all the even frequency components.

The final estimate of this frequency offset, $\hat{g}$, can then be used to finely

correct the carrier frequency offset to obtain $\widehat{\Delta f}$ using equation 6.19.

$$\widehat{\Delta f} = \frac{\hat{\phi}}{\pi T} + \frac{2\hat{g}}{T} \tag{6.19}$$

This method can be used with or without a cyclic prefix which makes it possible to be used with the proposed system.

6.5 Dealing with Multiplexed Multimedia Data

In a video data stream transmitted via the DVB-T technique the multimedia data transmitted consists of a multiplexed stream, the standard adopted in this type of system is the MPEG-2 standard [107] where encoded video and audio is multiplexed together with system data before being processed by the OFDM system.

In the proposed system the performance of multiplexed data streams was considered, this meant an analysis needed to be performed on how the quality of audio could be affected by the compressive OFDM method and whether this type of data needed to be treated differently to the image data. Figure 6.10 shows the results obtained when compressing and transmitting audio and images in the new compressive OFDM system.

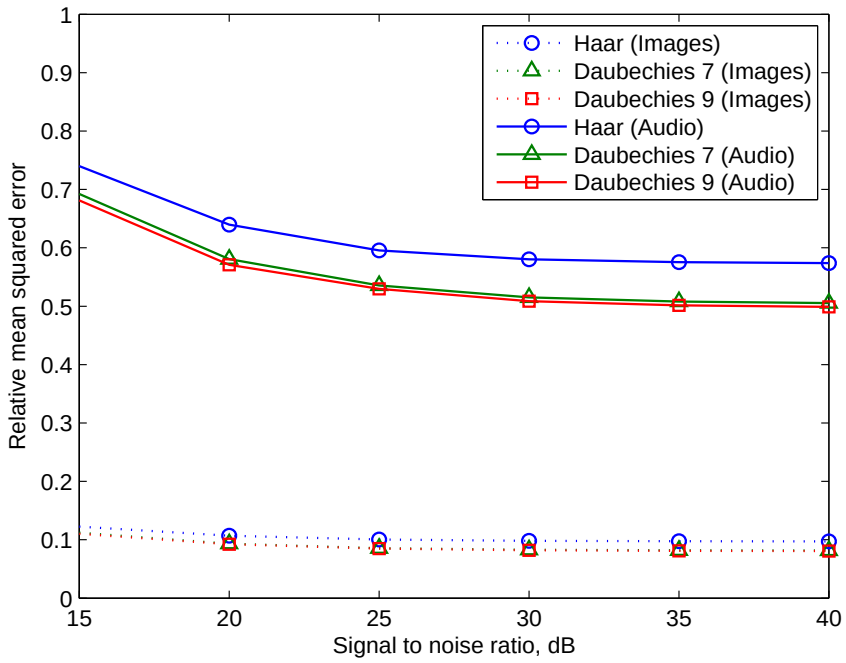

Figure 6.10: Comparing the results from the proposed system for both images and audio data.

Looking at figure 6.10 gives an indication of the reduction in quality obtained in the case of audio data transmission. In this situation there was a RMSE increase of 0.419 at a signal-to-noise ratio of 40 dB.

This result means that audio certainly would need to be treated differently to the image/video data when being transmitted as a multiplexed stream using the proposed compressive OFDM technique. A logical way to solve this problem would be to modulate the audio component as a non-compressed stream using one of the more traditional methods of OFDM transmission while the video frames could be transmitted simultaneously on separate subcarriers using the compressive OFDM method which is shown to perform well with image and

video data (this will be considered in more depth in chapter 7).

This solution would not affect the compression aspect of the system considerably since audio is a relatively small component of the MPEG multiplexed data stream only contributing to approximately 16% of the overall data contained in the MPEG stream [107].

6.6 Conclusions

This chapter has addressed some of the important blocks in an OFDM system and considered appropriate methods of implementing these blocks in the new compressive OFDM system. It has also considered multiplexed multimedia data streams and looked at how the system could handle this type of data.

In this chapter the issue of the channel coding was firstly addressed, most OFDM standards consist of two types of channel coding, in the DVB-T standard these are outer Reed-Solomon coding and and inner convolutional encoder, in the IEEE 802.11a standard convolutional encoding is used in the channel coding stage. This chapter looked at Reed-Solomon encoding and examined how this type of encoding works, this chapter also looked at turbo-coding which has been considered as a good replacement for basic convolutional encoding since its structure of two concatenated convolution encoders allows good performance to be achieved in OFDM systems, [101], [103].

The second issue addressed in this chapter was the need for a cyclic prefix, the cyclic prefix is defined as a number of redundant samples from the end of an OFDM block being appended to the start of an OFDM block. The purpose of this cyclic prefix is to reduce the ICI and IBI occurring to the data due to

multi-path fading channel effects at transmission. In the literature the cyclic prefix was found to be beneficial to DFT-based OFDM [21], [23], [33], [83],[93] where the DFT-process and transmit filtering results in a harsh truncation of the transmitted OFDM symbols. This harsh truncation results in a spectrum that resembles a sinc function with large amounts of spectral overlap occurring between neighbouring subcarriers. This chapter also addressed how the wavelet transform and wavelet filtering of OFDM symbols has shown to reduce the effect of this spectral overlap. This has allowed wavelet-based OFDM, such as the proposed compressive OFDM system, to improve on the spectral containment properties of OFDM systems. In wavelet based systems the literature has shown that cyclic prefixes are of less importance and can be removed to improve on data transmission efficiency [33], [36], [38].

Thirdly this chapter addressed the issues of symbol timing and frequency offset in received OFDM symbols. Synchronisation is extremely important in all transmission systems and needs to be addressed in a system to allow correct reception of data. This chapter looked at the two main symbol timing and frequency synchronisation techniques that are commonly used in OFDM systems, firstly a method of synchronisation was analysed which made use of the cyclic prefix extension in synchronising the system [97]. The second method considered was for the case where no cyclic prefix is used; it is this method that was considered more appropriate for the proposed wavelet-based OFDM system as the cyclic prefix is unnecessary. The latter method considered uses time-symmetric training sequences to aid in time and frequency synchronisation of the incoming OFDM symbols [99].

Lastly this chapter considered multiplexed multimedia data such as MPEG

encoded data and looked at how the system could handle this type of data. From experiments it was found that the audio would have to be considered separately to the video and would need to be transmitted using a non-compressive transmission method. This method of handling multiplexed multimedia data was also found to not dramatically reduce the compressive aspect of the new system as audio only contributes to around 16% of the total data in a multiplexed multimedia data stream.

Chapter 7

Results and Performance Analysis of the New Compressive OFDM System

7.1 Introduction

The previous chapter described a novel system where the attributes of wavelet transforms and filters were utilised to produce a system that both compresses data and is able to filter the data so as to obtain the orthogonality required to be transmitted using orthogonal frequency division multiplexing (OFDM). The system is unique in that it combines the compression and transmission blocks into one and reduces the computational complexity of the transmission system.

This chapter will look at the performance of this compressive OFDM transceiver system and consider its strengths and weaknesses in the transmission of image and video data.

The first part of this chapter will describe the specific parameters used in the MATLAB simulations and will describe the error measures used in the results analysis. The second part will look in detail at the performance of the system when transmitting image and video data. The chapter will conclude with a summary of the system performance and where improvements can be made.

7.2 Simulation Results of Compressive Transceiver

The novel compressive transceiver system described in chapter 5 and chapter 6 was simulated using the MATLAB simulation software package. Simulations were performed on image and video frame samples to get an indication of the results that would be obtained with multimedia information signals.

The same image and video data set was used in these experiments as was described in chapter 4. The image set was obtained from the USC-SIPI Image Database [86] and the video database was obtained from the Arizona State University Trave video library [87].

The raw data from these multimedia sources were firstly mapped onto 256-QAM constellation symbols and input into the compressive block of the transmitter. In this compressive block a 2-level wavelet decomposition was performed on the data. Several different wavelets from the Daubechies wavelet family were included to consider the effect the wavelet order has on the system being simulated. After the wavelet decomposition was performed on the data the result was subsequently low pass filtered to remove the high frequency components from the wavelet coefficients, these low-pass coefficients were then OFDM transmitted through a multipath fading channel with additive white Gaussian noise

(AWGN) in the same manner as described in section 4.2.

The number of OFDM subcarriers, N, used in this system was 16 and due to the spectral containment of wavelet filters in the transceiver there was no need for a cyclic prefix to be appended to the OFDM data symbols (see section 3.4.2 for more information on this point). The signal-to-noise ratio in these experiments was defined as the ratio of the average QAM-symbol energy over the noise energy per QAM-symbol.

The following subsections will look at the results obtained from firstly transmitting the image data using this compressive system and secondly the results from the video transmission. Each simulation was performed 100 times and the results averaged to give a good indication of the expected performance of the system.

7.2.1 Image Transmission

From the USC-SIPI Image Database [86] 69 images were selected of various subjects, these images were then processed in the compressive transceiver system as described in chapters 5 and 6. As discussed in section 4.2, relative mean squared error (RMSE) was used as one of the measures of transmission error. RMSE is defined as:

$$\text{RMSE} = \sum_{i=1}^{M}\sum_{j=1}^{N}[x(i,j) - x_r(i,j)]^2 / \sum_{i=1}^{M}\sum_{j=1}^{N}[x(i,j)]^2 \tag{7.1}$$

where x and x_r are the original and reconstructed data sets respectively, N is the number of rows in the data set and M is the number of columns in the data set. For an image $N > 1$ and $M > 1$.

The second measure of performance used for images is structural similarity (defined in section 4.2) [88] where contrast, luminance and pixel structure are considered in order to calculate a percentage value for the perceived image quality and the last measure is PSNR also defined in section 4.2. The following results were obtained for images transmitted in this system.

Figure 7.1 shows the results of the average RMSE over all 69 images while figures 7.2 and 7.3 show the average structural similarity and PSNR for these same images respectively. The results shown are for eight different signal to noise ratios: 5, 10, 15, 20, 25, 30, 35 and 40 dB and for 3 Daubechies family wavelets: Haar, db7 and db9.

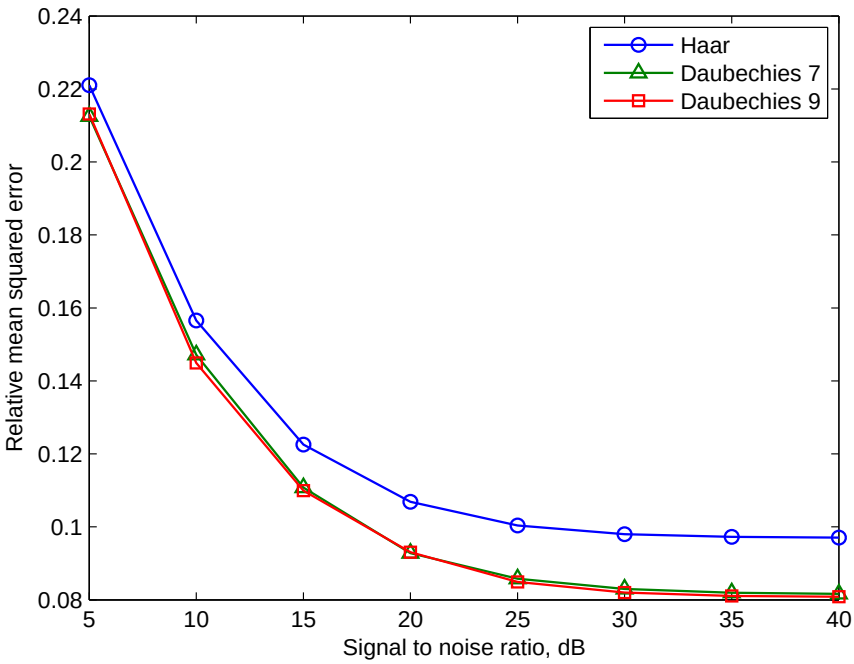

Figure 7.1: Root mean squared error of images for eight different SNRs

The Haar (or Daubechies 1) wavelet is a good control data set for results

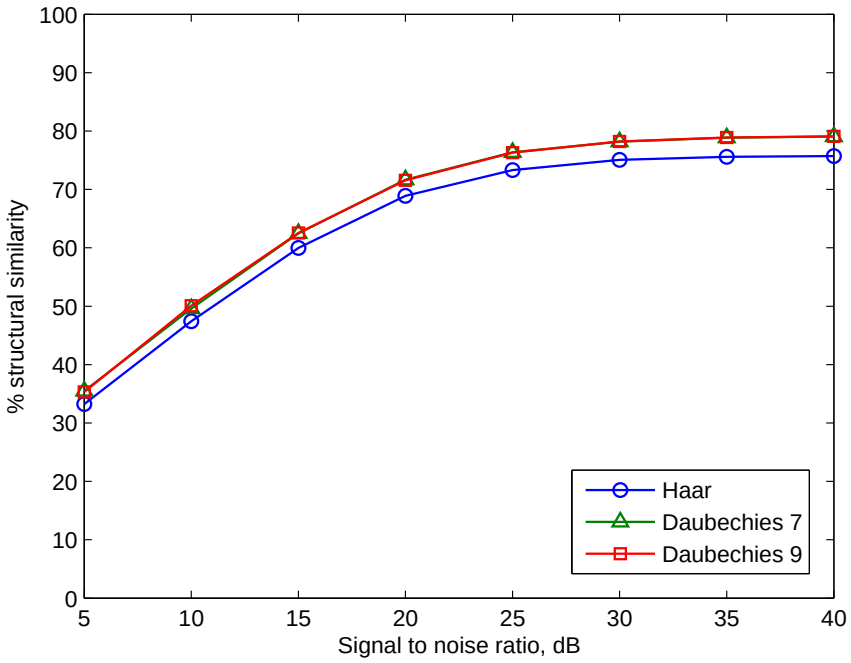

Figure 7.2: Structural similarity of images for eight different SNRs

obtained from wavelet decompositions as it is the simplest of all the wavelets. The Haar wavelet filter basis function is defined as [52]:

$$\psi(t) = \begin{cases} 1, & 0 \leqq t < \frac{1}{2}, \\ -1, & \frac{1}{2} \leqq t < 1, \\ 0, & \text{otherwise}, \end{cases} \tag{7.2}$$

This corresponds to the wavelet basis function shown in figure 7.4

Because of the simplicity of this wavelet basis function the results from a Haar decomposition can be crude and produce some error, it can be seen from figures 7.1, 7.2 and 7.3 that this wavelet's performance is not the best for this

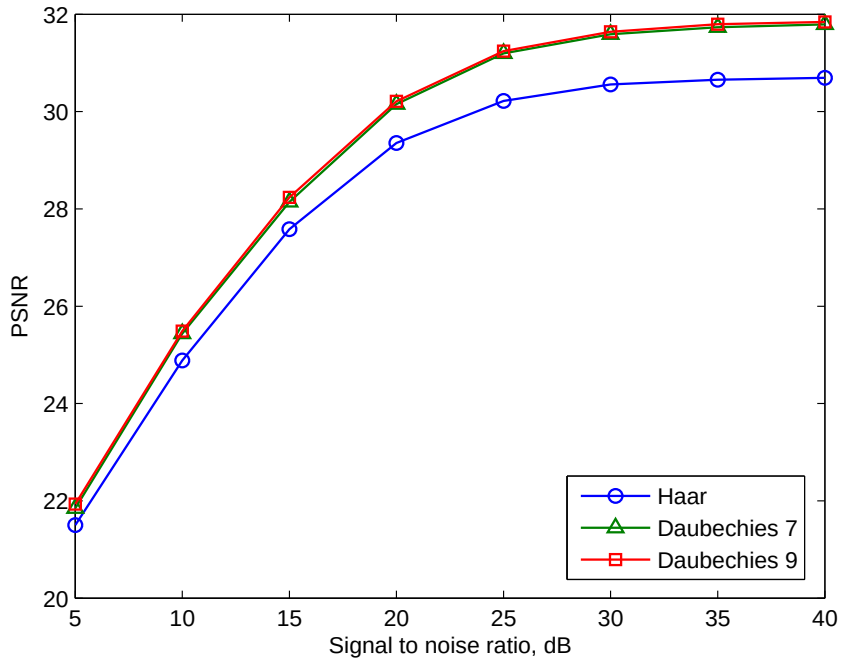

Figure 7.3: PSNR of images for eight different SNRs

application, these figures show more error in the case of the Haar wavelet.

A more desirable type of wavelet for OFDM applications is the Daubechies wavelet family (Haar is also considered one of the Daubechies wavelets but Daubechies order 2+ will be considered here). Daubechies wavelet filters are ideal for use as synthesis and analysis filters in OFDM transmultiplexers due to the wavelet's orthonormal properties. This property is defined as follows; a wavelet is considered orthogonal and perpendicular/normal (i.e. orthonormal) if its scaling functions ($\phi(t)$) and its wavelet function ($\psi(t)$) have the following properties for their inner product [56]:

$$\langle \phi(t-k), \psi(t) \rangle = 0, \text{ for all } k \tag{7.3}$$

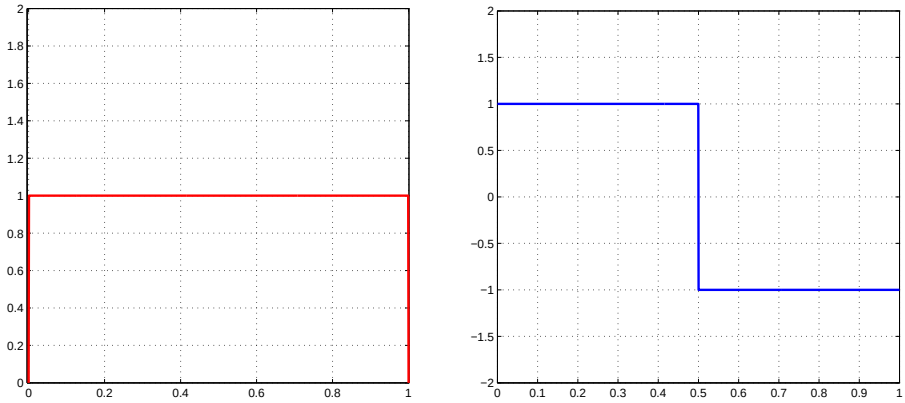

Figure 7.4: The scaling function ($\phi(t)$) and the wavelet function ($\psi(t)$) for the Haar basis

$$\langle \phi(t+l), \phi(t-k) \rangle = \delta[k-l] \tag{7.4}$$

These properties allow orthogonality to be maintained in the OFDM symbols which is a requisite for effective OFDM transmission. An example of the Daubechies 7 scaling and wavelet functions are shown in figure 7.5

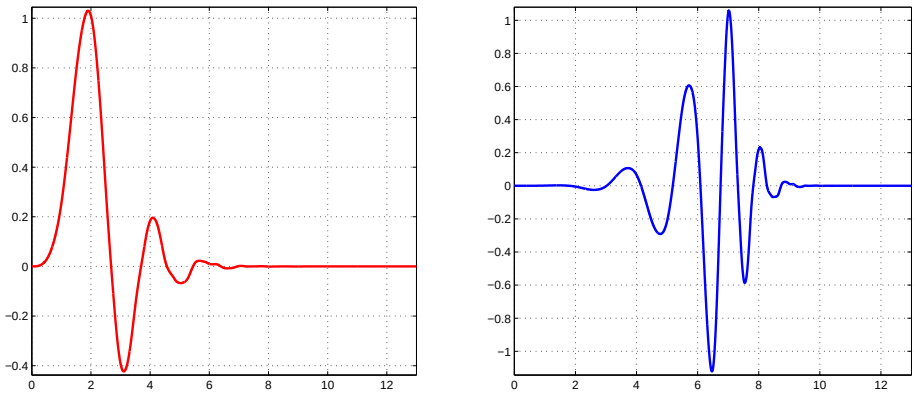

Figure 7.5: The scaling function ($\phi(t)$) and the wavelet function ($\psi(t)$) for the Daubechies 7 wavelet

From figures 7.1, 7.2 and 7.3 it can be seen that the results for the Daubechies 7 and 9 wavelet filters produced very close to the same results for RMSE, structural similarity and PSNR of the received images with results of RMSE $\approx$ 0.081, SSIM $\approx$ 79% and PSNR $\approx$ 31.8dB for a SNR = 40dB.

Another aspect to be considered is the results of this transmission for individual images. Figures 7.6 and 7.7 show the RMSE and structural similarity of the individual received images.

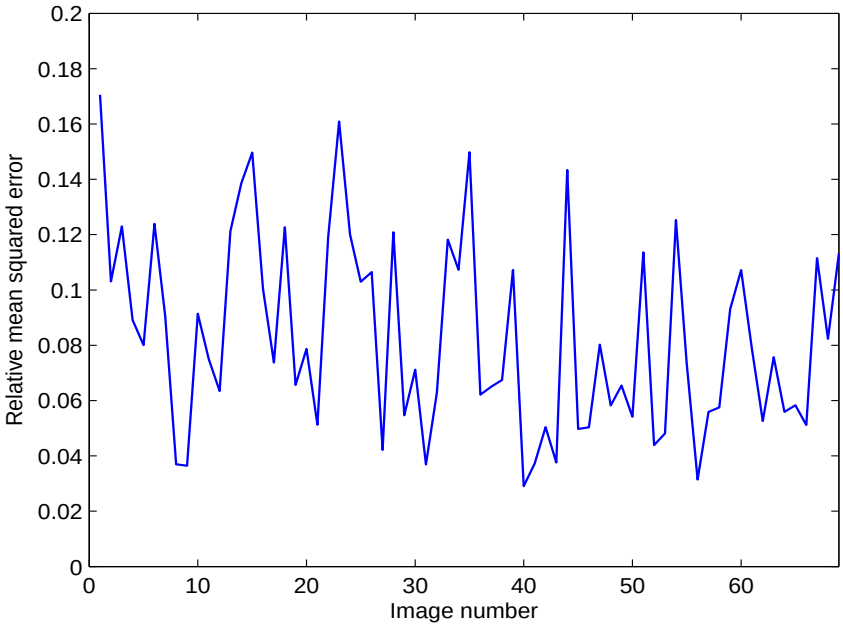

Figure 7.6: Root mean squared error for individual images at SNR = 35 dB

These results were obtained from the image transmission using the Daubechies 7 wavelet for the compression, synthesis filter and analysis filter blocks of the transceiver. Also the signal-to-noise ratio selected was 35 dB which represents a fairly good SNR for wireless transmission.

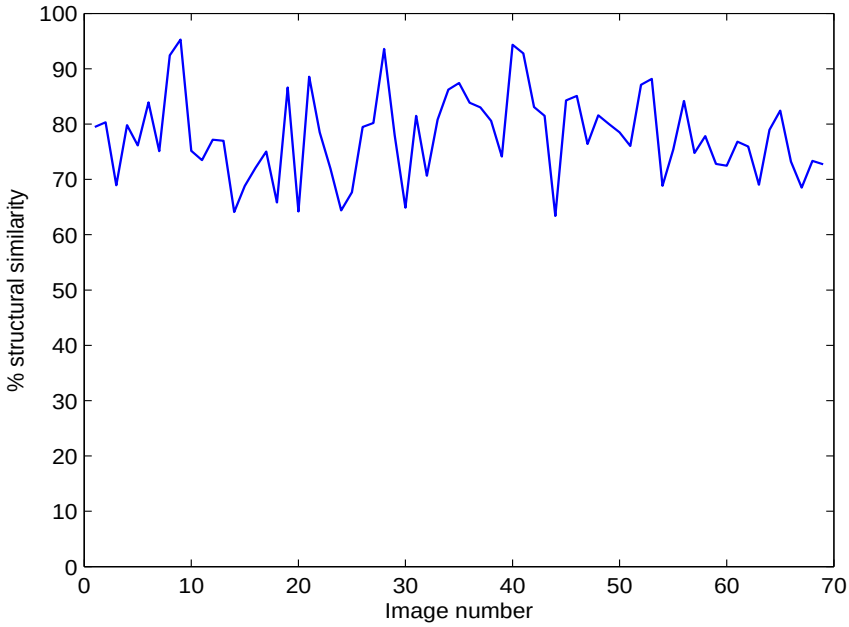

Figure 7.7: Structural similarity of individual images at SNR = 35 dB

The interesting thing about these results is the fact that certain images compressed and reconstructed better than others. The way a wavelet decomposition operates on an image is dependent on the spatial frequency of that particular image. If the image contains large variations in pixel values (particularly black pixels next to white pixels) the image will generally have a higher spatial frequency [46]. As this effect corresponds to large variations in the QAM-mapping (see section 5.2.2 for details on this) the wavelet decomposition of the QAM-symbols will have a large high frequency component which, using the proposed technique, is removed at the compression point. Consequently this will give more error.

The complete set of images used in these experiments are given in appendix

A and can be referred to for more information on the images that compressed well or poorly. The experimental images 8, 9, 40 and 56 were shown to compress well, these images generally consisted of unchanging values of pixels, these represent images with low spatial frequencies. The subjects of these images are either flat, grey textures or are small objects with a large portion of flat, grey background around them (as with the jelly beans in image 40 and the aeroplane in image 56). These images have most of their wavelet coefficients concentrated in the low subband regions which are not removed in this transmission method.

The experimental images 1, 15, 23 and 44 compressed less impressively as they have high spatial frequencies and consist of textures (such as grass in image 1 and roof tiles in image 15) where there is constant light to dark transitions between neighbouring pixels. Because these images have a high spatial frequency when the high-pass wavelet subbands are discarded in the compression process much of the fine details are also discarded giving less structural similarity and more error in the received images.

7.2.2 Video Transmission

The following section will now look at the behaviour of the proposed system with video input instead of images. Again the three different wavelet orders will be assessed: Haar, Daubechies 7 and Daubechies 9.

Figures 7.8, 7.9 and 7.10 give the results obtained from transmitting the video frames via the compressive OFDM technique.

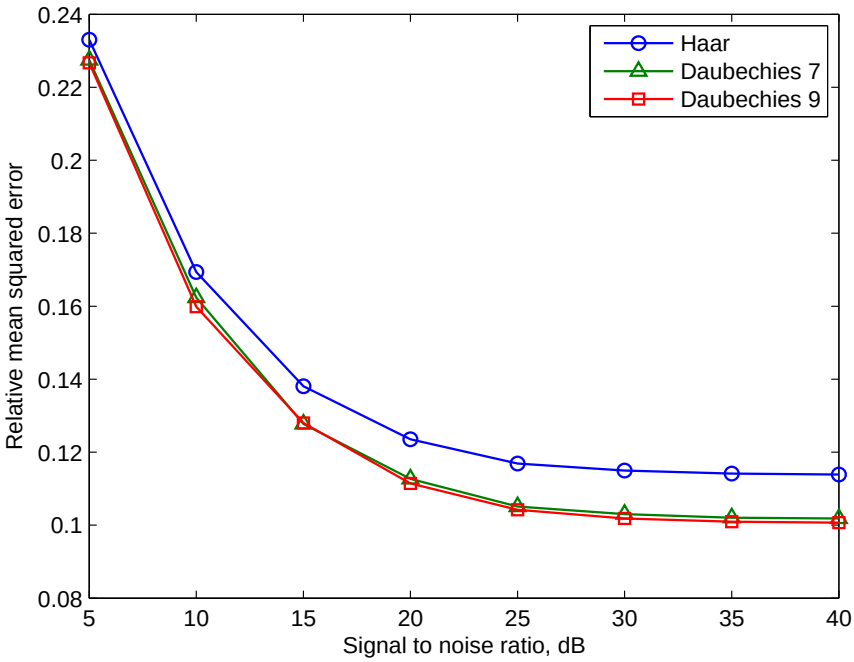

Figure 7.8: Root mean squared error of video frames for eight different SNRs

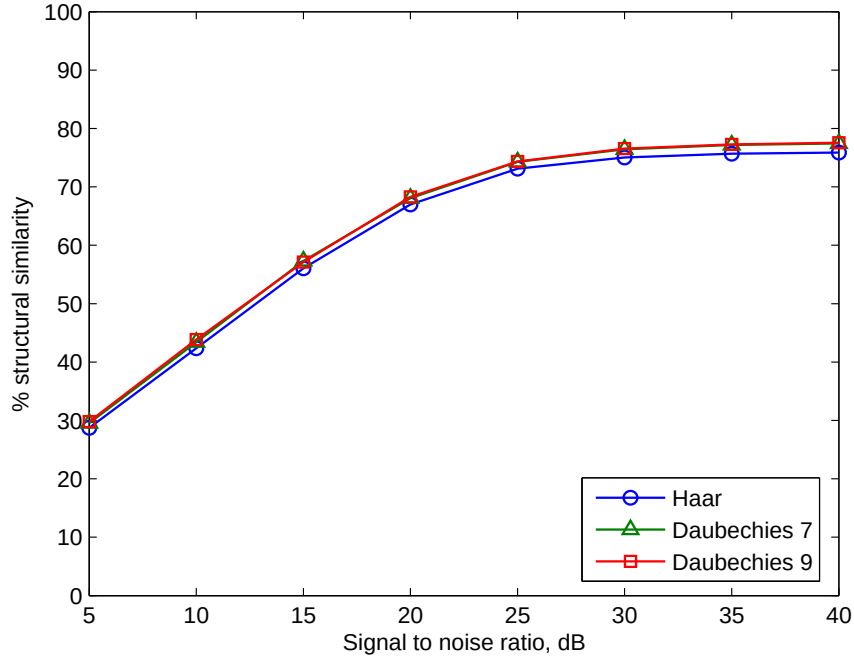

Figure 7.9: Structural similarity of video frames for eight different SNRs

These results show a very similar performance as that shown for image transmission, a slight increase in error was observed which was mainly noticeable in the RMSE results where images had a minimum RMSE of around 0.08 while for the videos the RMSE was closer to 0.1. Again the Haar wavelet has given poorer performance than the other Daubechies family wavelets which have both performed comparably with each other.

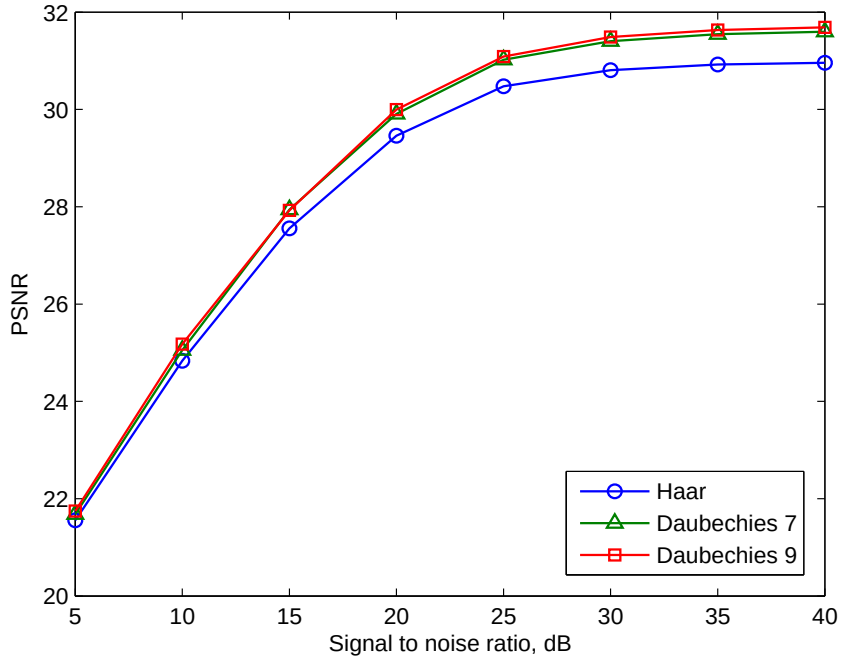

Figure 7.10: PSNR of video frames for eight different SNRs

Similarly to the case of the images the videos achieved a 77.5% average structural similarity at signal-to-noise ratios above around 30dB while dropping to just under 30% structural similarity at a signal-to-noise ratio of 5dB. PSNR also showed a similar behaviour with 31.6dB achieved at 30dB or higher and 21.7dB at low signal-to-noise ratios (i.e. 5dB). These results are considerably closer

to the results obtained for the DFT-OFDM transmission with no compression applied and the next section will look at this comparison in much more detail.

7.2.3 Effects on Computational Complexity

This section will look at the amount of time taken to simulate the processing and transmission of both image and video data using both the traditional DFT-OFDM method with a separate compression block and the proposed compressive OFDM method where compression and transmission are combined. The computer used to perform the MATLAB simulations was running Microsoft Windows XP, it had an Intel Core 2 Duo CPU operating at 3.16 GHz and it had 3.48 Gb of RAM.

Table 7.1 shows the simulation times for both types of OFDM so as to contrast the computational complexity reduction achieved by using the proposed compressive transmission method. These computation times were calculated by averaging the time taken to process different sized images or by averaging the time taken to process the individual frames of videos.

Table 7.1: Computation Times for Image and Video Transmission.

Data Types	**Traditional DFT-OFDM**	**Proposed Method**
256 x 256 pixel images	1.6 sec	0.3 sec
512 x 512 pixel images	4.3 sec	1 sec
1024 x 1024 pixel images	4.3 sec	1 sec
Small (176 x 144 pixel) video	4.8 sec/frame	2.7 sec/frame
Large (352 x 288 pixel) video	14.9 sec/frame	10 sec/frame

Table 7.1 shows the reduction in computation time when using the new compressive OFDM technique. Using the new compressive OFDM technique has reduced the computation time to a quarter of that given by the DFT-OFDM method. This is the case for each of the different sized images. In the case of videos the time has not been reduced by as much but there has been a reduction of almost half when using the new compressive OFDM method.

7.3 Performance Comparison with Traditional DFT-OFDM

To examine the effectiveness of the compressive OFDM transceiver discussed in chapters 5 and 6 the results from this chapter will be compared to the results obtained in chapter 4 for the traditional DFT-based OFDM method with wavelet subband compression prior to transmission. These results will also be compared to DFT-OFDM with no compression applied to the data at all. The following sections will look at these comparisons for image and video data transmission.

7.3.1 Image Transmission Performance

Figures 7.11, 7.12 and 7.13 show a performance comparison of the relative RMSE, structural similarity and PSNR between images transmitted via the traditional OFDM method and the new compressive OFDM system.

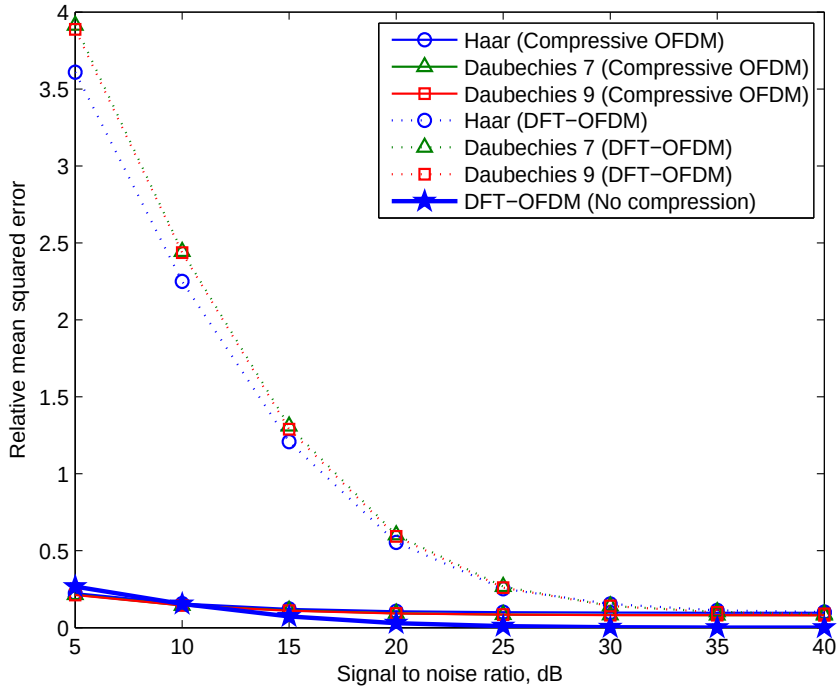

Figure 7.11: Relative RMSE of images transmitted via compressive transceiver system (solid line) and standard DFT-OFDM (dotted line)

These figures show the new compressive method performs particularly well in high noise situations, the results obtained from this method shows a very similar performance to the standard OFDM method with no compression applied to the data. At high signal-to-noise ratios (above approximately 30 dB) both OFDM schemes with compression applied have a similar performance.

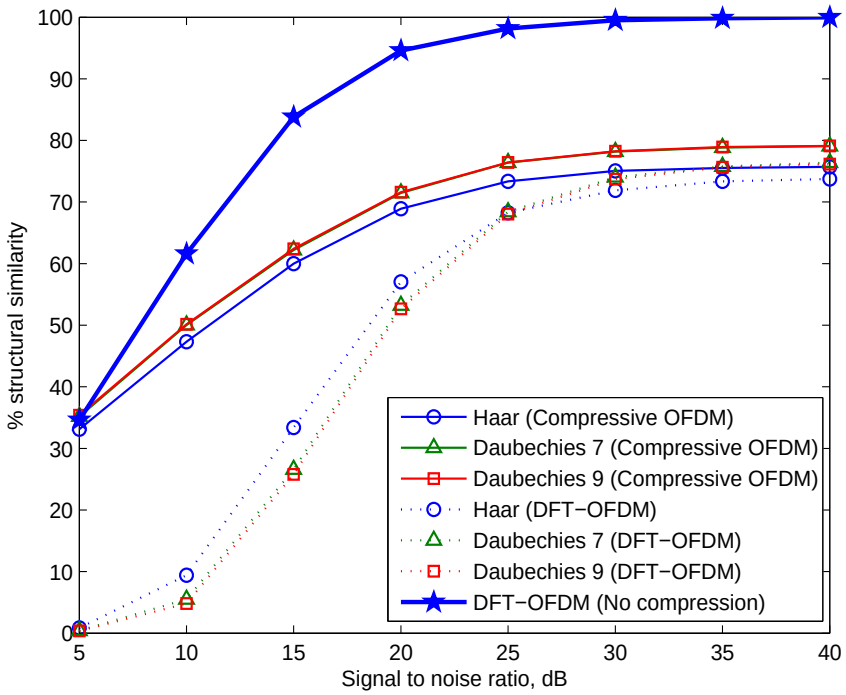

Figure 7.12: Structural similarity of images transmitted via compressive transceiver system (solid line) and standard DFT-OFDM (dotted line)

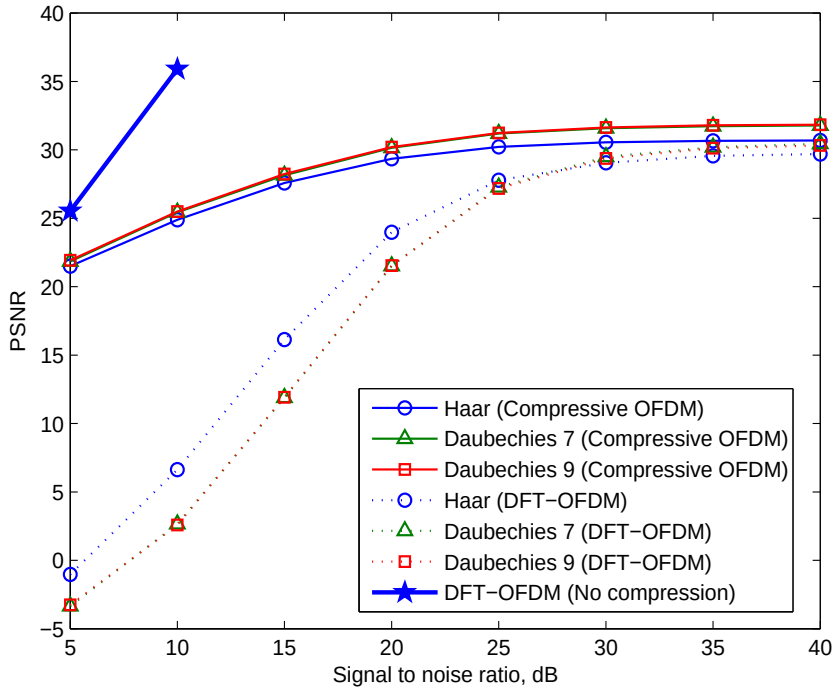

Figure 7.13: PSNR of images transmitted via compressive transceiver system (solid line) and standard DFT-OFDM (dotted line)

The non-compressed OFDM's RMSE error for the high SNRs tends to zero, while the structural similarity approaches 100% and PSNR approaches ∞. This result is to be expected as the compressive schemes used comprise of a lossy compression algorithm, therefore there will always be some loss of quality when compared to the non-compressed OFDM.

With this compression method, as more high frequency wavelet subbands are removed from the image, blurring will occur in the final reconstructed image which will give a structural similarity less than that obtained in an image with no compression applied. As an example, figure 5.3 given in section 5.2.2 shows a reconstructed image after only four high frequency subbands are removed. The reconstructed image has resulted in little visible loss and has a structural similarity of 92%. If the number of subbands removed from this data was increased beyond the four in this example the structural similarity will further decrease and this data loss will become more apparent to the human eye.

The results obtained in this section are good since the total amount of data transmitted in the compressive OFDM method is reduced considerably in relation to the original raw data, in fact the compression ratio for the compressive system is approximately 2.6:1 (this ratio varies slightly for the different wavelet families), therefore to obtain error results so close to the non-compressed OFDM (particularly in low SNRs) is a good initial result for this type of system.

7.3.2 Video Transmission Performance

This section will show the comparison of video transmission using the proposed compressive OFDM system. Again the results from this system will be compared against the DFT-OFDM system with wavelet compression occurring before transmission as well as the DFT-OFDM system with no compression applied to the data at all.

Figures 7.14, 7.15 and 7.16 show RMSE, SSIM and PSNR results obtained for the video frames transmitted.

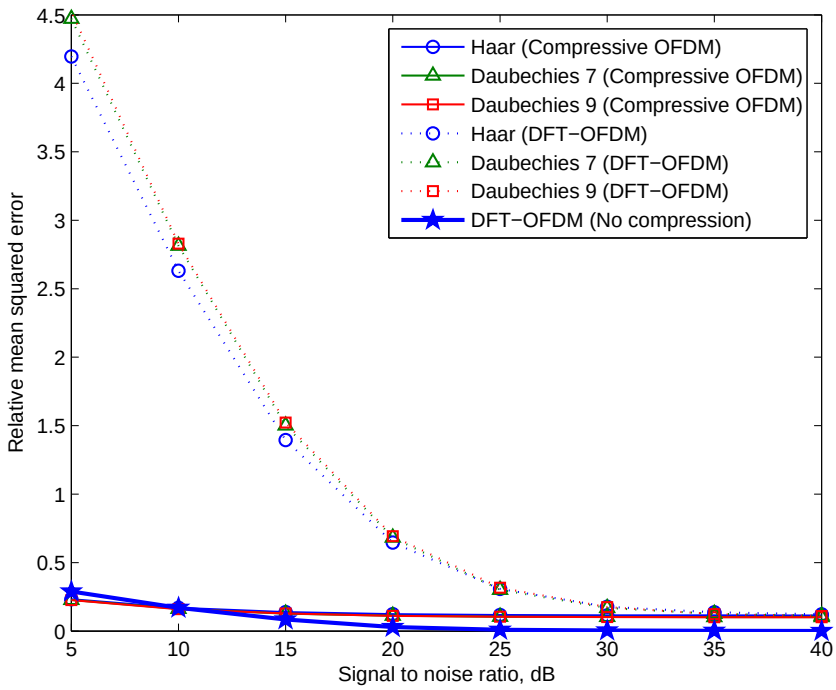

Figure 7.14: Relative RMSE of video frames transmitted via the OFDM transmission systems.

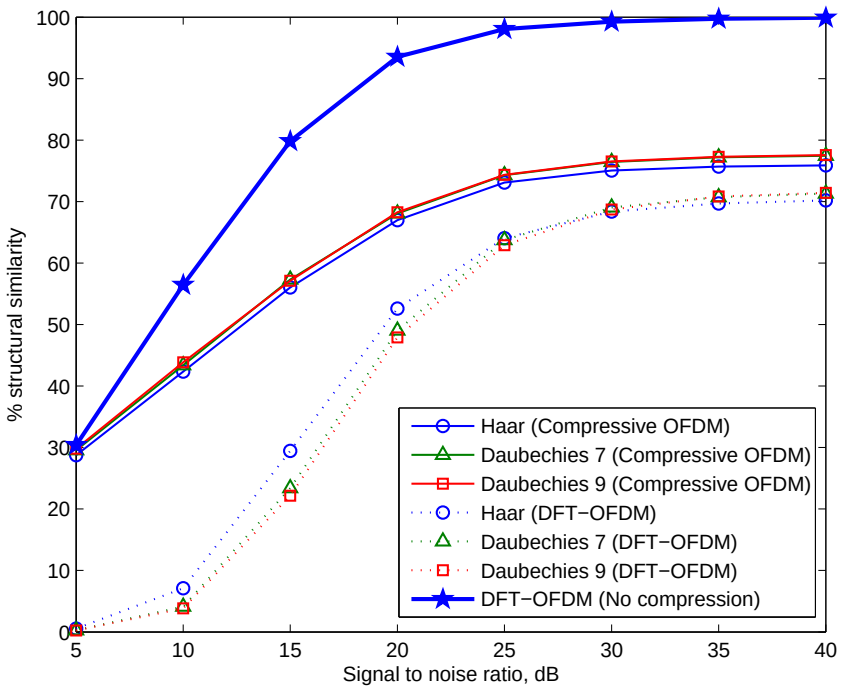

Figure 7.15: Structural similarity of video frames transmitted via the OFDM transmission systems.

These figures show much the same results at those obtained for the images transmitted via the three systems. Again the new compressive method performs well in the high noise situations and again show similar performance to the DFT-OFDM method with no compression and as before the results for videos transmitted through channels with a SNR above 30 dB showed both OFDM schemes with compression applied have similar performance.

This result shows that for both videos and images a consistent performance is expected in these systems.

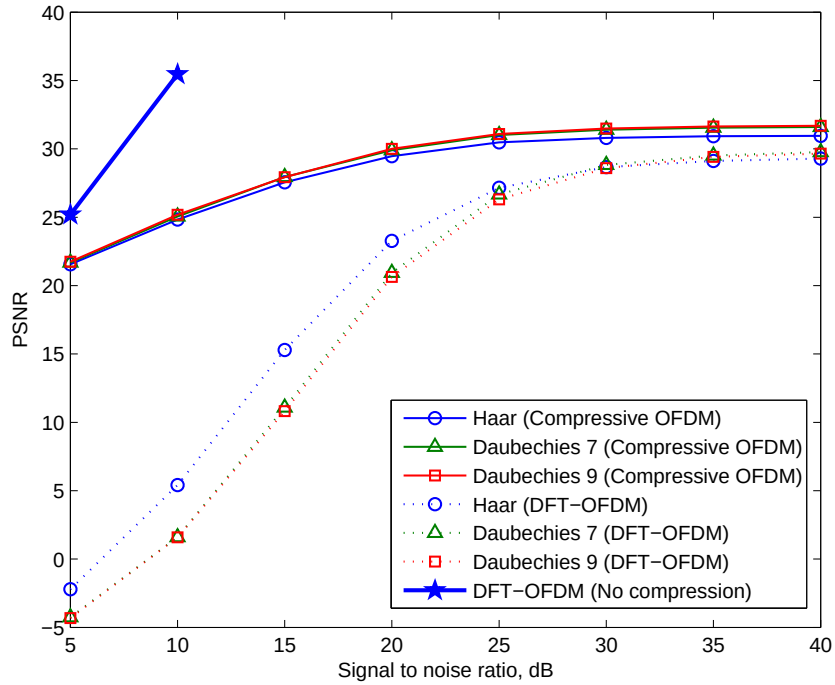

Figure 7.16: PSNR of video frames transmitted via the OFDM transmission systems.

7.4 Conclusions

This chapter has examined the performance of the new compressive OFDM transmission system on the transmission of both image and video signals. It was found in these results that the compressive method worked very well in noisy channel environments. It was also shown that generally the wavelet type made little difference to the performance of the system with only the Haar wavelet contributing to a substantial reduction in system performance.

When compared to traditional DFT-OFDM with wavelet subband compression applied prior to transmission, the proposed compressive method gave superior performance. For the new method the error rate stayed relatively consistent

with a RMSE error rate of between 0.1 and 0.24 for the observed signal-to-noise ratios. This was compared to the DFT-OFDM method with compression applied prior where a large variation in error rates were observed with a dramatic drop in performance at SNRs less than 25 dB. This result alone shows that system performance can be improved when incorporating compression at the time of transmission of the data. Apart from this, computation time was also considered and was also shown to be less when using the new compressive OFDM technique with reductions of 3/4 of the time achieved for image transmission and a reduction of a half the time in the case of videos.

The final comparison presented in this chapter was with DFT-OFDM with no compression applied to the data. As expected this method performed the best with RMSE results of zero at signal-to-noise ratios above 30 dB, but with a data rate approximately 2.6 times greater than that of the other two methods, efficiency was a downside to this system.

Chapter 8

Conclusions and Future Directions

This thesis has presented a study in OFDM techniques in the transmission of image and video data. Experiments have been conducted in image and video transmission using both traditional DFT-OFDM techniques and a novel compressive technique. Both techniques make use of wavelets for compression and experiments have looked at how wavelet subband compression can be implemented in the two different OFDM transmission schemes.

In Chapter 4 results were presented on the performance of traditional DFT-OFDM. Both image transmission and video transmission was considered to get a good indication of the performance of this technique. The results presented in this chapter looked firstly at the effects wavelet subband compression has on the quality of transmitted data as well as the effect different QAM constellation mappings had on the transmission error. For the results considering the effects compression has on data quality, wavelet subband compression was used on the data. Relative mean squared error, structural similarity of the images/videos and PSNR were then all considered when looking at the effects this type of

compression has on the data.

It was found in this chapter that:

- For images and videos transmitted using DFT-OFDM without compression an error rate close to zero as well as a structural similarity of 100% and PSNR of infinity were obtained at signal-to-noise ratios above 35 dB. This result allowed for a quantification of how much error is obtained from the lossy wavelet compression method applied to the data before transmission. For the compressed data at these same signal-to-noise ratios a maximum structural similarity of 71% was achieved and a PSNR of 30dB was also achieved. This shows the level of reduction purely due to compression.

- 16-QAM constellation mapping was the most effective method of baseband encoding when the intended transmission method was DFT-OFDM.

  The results from this chapter showed that by using 16-QAM the RMSE obtained was far less that that obtained when using 32- or 64-QAM. This result was understandable since the Euclidean distance between constellation points in 16-QAM is much greater than for the other studied QAM encoding methods. Using constellation encoding methods with this attribute allows for greater flexibility at the receiver before an error in detection occurs [4].

- Relative mean squared error, structural similarity and PSNR obtained from the experiments were dependent on the type of images being transmitted.

This could be seen to be caused by the correlation in the data and the way the wavelet decomposition affects the data. It was interesting though to look at the types of images that were adversely affected during the transmission simulations. The images that compressed poorly were, as expected, the ones with a lot of black to white transitions between neighbouring pixels. These images tend to have a higher spatial frequency, the images that compressed well tended to be flat shades.

Chapter 7 presented results from simulations of a novel compressive OFDM system. This system combines data compression and transmission into the one block in order to decrease the computational complexity of the system.

Results in this chapter present RMSE, structural similarity and PSNR for the transmission of image data. Results were also discussed for the error obtained for different wavelets being used for the compression and OFDM transmission.

The second part of this chapter also gives a comparison of the novel compressive OFDM method and the traditional DFT-OFDM (with and without compression) and looks at the differences in the three methods.

It was found in this chapter that:

- The novel compressive transceiver system performed well in all channel conditions for the transmission of images.

  This new technique proved to be very resilient to noise corrupting a channel which was a very good result. When compared to the results obtained from traditional DFT-based OFDM with compression applied, error re-

mained very low even at SNRs of 5dB where the DFT-OFDM method proved to work very poorly. For SNRs that were higher (greater than 30 dB) the proposed method had a slightly better performance than the DFT-OFDM with compression applied. Even when considering the structural similarity of the received images the proposed method gave better structural similarity than that obtained using the traditional OFDM method over all signal-to-noise ratios.

The proposed method was also shown to perform slightly worse than the DFT-OFDM without compression with a SSIM value of 21% less than the non-compressed image transmission experiment. This result was to be expected as a lossy compression technique is used in the proposed method which will reduce the quality of the data. As far as efficiency is concerned the loss of structural similarity is balanced out by the data reduction from the compression method with a 2.6:1 compression ratio being achieved for the proposed method. This had an obvious effect on simulation time with simulations of the proposed method taking approximately half the amount of time as the DFT-OFDM simulations with compression.

- The wavelet used had very little effect on the results obtained for both the transmission of image and video data. It was found that using the Haar wavelet contributed to the most quality reduction with a 0.014 - 0.016 RMSE reduction between the Haar wavelet and the Daubechies 9 wavelet for video and image transmission respectively. This translated to a SSIM reduction of 1.7% and a 0.73dB reduction in PSNR.

  While system performance did decrease when using the Haar wavelet ba-

sis function, all the other Daubechies family wavelets performed comparably well. The Haar basis function is a very basic, simplistic wavelet and can end up giving a crude decomposition to the signal so it was not unexpected that this wavelet did not perform as well for the proposed system being examined. The Daubechies wavelets (Db2+) are preferred in wavelet based OFDM transmission systems with no advantage of using one over the other when it came to performance [38], the results in this chapter also confirm that this is also the case in the proposed system.

Another consideration is increasing the wavelet order also increases the number of coefficients produced by the DWT process. Since there is a negligible improvement in data quality using wavelet filter orders above Daubechies 2, the wavelet order should be selected to reduce the coefficients as much as possible to produce the most efficient data compression possible.

- Computational complexity is reduced in the proposed system with a simulation time of almost half achieved using the new method with video and a 3/4 reduction in time for images.

  Simulation time for the proposed compressive OFDM technique was found to be approximately half the time taken to simulate the DFT-based OFDM system with video and 3/4 less for images. This is a highly desirable characteristic in the system as computational complexity can delay transmission of the data and slow the whole system down. Computational complexity was already proven to be better in wavelet based OFDM systems [38], but by merging the compression and transmission blocks into

one as well as using a wavelet based transmission method a much more efficient system is again produced.

Future Directions

The proposed technique has many areas which need to be explored and developed which are beyond the scope of this thesis, some of the future research directions that need to be further assessed in this transmission method include the following:

1. In this research the transmission method was considered in a wireless environment, further research could examine the feasibility of this system in other applications that employ OFDM. As mentioned in this research power line communications and ADSL internet are other applications that are based on OFDM and this new technique may also work well in these systems.

   By looking at these other OFDM systems different channel models would need to be considered as some OFDM applications are wireless and others are wired. The channel simulated in this research was a multipath fading channel with AWGN which is a typical wireless channel model. Another direction this research could consider is the effect different channel models have on the quality of the data being transmitted and received.

2. Another direction is to consider more diverse data types being transmitted. This thesis has focused on system performance when transmitting greyscale, still images as well as video. Other data types such as audio and data such as computer files could also be considered and system effectiveness for these different data types could be assessed.

Another aspect of this future work that would need to be considered is the MPEG encoding that usually occurs to video being transmitted wirelessly. In OFDM based systems such as digital television broadcasting, MPEG encoding is applied to the data before any processing occurs for transmission [24]. In these cases the video and image data are not going to be in the same form as a raw image or video frame, in future research this will also need to be considered to see how this type of data encapsulation method could effect the quality of the data being transmitted through the OFDM system.

Finally in this colour images and video should be considered. It would be expected these would perform in the same way as the same process would just be applied to the red, green and blue layers but this is also another consideration to explore in future work.

Appendix A

The following pages show the images used in the experiments performed in this work. These images were sourced from the SIPI database, [86].

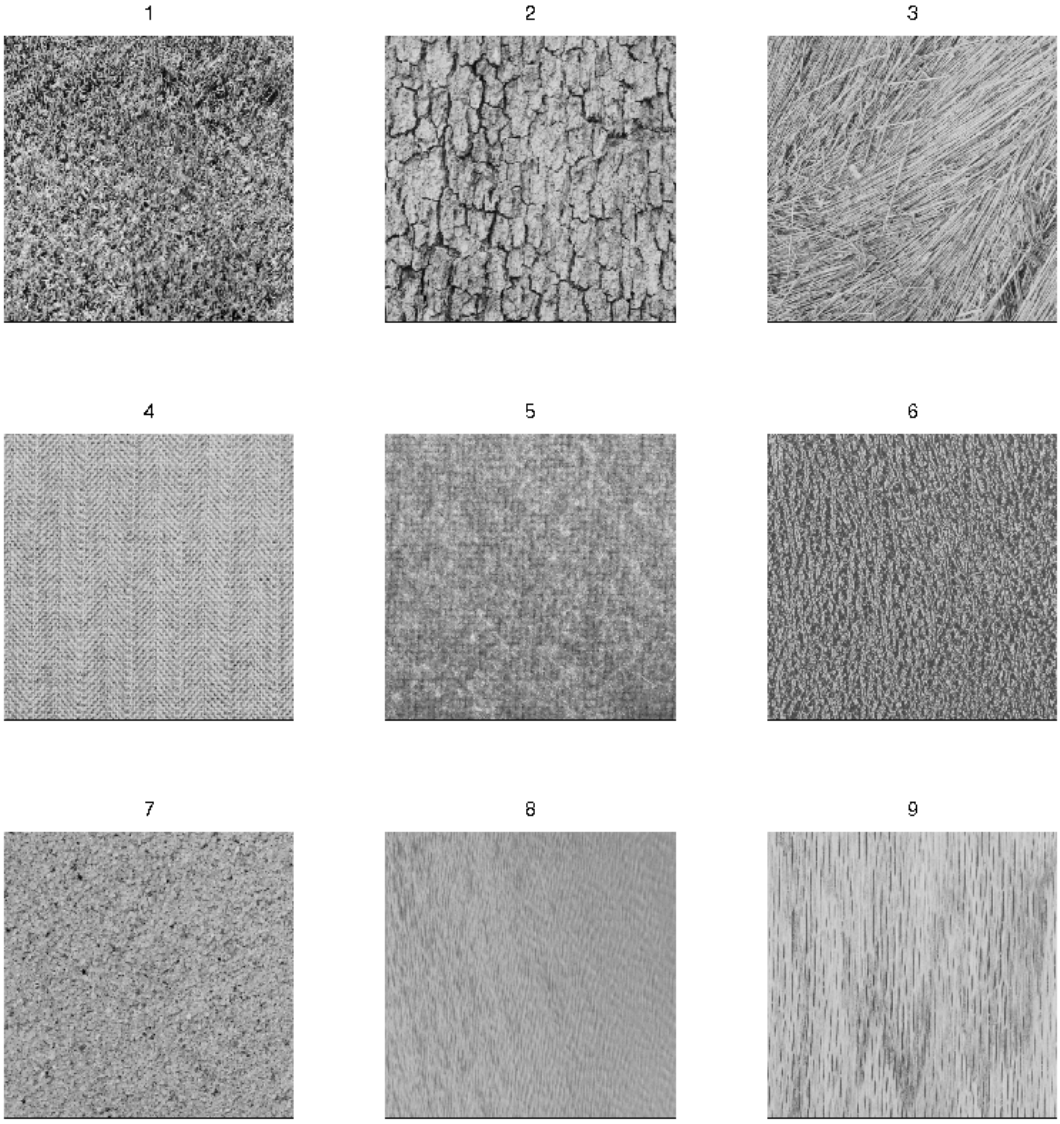

Figure A.1: Experimental images no. 1 - 9

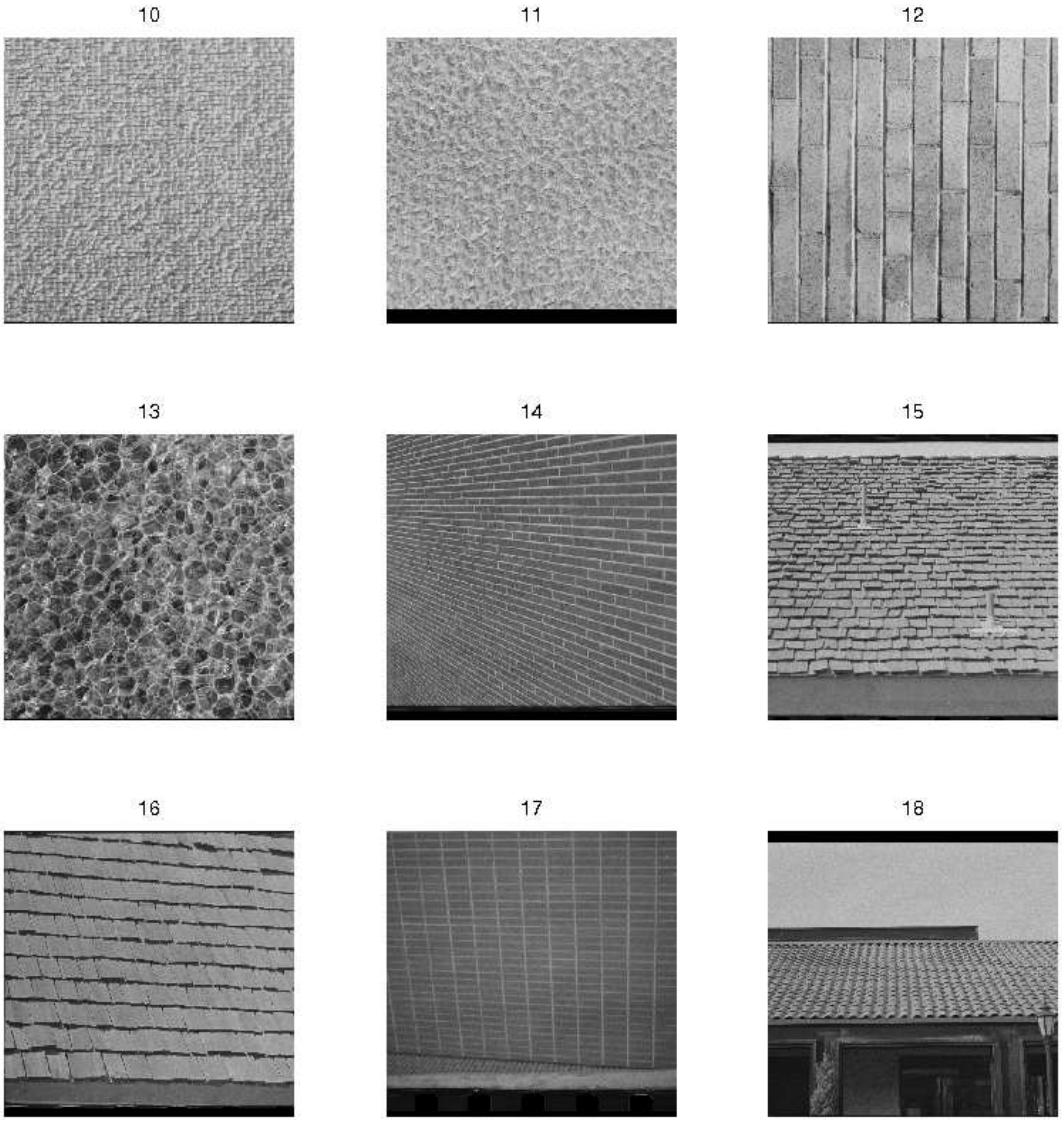

Figure A.2: Experimental images no. 10 - 18

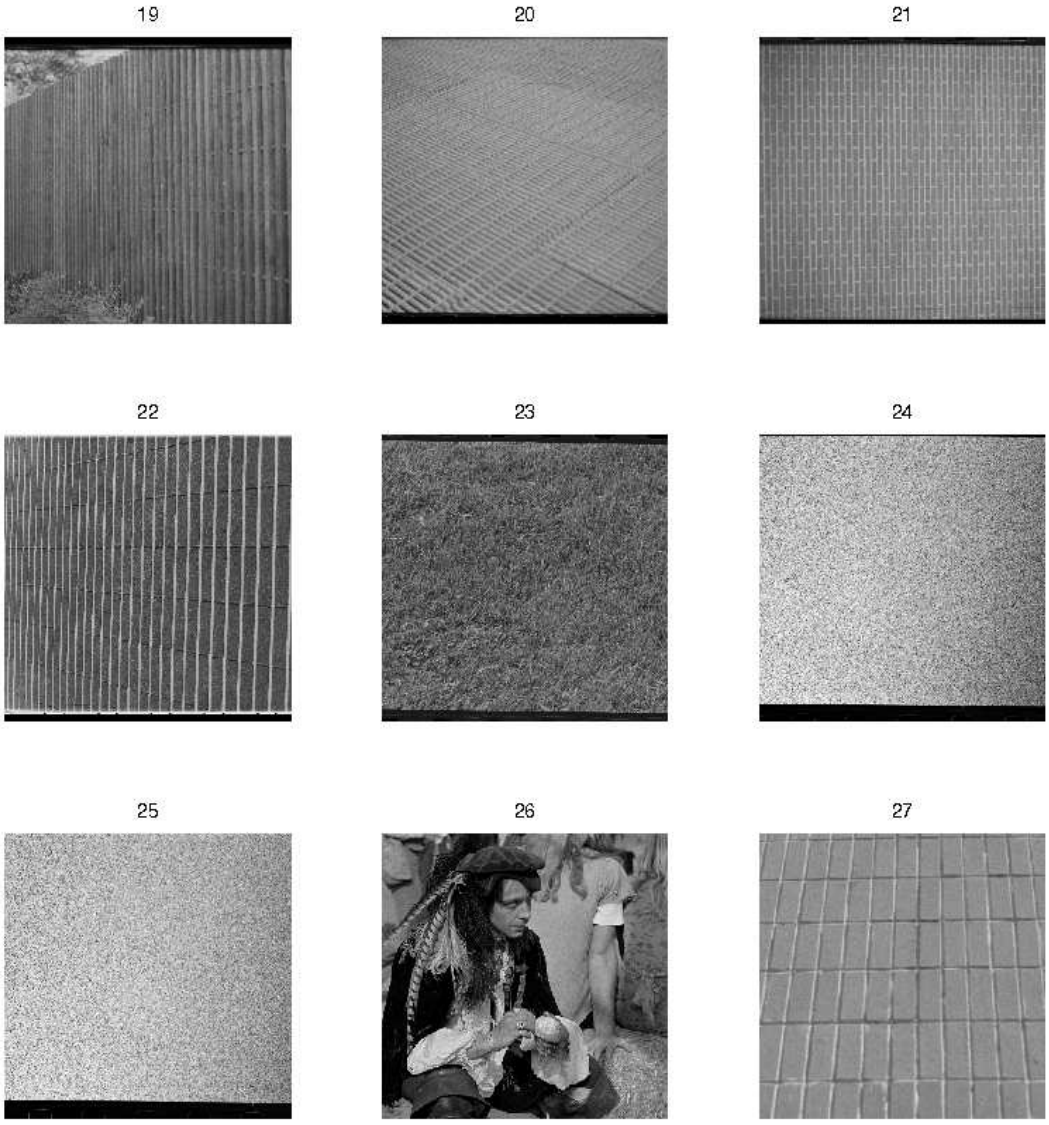

Figure A.3: Experimental images no. 19 - 27

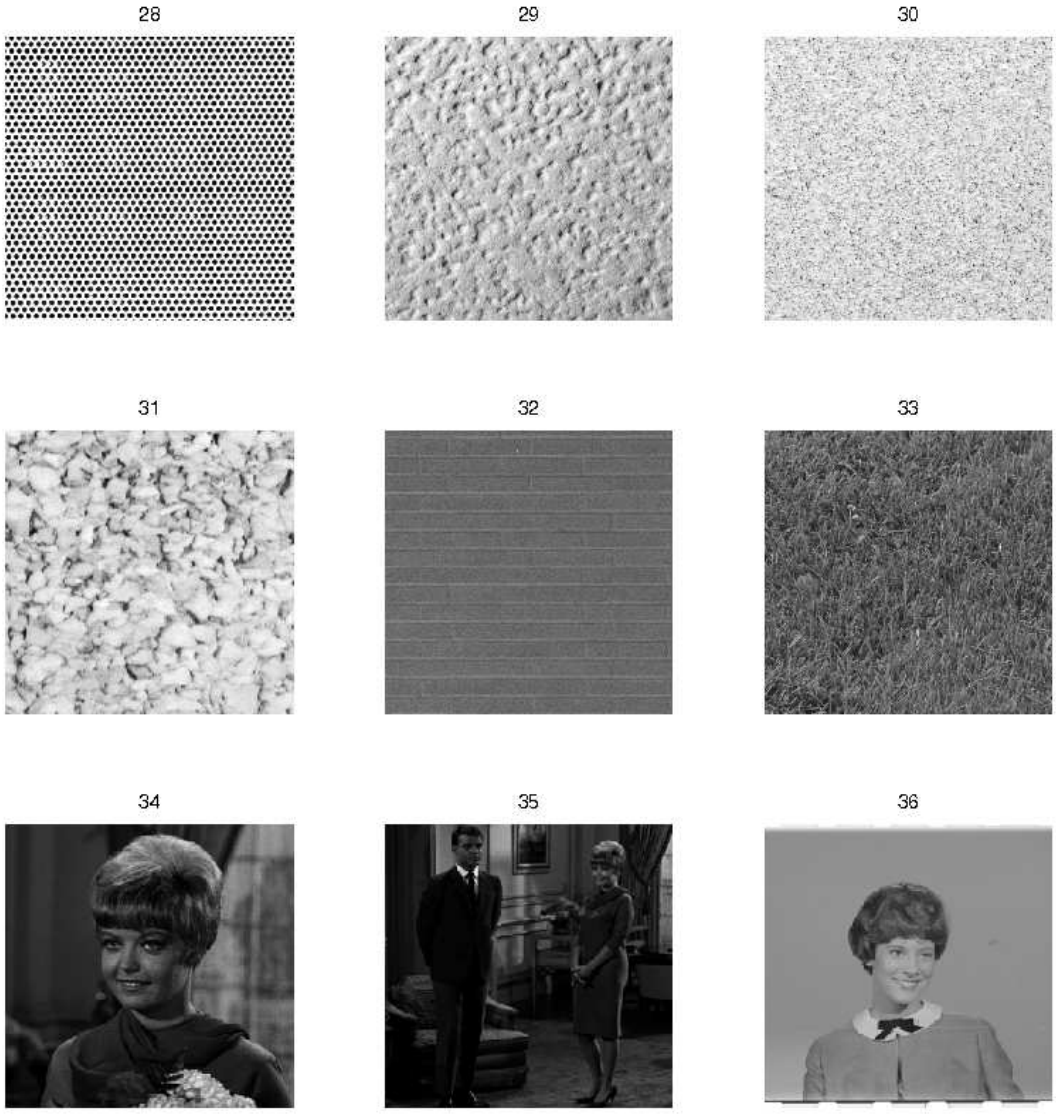

Figure A.4: Experimental images no. 28 - 36

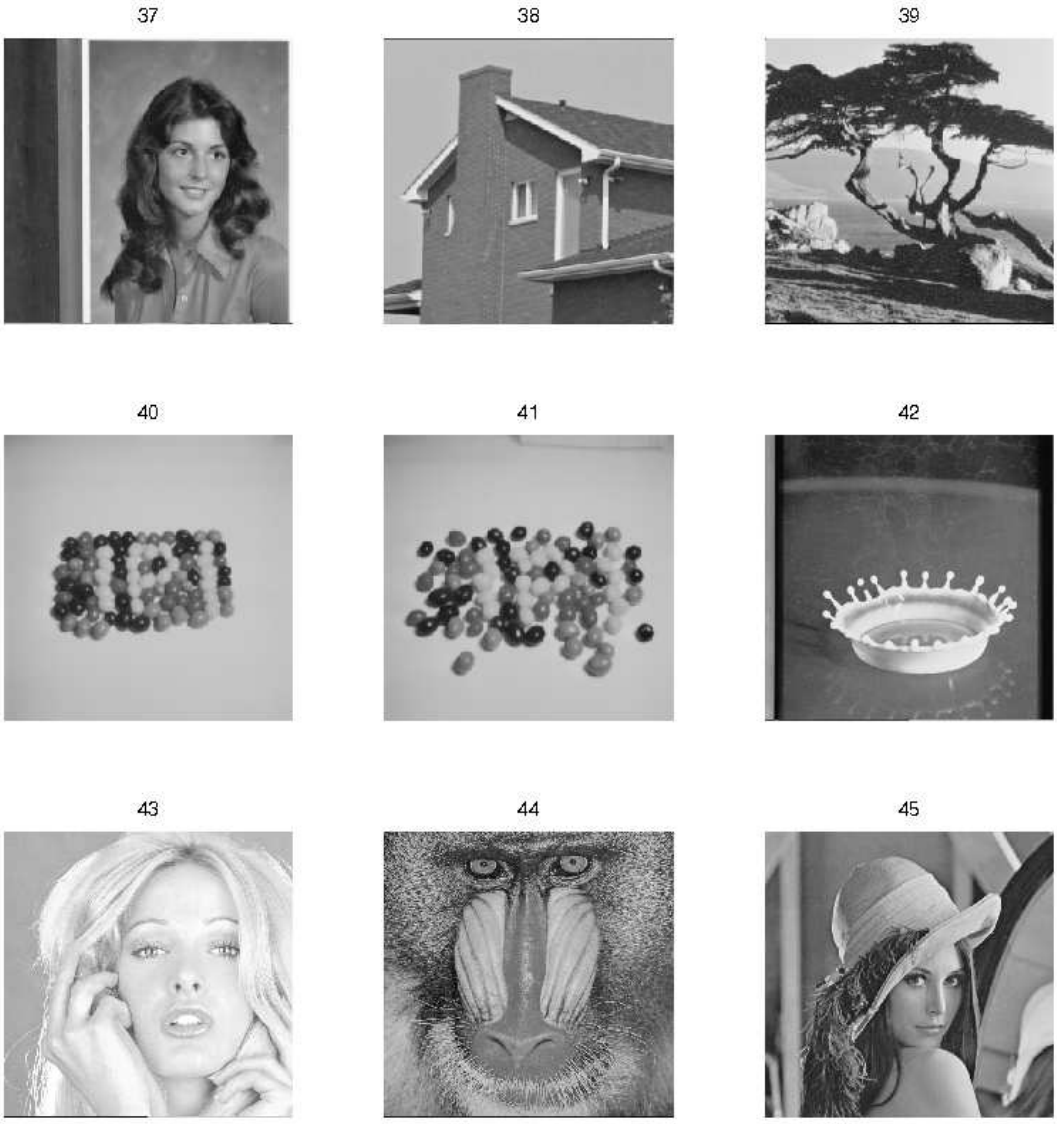

Figure A.5: Experimental images no. 37 - 45

Figure A.6: Experimental images no. 46 - 54

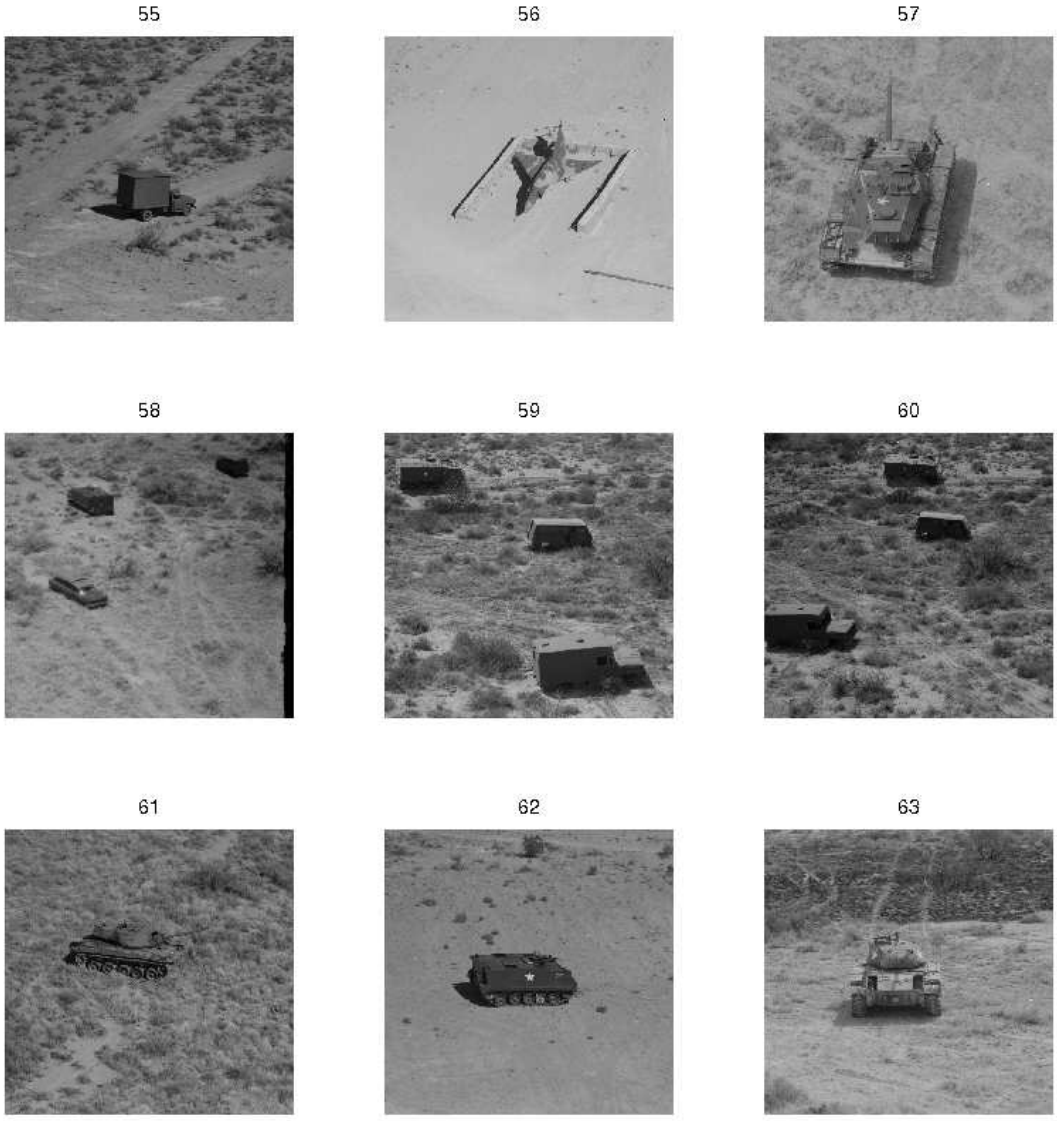

Figure A.7: Experimental images no. 55 - 63

Figure A.8: Experimental images no. 64 - 69

Bibliography

[1] S. F. B. Morse, "Improvement in the Mode of Communicating Information by Signals by the Application of Electro-Magnetism", U.S. Patent 1647, June 20, 1840.

[2] G. Marconi, "Improvements in Transmitting Electrical Impulses and Signals, and in Apparatus Therefor", British Patent 12,039, July 2, 1897.

[3] G. Marconi, "Apparatus for Wireless Telegraphy", U.S. Patent 676332, June 11, 1901.

[4] J. G. Proakis, and M. Salehi, *Communication Systems Engineering, Second Edition*, Prentice Hall, New Jersey, 2002.

[5] M. S. Roden, *Analog and Digital Communication Systems, Fourth Edition*, Prentice Hall, New Jersey, 1996.

[6] D. R. Smith, *Digital Transmission Systems, Third Edition*, Kluwer Academic Publishers, Massachusetts, 2004.

[7] R. W. Chang, "Synthesis of Band-Limited Orthogonal Signals for Multichannel Data Transmission," *Bell Systems Technical Journal*, Vol. 45, No. 2, pp 1775-1796, Dec 1966.

[8] L. J. Cimini, "Analysis and Simulation of a Digital Mobile Channel Using Orthogonal Frequency Division Multiplexing," *IEEE Transactions on Communications*, Vol. COM-33, No. 7, pp 665-675, July 1985.

[9] A. N. Akansu, P. Duhamel, X. Lin, and M. de Courville, "Orthogonal transmultiplexers in communication: A review," *IEEE Transactions on Signal Processing*, Vol. 46, pp. 979-995, Apr. 1998.

[10] L. W. Couch, *Digital and Analog Communication Systems, Sixth Edition*, Prentice Hall, New Jersey, 2001.

[11] K. Sayood, *Introduction to Data Compression, Third Edition*, Morgan Kaufmann, San Fransisco, 2006.

[12] K. Neville, and Z. M. Hussain, "FFT-OFDM for Compressed Image Transmission: Performance using Structural Similarity," Proceedings of *IEEE Advanced Technologies in Commmunication Conference (ATC'08)*, Hanoi, Vietnam, Oct. 2008.

[13] K. L. Neville and Z. M. Hussain, "Effects of Wavelet Compression of Speech on its Mel-Cepstral Coefficients," Proceedings of *International Conference on Communication, Computer and Power (ICCCP'09)*, Muscat, Feb. 2009.

[14] S. M. Lajevardi, K. L. Neville and Z. M. Hussain, "Facial Expression Recognition Over FFT-OFDM," Proceedings of *IEEE Advanced Technologies in Communications (ATC'09)*, Haiphong, Vietnam, October 12-14, 2009.

[15] G. Smithson, "Introduction to digital modulation schemes,", *IEE Collo-*

quium on the Design of Digital Cellular Handsets., Vol. 2, pp. 1-9, March 1998.

[16] I. A. Glover, and P. M. Grant, *Digital Communications, 2nd edition* Pearson Education, Essex, 2004.

[17] J. D. Oetting, "A Comparison of Modulation Techniques for Digital Radio," *IEEE Transactions on Communicatons*, Vol. COM-27, No. 12, pp. 1752-1762, Dec 1979.

[18] S. Haykin, *An Introduction to Analog and Digital Communications*, John Wiley and Sons, New York, 1989.

[19] R. W. Chang, and R. A. Gibby, "A Theoretical Study of Performance of an Orthogonal Multiplexing Data Transmission Scheme," *IEEE Transactions on Communication Technology*, Vol. COM-16, No. 4, pp 529-540, Aug 1968.

[20] B. R. Saltzberg, "Performance of an Efficient Parallel Data Transmission System," *IEEE Transactions on Communication Technology*, Vol. COM-15, No. 6, pp 805-811, Dec 1967.

[21] S. B. Weinstein, and P. M. Ebert, "Data Transmission by Frequency-Division Multiplexing using the Discrete Fourier Transform," *IEEE Transactions on Communications*, Vol. COM-19, No. 5, pp 628-634, Oct 1971.

[22] J. A. C. Bingham, "Multicarrier Modulation for Data Transmission: An Idea Whose Time Has Come," *IEEE Communications Magazine*, Vol. 28, No. 5, pp. 5-14, May. 1990.

[23] H. C. Wu, "Analysis and Characterization of Intercarrier and Interblock Interferences for Wireless Mobile OFDM Systems," *IEEE Transactions on Broadcasting*, Vol. 52, No. 2, pp. 203-210, June. 2006.

[24] *Digital Video Broadcasting (DVB); Framing structure, channel coding and modulation for digital terrestrial television*, ETSI Std EN 300 744 v1.6.1 (2009-01), 2009.

[25] N. Al-Hinai, K. Neville, A. Z. Sadik, and Z. M. Hussain, "Compressed Image Transmission over FFT-OFDM: A Comparative Study," Proceedings of *Australasian Telecommunication Networks and Applications Conference (ATNAC'07)*, Christchurch, New Zealand, pp.465 - 469, 2007.

[26] A. E. Jones, T. A. Wilkinson, and S. K. Barton, "Block Coding Scheme for Reduction of Peak to Mean Envelope Power Ratio of Multicarrier Transmission Schemes," *IEEE Electronic Letters*, Vol. 30, No. 25, pp 2098-2099, Dec. 1994.

[27] T. A. Wilkinson, and A. E. Jones, "Minimisation of the Peak to Mean Envelope Power Ratio of Multicarrier Transmission Schemes by Block Coding," Proceedings of the *IEEE Vehicular Technology Conference (VTC'95)*, Vol. 2, Chicago, USA, pp 825-829, Jul. 1995.

[28] Y. Park, and S. L. Miller, "Peak-to-Average Power Ratio Suppression Schemes in DFT Based OFDM," Proceedings of the *IEEE Vehicular Technology Conference (VTC 2000)*, Vol. 1, Tokyo, Japan, pp 292-297, Sep. 2000.

[29] S. Galli, and O. Logvinov, "Recent Developments in the Standardization of Power Line Communications within the IEEE," *IEEE Communications Magazine*, Vol. 46, No. 7, pp 64 - 71 , Jul. 2008.

[30] H. C. Ferreira, H. M. Grové,O. Hooijen, and A. J. Han Vinck, "Power Line Communications: an Overview," Proceedings of *IEEE AFRICON '96*, South Africa, Vol. 2, pp 558-563 , Sep. 1996.

[31] P. K. Van Der Gracht, and R. W. Donaldson "Communication Using Pseudonoise Modulation on Electric Power Distribution Circuits," *IEEE Transactions on Communications*, Vol. COMM-33, No. 9, pp 964-974, Sep. 1985.

[32] J. B. O'Neal, "The Residential Power Circuit as a Communication Medium," *IEEE Transactions on Consumer Electronics*, Vol. CE-32, No. 3, pp 567-577, Aug. 1986.

[33] S. D. Sandberg, and M. A. Tzannes, "Overlapped Discrete Multitone Modulation for High Speed Copper Wire Communications," *IEEE Journal on Selected Areas in Communications*, Vol. 13, No. 9, pp 1571-1585, Dec. 1995.

[34] M. Kuhn, D. Benyoucef, and A. Wittneben, "Linear Block Codes for Frequency Selective PLC Channels With Colored Noise and Multiple Narrowband Interference," Proceedings of the *IEEE Vehicular Technology Conference 2002*, Birmingham, USA, Vol. 4, pp 1756-1760, May 2002.

[35] White Paper: OPERA Technology, *Open PLC European Reasearch Alliance*, Retrieved July 8th, 2009 from: http://www.ist-opera.org/

[36] Y. Zhang, and S. Cheng, "A Novel Multicarrier Signal Transmission System Over Multipath Channel of Low-Voltage Power Line," *IEEE Transactions on Power Delivery*, Vol. 19, No. 4, pp 1668-1672, Oct. 2004.

[37] S. Galli, H. Koga, and N. Kodama, "Advanced Signal Processing for PLCs: Wavelet-OFDM," Proceedings of the *IEEE International Symposium on Power Line Communications and its Applications (ISPLC2008)*, Jeju Island, Korea, pp 187-192, Apr. 2008.

[38] M. Oltean, and M. Naforniţă, "Efficient Pulse Shaping and Robust Data Transmission Using Wavelets," Proceedings of the *IEEE International Symposium on Intelligent Signal Processing, 2007 (WISP 2007)*, Alcala De Henares, Spain, pp 1-6, Oct. 2007.

[39] S. Wei, R. Han, F. Cheng, Y. Chen, and W. Liu, "Performance of Wavelet OFDM in Underground Coal Mine PLCs," Proceedings of the *Second International Symposium on Intelligent Information Technology Application, 2008 (IITA '08)*, Shanghai, China, Vol. 2, pp 723-727, Dec. 2008.

[40] M. A. Tzannes, M. C. Tzannes, J. Proakis, and P. N. Heller, "DMT Systems, DWMT Systems and Digital Filter Banks," Proceedings of the *IEEE International Conference on Communications, 1994 (ICC '94)*, New Orleans, USA, pp 311-315, May. 1994.

[41] K. Abdullah, and Z. M. Hussain, "Performance of Fourier-Based and Wavelet-Based OFDM for DVB-T Systems," Proceedings of the *Australasian Telecommunication Networks and Applications Conference, 2007 (ATNAC '07)*, Christchurch, New Zealand, pp 475-479, Dec. 2007.

[42] C. Van Bouwel, J. Potemans, S. Schepers, B. Nauwelaers, and A. Van de Capelle, "Wavelet Packet Based Multicarrier Modulation," Proceedings of the *Symposium on Communications and Vehicular Technology (SCVT-2000)*, Leuven, Belgium, pp 131-138, 2000.

[43] S. Baig, F. U. Rehman, and M. J. Mughal, "Performance Comparison of DFT, Discrete Wavelet Packet and Wavelet Transforms, in an OFDM Transceiver for Multipath Fading Channel," Proceedings of the *IEEE International Multitopic Conference (INMIC 2005)*, Karachi, Pakistan, pp 1-6, Dec. 2005.

[44] A. R. Lindsey, "Wavelet Packet Modulation for Orthogonally Multiplexed Communication," *IEEE Transactions on Signal Processing*, Vol. 45, No. 5, pp 1336-1339, May 1997.

[45] A. Jamin, and P. Mähönen "Wavelet Packet Modulation for Wireless Communications," *Wireless Communications and Mobile Computing*, Vol. 5, pp 123-137, Dec 2005.

[46] D. Salomon, *Data Compression The Complete Reference, Fourth Edition*, Springer-Verlag London Limited, London, 2007.

[47] S. D. Bradley, "Optimizing a Scheme for Run Length Encoding," *Proceedings of the IEEE*, Vol. 57, No. 1, pp 108-109, Jan. 1969.

[48] N. Ahmed, T. Natarajan, and K. R. Rao, "Discrete Cosine Transform," *IEEE Transactions on Computers*, Vol. C-23, No. 1, pp 90 - 93 , Jan. 1974.

[49] *Information Technology - Digital Compression and Coding of Continuous-tone Still Images: Requirements and Guidelines*, ISO/IEC Std 10918-1, 1994.

[50] W. B. Pennebaker, and J. L. Mitchell, *JPEG Still Image Compression Standard*, Van Nostrand Reinhold, New York, 1993.

[51] L. McMillan, L. Westover, "A Forward-Mapping Realization of the Inverse Discrete Cosine Transform," *Data Compression Conference 1992*, pp 219 - 228, 24-27 March 1992.

[52] I. Daubechies, "Orthonormal Bases of Compactly Supported Wavelets," *Communications on Pure and Applied Mathematics*, Vol. 41, pp. 909-996, 1988.

[53] I. Daubechies, "The Wavelet Transform, Time-Frequency Localization and Signal Analysis," *IEEE Transactions on Information Theory*, Vol. 36, No. 5, pp 961 - 1005, Sep. 1990.

[54] I. Daubechies, "Orthonormal Bases of Compactly Supported Wavelets II. Variations on a Theme," *SIAM Journal on Mathematical Analysis*, Vol. 24, No. 2, pp. 499-519, Mar. 1993.

[55] S. G. Mallet, "A Theory for Multiresolution Signal Decomposition: The Wavelet Representation," *IEEE Transactions on Pattern Analysis and Machine Intelligence*, Vol. 11, No. 7, pp 674 - 693 , Jul. 1989.

[56] M. Vetterli, and J. Kovacevic, *Wavelets and Subband Coding*, Prentice Hall, New Jersey, 1995.

[57] X. P. Zhang, L. S. Tian, and Y. N. Peng, "From the Wavelet Series to the Discrete Wavelet Transform - The Initialization," *IEEE Transactions on Signal Processing*, Vol. 44, No. 1, pp 129 - 133 , Jan. 1996.

[58] O. Rioul, and P. Duhamel, "Fast Algorithms for Discrete and Continuous Wavelet Transforms," *IEEE Transactions on Information Theory*, Vol. 38, No. 2, pp 569 - 586 , Mar. 1992.

[59] R. Kronland-Martinet, J. Morlet, and A. Grossman, "Analysis of Sound Patterns Through Wavelet Transforms," *International Journal of Pattern Recognition and Artificial Intelligence*, Vol. 1, No. 2, pp 273 - 302 , 1987.

[60] W. Kinsner, and A. Langi, "Speech and Image Signal Compression with Wavelets," Proceedings of the *IEEE Conference on Communications, Computers and Power in the Modern Environment*, Saskatoon, Canada, pp 368 - 375, 17-18 May 1993.

[61] R. R. Coifman, Y. Meyer, and V. Wickerhauser, "Wavelet Analysis and Signal Processing," in *Wavelets and their Applications*, Springer-Verlag London Limited, London, 1992.

[62] M. Antonini, M. Barlaud, P. Mathieu, and I. Daubechies, "Image Coding Using Vector Quantization in the Wavelet Transform Domain," Proceedings of the *International Conference on Acoustics, Speech, and Signal Processing (ICASSP-90)*, Vol. 4, pp 2297 - 2300, 3-6 Apr. 1991.

[63] M. Antonini, M. Barlaud, P. Mathieu, and I. Daubechies, "Image Coding Using Wavelet Transform," *IEEE Transactions on Image Processing*, Vol. 1, No. 2, pp 205 - 220 , Apr. 1992.

[64] J. I. Agbinya, "Discrete Wavelet Transform Techniques in Speech Processing," *IEEE TENCON - Digital Signal Processing Applications*, Vol. 2, pp 514 - 519, Nov. 1996.

[65] G. Franceschetti, and S. Stornelli, *Wireless Networks*, Academic Press, Elsevier, Burlington, 2006.

[66] W. Hwang, and K. Kim, "Performance Analysis of OFDM on the Shadowed Multipath Channels," *IEEE Transactions on Consumer Electronics*, Vol. 44, No. 4, pp 1323 - 1328, Nov. 1998.

[67] E. Viterbo, and K. Fazel, "How to Combat Long Echoes in OFDM Transmission Schemes: Sub-Channel Equalization or More Powerful Channel Coding," Proceedings of the *IEEE Global Telecommunications Conference (GLOBECOM'95)*, Singapore, Vol. 3, pp 2069 - 2074, Nov. 1995.

[68] H. Arslan, L. Krasny, D. Koilpillai, and S. Chennakeshu, "Doppler Spread Estimation for Wireless Mobile Radio Systems," Proceedings of the *IEEE Wireless Communications and Networking Conference*, Chicago, USA, Vol. 3, pp 1075 - 1079, Sep. 2000.

[69] Q. Lu, X. T. Chen, and B. Long, "A Doppler Spread Estimation Design for Mobile OFDM Systems," Proceedings of the *IEEE International Conference on Communication Systems*, Guangzhou, China, pp 1046 - 1049, Nov. 2008.

[70] J. Tao, and C. Xiao, "Doppler Spread Estimation for Broadband OFDM Systems," Proceedings of the *IEEE Global Telecommunications Conference (GLOBECOM'07)*, Washington DC, USA, pp 2878 - 2882, Nov. 2007.

[71] J. G. Proakis, *Digital Communications, Fourth Edition*, McGraw Hill New York, 2001.

[72] W. C. Jakes, "Mobile Radio Propagation," in *Microwave Mobile Communications*, John Wiley and Sons New York, 1974.

[73] *Radio Broadcasting Systems; Digital Audio Broadcasting to mobile, portable and fixed receivers*, ETSI Std EN 300 401 v1.4.1 (2006-06), 2006.

[74] R. K. Jurgen, "Broadcasting with Digital Audio," *IEEE Spectrum Magazine*, Vol. 33, iss. 3, pp 52 - 59, Mar. 1996.

[75] B. W. Kroeger, and P. J. Peyla, "Compatibility of FM Hybrid In-Band On-Channel (IBOC) System for Digital Audio Broadcasting," *IEEE Transactions on Broadcasting*, Vol. 43, No. 4, pp 421 - 430, Dec. 1997.

[76] *IEEE Standard for Wireless LAN Medium Access Control (MAC) and Physical Layer (PHY) Specifications*, IEEE Std 802.11a-1999(R2003), 2003.

[77] IEEE P1901 Draft Standard for Broadband over Power Line Networks: Medium Access Control and Physical Layer Specifications, *IEEE P1901 Working Group*, Retrieved June 24th, 2009 from: http://grouper.ieee.org/groups/1901/

[78] D. R. Gimlin, and C. R. Patisaul, "On Minimizing the Peak-to-Average Power Ratio for the Sum of N Sinusoids," *IEEE Transactions on Communications*, Vol. 41, No. 4, pp 631 - 635 , Apr. 1993.

[79] S. H. Han, and J. H. Lee, "An Overview of Peak-to-Average Power Ra-

tion Reduction Techniques for Multicarrier Transmission," *IEEE Wireless Communications*, pp 56 - 65 , Apr. 2005.

[80] A. K. Gurung, F. S. Al-Qahtani, A. Z. Sadik, and Z. M. Hussain, "One-Iteration-Clipping-Filtering (OICF) Scheme for PAPR Reduction of OFDM Signals," Proceedings of the *International Conference on Advanced Technologies for Communications (ATC'08)*, Hanoi, Vietnam, pp 207 - 210 , Oct. 2008.

[81] R. O'Neill, and L. B. Lopes, "Envelope variations and spectral splatter in clipped multicarrier signals," Proceedings of the *IEEE International Symposium on Personal, Indoor and Mobile Radio Communications (PIMRC'95)*, Toronto, Canada, pp 71 - 75, Sep. 1995.

[82] B. S. Krongold, and D. L. Jones, "PAR Reduction in OFDM via Active Constellation Extension," *IEEE Transactions on Broadcasting*, Vol. 49, No. 3, pp 258 - 268, Sep. 2003.

[83] S. Celebi, "Interblock Interference (IBI) and Time of Reference (TOR) Computation in OFDM Systems," *IEEE Transactions on Communications*, Vol. 49, No. 11, pp 1895 - 1900, Nov. 2001.

[84] A. Peled, and A. Ruiz, "Frequency Domain Data Transmission using Reduced Computational Complexity Algorithms," Proceedings of the *IEEE International Conference on Acoustics, Speech and Signal Processing (ICASSP'80)*, Denver, Colorado, Vol. 5, pp 964 - 967 , Apr. 1980.

[85] T. Han, and X. Li, "Minimum-Output-Energy Method for Blind Equalization of OFDM and Systems With Sufficient of Insufficient Cyclic Prefix,"

Proceedings of the *IEEE International Conference on Acoustics, Speech, and Signal Processing (ICASSP'03)*, Hong Kong, Vol. 4, pp. 225 - 228, Apr 2003.

[86] University of Southern California, *USC-SIPI Image Database*, Retrieved June 23rd, 2009 from: http://sipi.usc.edu/database/

[87] Arizona State University, *Trace Video Library*, Retrieved November 16th, 2009 from: http://trace.eas.asu.edu/yuv/

[88] Z. Wang, A. C. Bovik, H. R. Sheikh, and E. P. Simoncelli "Image Quality Assessment: From Error Visibility to Structural Similarity," *IEEE Transactions on Image Processing*, Vol. 13, No. 4, pp 600 - 612, Apr. 2004.

[89] Q. Huynh-Thu, and M. Ghanbari, "Scope of Validity of PSNR in Image/Video Quality Assessment," *Electronic Letters*, Vol. 44, No. 13, pp 800 - 801, Jun. 2008.

[90] A. R Prasad, R. Esmailzadeh, S. Winkler, B. Rohani, B. Pinguet, and M. Capel, "Perceptual Quality Measurement and Control: Definition, Application and Performance," Proceedings of the *4th International Symposium on Wireless Personal Multimedia Communication (WPMC'01)*, Aalborg, Denmark, pp 547-552, Sept. 2001.

[91] B. G. Negash, and H. Nikookar, "Wavelet Based OFDM for Wireless Channels," Proceedings of the *IEEE Vehicular Technology Conference (VTC'01)*, Rhodes, Greece, Vol. 1, pp. 688 - 691, May 2001.

[92] M. K. Lakshmanan, and H. Nikookar "A Review of Wavelets for Digital

Wireless Communication,", *Springer Journal on Wireless Personal Communications*, Vol. 37, pp. 387Ű420, May 2006.

[93] J. L. Seoane, S. K. Wilson, and S. Gelfand "Analysis of Intertone and Interblock Interference in OFDM when the length of the Cyclic Prefix is shorter than the Length of the Impulse Response of the Channel," Proceedings of the *IEEE Global Telecommunications Conference (GLOBECOM '97)*, Phoenix, Arizona, Vol 1, pp. 32 - 36, Nov 1997.

[94] B. Ai, Z. Yang, C. Pan, J. Ge, Y. Wang, and Z. Lu "On the Synchronization Techniques for Wireless OFDM Systems," *IEEE Transactions on Broadcasting*, Vol. 52, No. 2, pp. 236 - 244, Jun 2006.

[95] T. Keller, L. Piazzo, P. Mandarini, and L. Hanzo, "Orthogonal Frequency Division Multiplex Synchronization Techniques for Frequency-Selective Fading Channels," *IEEE Journal on Selected Areas in Communications*, Vol. 19, No. 6, pp 999 - 1008, Jun. 2001.

[96] D. Landström, S. K. Wilson, J. van de Beek, and P. Ödling, "Symbol Time Offset Estimation in Coherent OFDM Systems," Proceeding of the *IEEE International Conference on Communications*, Vancouver, Canada, pp 500 - 505, Jun. 1999.

[97] J. van de Beek, M. Sandell, and P. O. Börjesson, "ML Estimation of Time and Frequency Offset in OFDM Systems," *IEEE Transactions on Signal Processing*, Vol. 45, No. 7, pp 1800 - 1805, Jul. 1997.

[98] J. van de Beek, M. Sandell, M. Isaksson, and P. O. Börjesson, "Low-Complex Frame Synchronization in OFDM Systems," Proceeding of the

Fourth IEEE International Conference on Universal Personal Communications, Tokyo, Japan, pp 982 - 986, Nov. 1995.

[99] T. M. Schmidl, and D. C. Cox "Robust Frequency and Timing Synchronization of OFDM," *IEEE Transactions on Communications*, Vol. 45, No. 12, pp. 1613 - 1621, Dec. 1997.

[100] M. Schellmann, "Synchronization in OFDM Systems Based on a Multi-Periodic Preamble," *International Symposium on Wireless Communication Systems*, Siena-Tuscany, Italy, pp 211 - 215, Sept. 2009.

[101] A. G. Burr, and G. P White "Performance of Turbo-coded OFDM," Proceedings of the *IEE Colloquium on Turbo codes in Digital Broadcasting*, London, UK, Vol. 8, pp. 1 - 8, Nov. 1999.

[102] C. Berrou, A. Glavieux and P. Thitimajshima "Near Shannon Limit Error - Correcting Coding and Decoding: Turbo Codes (1)," Proceedings of the *IEEE International Conference on Communications (ICC'93)*, Geneva, Switzerland, Vol. 2, Iss. 1, pp. 1064 - 1070, May. 1993.

[103] M. Torabi, and M. R. Soleymani "Turbo Coded OFDM for Wireless Local Area Networks," Proceedings of the *Canadian Conference on Electrical and Computer Engineering (CCECE'02)*, Winnipeg, Canada, Vol. 3, pp. 1363 - 1367, May. 2002.

[104] I. S. Reed, and G. Solomon "Polynomial Codes Over Certain Finite Fields," *Journal of the Society for Industrial and Applied Mathematics*, Vol. 8, No. 2, pp. 300 - 304, Jun. 1960.

[105] B. Sklar, *Reed-Solomon Codes*, Retrieved July 13th, 2010 from: http://ptgmedia.pearsoncmg.com/images/art_sklar7_reed-solomon/elementLinks/art_sklar7_reed-solomon.pdf

[106] B. Sklar, "A Primer on Turbo Code Concepts," *IEEE Communications Magazine*, Vol. 35, Iss. 12, pp. 94 - 102, Dec. 1997.

[107] *Information Technology - Coding of Moving Pictures and Associated Audio for Digital Storage Media at up to about 1.5 Mbits/s*, ISO/IEC Std 11172, 1993.